THE FER TYROSINE KINASE CONTRIBUTES TO ABERRANT ANDROGEN RECEPTOR SIGNALING IN PROSTATE CANCER

Seta Derderian

Faculty of Medicine, Division of Experimental Medicine

McGill University, Montreal

April 2018

A thesis submitted to McGill University in partial fulfillment of the requirements

of the degree of Master of Science

ABSTRACT

Prostate cancer (PCa) is the most common cancer in Canadian men and the third leading cause of cancer mortality. Despite castration resistance (CRPC) in advanced disease, the androgen receptor (AR) remains transcriptionally active in prostate tumor cells. Our lab has reported on the interleukin (IL)-6 activated tyrosine (Y) kinase (TK) Fer, which phosphorylates and forms nuclear complexes with key transcription factors (TFs) involved in CRPC: signal transducer and activator of transcription (STAT)3 (Y705) and AR (Y223). Recent AR chromatin immunoprecipitation data on PCa tissues from CRPC patients indicates aberrant AR binding to DNA motifs associated to STATs, Myc, and E2Fs. The central hypothesis was that nuclear Fer and possibly other TKs keep TFs activated to allow an integration of signals emanating from different pathways upregulated in advanced forms of human PCa. Accordingly, specific pY223AR and pY714Fer antibodies (Abs) generated in the host lab, along with Fer, AR, AR-V7 (constitutively active AR splice variant), STAT3, pSTAT3, c-Myc, E2F1, and pY Abs, were used as tools to characterize AR Y223 phosphorylation and the formation of complexes in PCa cell lines exposed to diverse stimuli. Our findings confirmed the activation of full-length AR by phosphorylation on Y223, mediated by IL-6 and R1881 (synthetic androgen) in LNCaP cells, whereas full-length AR and the AR-V7 variant are constitutively activated in the more aggressive 22RV1 PCa cell line. Further characterization of the interaction between activated pY223AR and pSTAT3 showed that it is mediated by the SH2 domain of STAT3 binding to the pY223 motif of AR. Of interest, the activation of STAT3 in 22RV1 cells and its interaction with activated AR-V7 are not constitutive but mediated by IL-6. The nuclear co-localization of AR was observed with activated STAT3, c-Myc, and E2F1. Furthermore, AR forms complexes with c-Myc upon exposure of LNCaP to IL-6, but not androgens. AR complexes with E2F1 were also observed under IL-6 or R1881. The pY223 motif of AR is required for these IL-6 mediated interactions, as shown in PC3 cells transfected with wild type vs mutant (Y223F) *AR* cDNAs. The possible Y-phosphorylation of both c-Myc and E2F1 was also observed in PC3 and LNCaP cells, especially in conditions favoring activation of TKs. Fer directly phosphorylates c-Myc, but not E2F1. Finally, we show clinical relevance of our findings in human prostate tumors, where high nuclear expression of STAT3 and c-Myc are predictive of biochemical recurrence. Taken together, AR activation by Y223 phosphorylation independently of androgens allows the

integration of signals emanating from upregulated pathways in CRPC. Aberrant AR signaling reorienting genomic programs may alter cell phenotypes, thereby favoring PCa progression.

RÉSUMÉ

Le cancer de la prostate (CaP) est le cancer le plus courant chez les hommes au Canada et la troisième cause de mortalité par cancer. Malgré la résistance à la castration (CRPC) dans la maladie avancée, le récepteur des androgènes (AR) reste actif sur le plan transcriptionnel dans les cellules tumorales. Notre laboratoire a étudié l'activation par l'interleukin (IL)-6 de la tyrosine (Y) kinase (TK) Fer qui phosphoryle et forme des complexes nucléaires avec deux facteurs de transcription (FTs) impliqués dans le CRPC: « signal transducer and activator of transcription » (STAT)3 (Y705) et AR (Y223). Une étude récente par immunoprécipitation du AR au niveau de la chromatine sur des tissus de prostate provenant de patients CRPC a indiqué une liaison aberrante du AR à des séquences de l'ADN associées aux FTs STATs, Myc et E2Fs. L'hypothèse centrale est que Fer nucléaire et d'autres TK maintiennent les FTs activés pour permettre une intégration de signaux émanant de différentes voies suractivées dans les formes avancées du CP humain. En conséquence, des anticorps pY223AR et pY714Fer spécifiques générés dans notre laboratoire, ainsi que des anticorps Fer, AR, AR-V7 (variant de AR constitutivement actif), STAT3, pSTAT3, c-Myc, E2F1 et pY ont été utilisés pour caractériser la phosphorylation du AR sur Y223 et la formation de complexes dans les lignées cellulaires du CaP exposées à diverses conditions. Nos résultats ont confirmé l'activation du AR par phosphorylation sur Y223, médiée par l'IL-6 et le R1881 (androgène synthétique) dans les cellules LNCaP, alors que le AR et le variant AR-V7 sont constitutivement activés dans les cellules 22RV1, aussi plus agressives. La caractérisation de l'interaction entre pY223AR activé et pSTAT3 a montré que ceci est médié par le domaine SH2 de STAT3 se liant au motif pY223 du AR. De plus, l'activation de STAT3 dans les 22RV1 et son interaction avec le AR-V7 activé ne sont pas constitutives, mais médiés par l'IL-6. La colocalisation nucléaire du AR a été observée avec STAT3 activé, c-Myc et E2F1. En outre, AR forme des complexes avec c-Myc dans les cellules LNCaP exposées à l'IL-6, mais pas aux androgènes. Des complexes AR avec E2F1 ont également été observés dans ces cellules sous l'IL-6 et le R1881. Dans les cellules PC3 transfectées avec l'ADNc du *AR* forme sauvage ou mutant (Y223F), on observe que le motif Y223 de AR est important pour ces interactions sous l'IL-6. Les FTs c-Myc et E2F1 peuvent également être phosphorylés sur Y dans les cellules PC3 et LNCaP, notamment dans des conditions favorisant l'activation des TK par le pervanadate. Fer phosphoryle directement c-Myc, mais pas E2F1. Enfin, nous montrons la connotation clinique de nos résultats dans des tumeurs

de prostate humaine, la forte expression nucléaire de STAT3 et c-Myc étant prédictives de la récidive biochimique. Pris ensemble, l'activation du AR par la phosphorylation sur Y223 indépendamment des androgènes permet l'intégration de signaux émanant des voies suractivées dans le CRPC. La signalisation aberrante du AR réorientant les programmes génomiques peut altérer les phénotypes des cellules et ainsi favoriser la progression du CaP.

TABLE OF CONTENTS

ACKNOWLEDGEMENTS

First, I would like to acknowledge my supervisor Dr. Simone Chevalier. Her endless passion for science and dedication to her work are a great motivation. She is truly an exemplary mentor, full of insight, always supportive, and pushing students to do their best.

I would also like to acknowledge my committee members: Dr. Jacques Lapointe, Dr. Teruko Taketo-Hosotani, and Dr. Christian Rocheleau. Their feedback was meaningful and useful, and their guidance was well appreciated.

I wish to thank the Uro-oncology Research group for their technical help, scientific advice, and criticism. I would especially like to thank Ms Fatima Zahra Zouanat for guiding me and teaching me everything she could, both in and out of the laboratory. I also thank Ms. Chrysoula Makris for her patience, her unshakeable honesty, and her remarkable talent of putting all of our problems into perspective.

I would also like to thank my family and friends, who were there to support, encourage, and distract me after long days of working in the lab.

I would like to acknowledge the financial support provided by Prostate Cancer Canada (PCC), Cancer Research Society (CRS), Astellas and Urology Research Funds.

PREFACE AND CONTRIBUTION OF AUTHORS

All the work presented was conducted at the Research Institute of the McGill University Health Center (RI-MUHC). For studies on human tissue by immunohistochemistry (IHC), the protocol BMD-10-1160 was approved by the ethics board of the research institute and renewed yearly.

Experimental planning, data collection and analysis, and preparation of the thesis were carried out by Seta Derderian, under the supervision of Dr. Simone Chevalier.

pY223AR and pY714Fer antibody production, purification, and testing were done by Dr Lucie Hamel and Ms Fatima Z. Zouanat. Ms Zouanat contributed to the experiment presented in Figure 16B. She also reviewed sections for STAT3 and c-Myc immunohistochemical staining (Chapter 7), which will also be reviewed by Dr F. Brimo, a genitourinary pathologist at the MUHC.

LIST OF ABBREVIATIONS

Abs: antibodies
ADT: androgen deprivation therapy
AR: androgen receptor
ARE: androgen response element
BCR: biochemical recurrence
BPH: benign prostatic hyperplasia
ChIP-seq: chromatin immunoprecipitation sequencing
CI: confidence interval
CRPC: castration resistant prostate cancer
CTD: C-terminal domain
DBD: DNA binding domain
EGF: epidermal growth factor
GS: Gleason score
HR: hazard ratio
HS: H score
ID: immunodetection
IF: immunofluorescence
IGF-1: insulin like growth factor 1
IP: immunoprecipitation
IL-6: interleukin-6
LBD: ligand binding domain
mCRPC: metastatic castration resistant prostate cancer
NE: neuroendocrine
NTD: N-terminal domain
PCa: prostate cancer
PTB: phosphotyrosine-binding domain
PTP: protein tyrosine phosphatase
pV: pervanadate
RP: radical prostatectomy
SH2: Src homology 2 domain
STAT3: signal transducer and activator of transcription 3
TMA: tissue microarray
TF: transcription factor
TK: tyrosine kinase
WL: whole cell lysate

LIST OF FIGURES AND TABLES

CHAPTER 1: Introduction

1. The Prostate

The prostate is an organ the size of a walnut, located at the base of the bladder, around the distal portion of the urethra (Fig. 1). As a part of the male reproductive tract, its primary function is to produce certain components of the semen. More specifically, it produces proteins important for sperm cell function and, consequently, for male fertility. The organ is divided into three histologically and anatomically distinct zones: transitional, central, and peripheral. Prostatitis and prostate cancer (PCa) occur principally in the peripheral zone, whereas benign prostatic hyperplasia (BPH) occurs mostly in the transitional zone [1].

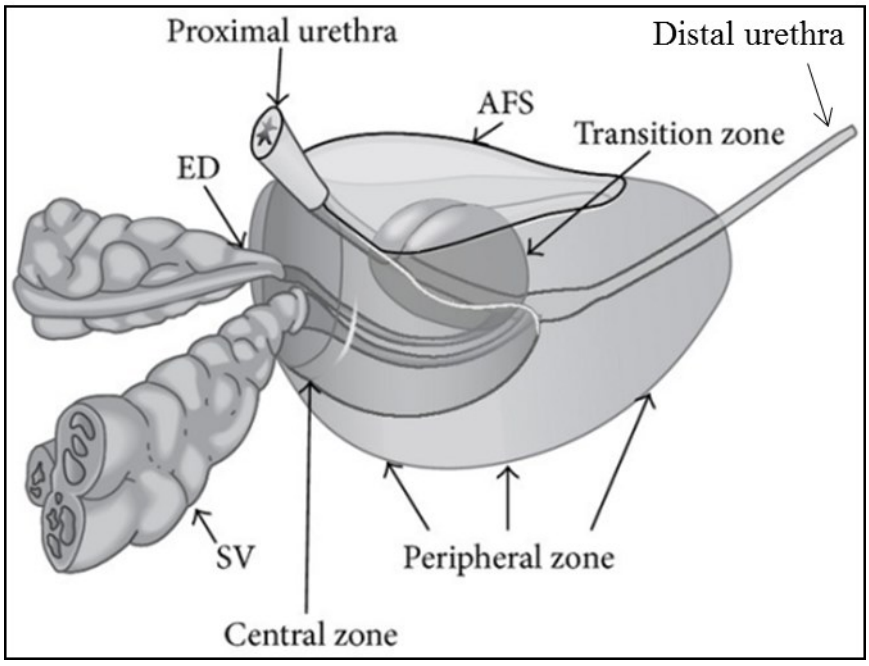

Figure 1: Anatomy of the human prostate. ED: ejaculatory duct. AFS: anterior fibromuscular stroma. SV: seminal vesicles. Adapted from: Bhavsar et Verma, 2014 [2].

The prostate is formed of glandular acini composed of basal and luminal epithelial layers making up secretory ducts, surrounded by a fibromuscular stroma of mesenchymal fibroblastic cells, blood vessels, and inflammatory cells. The interactions between these diverse cells affect

the development and maturation of the prostate [3]. Testosterone is produced in the testes before being liberated into the blood and reaching the prostate and other tissues. The androgen/androgen receptor (AR) axis is involved in regulating prostate homeostasis and function. It has been shown that upon castration of adult male mice, there is apoptosis of the prostatic luminal epithelial cells, leading to prostate involution; the epithelium can be restored by androgen supplementation [3]. It is believed that, in normal conditions, epithelial AR is necessary for homeostasis, controlling epithelial cell differentiation, while stromal AR promotes epithelial and fibroblastic cell growth through the regulation and secretion of different growth factors [3, 4]. Stromal AR is also responsible for prostate development [4]. Although AR signalling has different roles in epithelial and stromal prostate cells, many studies have shown that both epithelial and stromal AR are necessary for proper development, homeostasis, and function of the prostate [3-5].

2. Prostate Cancer

PCa is the most common cancer in Canadian men (1 in 7 men) and the third leading cause of cancer mortality. 21 300 new cases were expected in Canada in 2017, accounting for 21% of all cancers in men. Most of these cases (38%) are diagnosed between the ages of 60-69. However, there has been a gradual decrease in PCa cases since 2007 (5.3%/year; age-standardized). This is thought to be the result of a peak in incidence rates in 2001, due to an increase in PSA (prostate specific antigen) testing [6]. The American and Canadian Urological Associations recently promoted to stop at large screening, but the issue remains a matter of animated debate.

a. Detection and Diagnosis

PCa is detected by blood PSA coupled to digital rectal examination (DRE), followed by prostate biopsies confirming the presence of tumor cells. PSA (also called kallikrein-3) is a known AR target gene and prostate marker liberated in the blood of PCa patients. It is a serine protease normally produced by prostate luminal cells, secreted in the lumen of acini, and expulsed into ducts upon ejaculation as a semen constituent. PSA liquefies seminal fluid by

acting on semenogelin and fibronectin, thus increasing sperm motility [7]. PSA is not found in the blood of young adult males, but may be detected in patients with prostatitis and BPH; its normal concentration range increases with age as well [7-8]. Thus, it is not a specific diagnostic tool for PCa. The results of blood PSA tests must therefore be interpreted with caution along with DRE results. The histopathological examination of biopsy sections confirms the diagnosis.

Tests involving other serum or urine biomarkers have not yet performed better than PSA, and a definitive non-invasive blood or urine test for diagnosis is unavailable at present [6, 7]. PSA screening has played a role in increasing detection of PCa, although its contribution to the decreasing mortality rate remains unclear [6]. However, circulating PSA becomes a key biomarker to closely follow the response of PCa patients to therapies and indicate recurrences.

b. Grading and Staging

PCa grading is done using the Gleason system introduced in 1966, with the last major revision made in 2014 (Fig. 2) [9]. This system defines five patterns based on architectural features of tumors, and the Gleason score (GS) is determined by the sum of the two most common patterns [9].

PCa stage is determined using the tumor/node/metastases (TNM) system [11]. The tumor can be localized to the prostate (T1/T2) or spread to adjacent structures (T3/T4). N (lymph nodes) and M (distant metastases) define their presence (N1; M1) or absence (N0; M0), with sub-classifications for different metastatic sites, such as soft organs or bones [11].

PSA levels, GS, and stage are taken into account when assessing the severity of a case, but different guidelines exist to define low/intermediate/high risk disease [12].

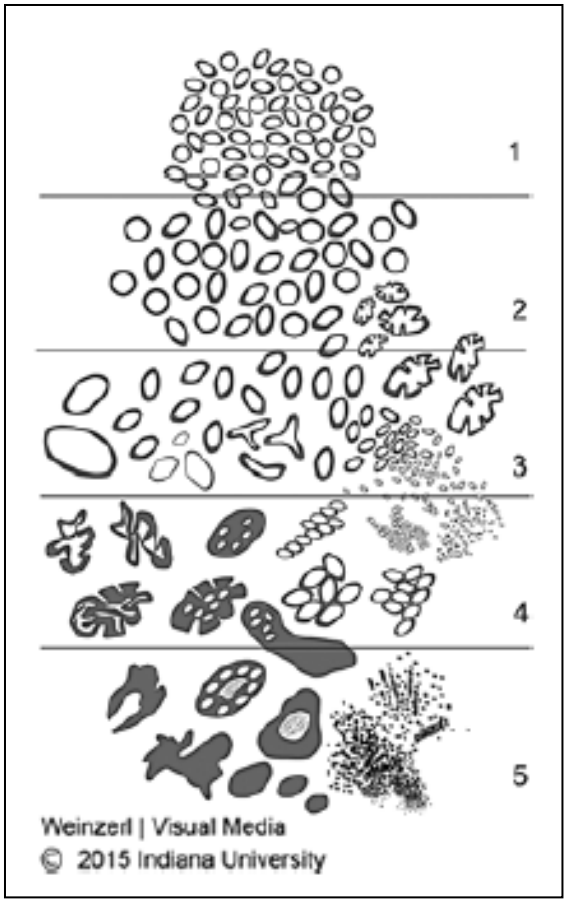

Figure 2: 2014 Modified International Society of Urological Pathology Gleason schematic diagram [10].

Grade Group 1: GS ≤ 6. Individual, discrete, well-formed glands. ***Grade Group 2***: GS 3+4=7. Like group 1, with few poorly-formed/fused/cribriform glands. ***Grade Group 3***: GS 4+3=7. Poorly-formed/fused/cribriform glands, with fewer individual, discrete, well-formed glands. ***Grade Group 4***: GS = 8 (4+4=8; 3+5=8; 5+3=8). Either predominantly poorly-formed/fused/cribriform glands, with lesser component lacking glands or else, predominantly lacking glands, with fewer well-formed glands. ***Grade Group 5***: GS > 8 (4+5=9; 5+4=9; 5+5=10). No glandular formation, or glands with necrosis; few poorly-formed/fused/cribriform glands may be present [10].

c. Treatment

Patients with small, low-grade tumors with low risk of progression are held under active surveillance, which involves periodic testing for rises in PSA levels as well as re-staging of the tumor by re-biopsy [13]. Although more advanced organ-confined disease can be cured by radical prostatectomy (RP) or radiation therapy, 25-35% of patients show recurrence [14]. Recurrent non-organ-confined or locally advanced disease is treated by androgen deprivation therapy (ADT) which consists of surgical or chemical castration in combination with antiandrogens (drugs inhibiting AR action). Chemical castration is achieved using luteinizing hormone/gonadotropin-releasing hormone (LHRH/GnRH) agonists or antagonists, which inhibit testosterone production by Leydig cells in the testes. Serum testosterone levels are reduced to under 0.5 ng/mL, believed to be too low to activate AR signaling in tumor cells. 5α-reductase inhibitors are also used in order to inhibit the conversion of testosterone to dihydrotestosterone (DHT) in prostate cells [14-17]. Biochemical recurrence (BCR) after ADT (i.e. progression despite castrate levels of androgens), termed castration-resistant prostate cancer (CRPC), is inevitable and, hitherto, incurable. The most common sites for PCa metastases to develop are regional lymph nodes, lungs, liver, brain, and bones. Chemotherapy (taxol derivatives e.g. docetaxel, cabazitaxel), and other drugs targeting AR (abiraterone, enzalutamide, bicalutamide) can delay but not prevent further progression of metastatic (m)CRPC [14-18]. Most men with mCRPC die within the next 2 to 3 years.

3. Androgen/Androgen Receptor Axis

AR is a 919 amino acid (aa) (110kDa) protein of the steroid hormone receptor family. Its gene and protein structure are schematized in Figure 3. It comprises of an N-terminal domain (NTD; exon 1), a DNA binding domain (DBD; exons 2-3), a hinge region (HR; exon 4) which contains a NLS (nuclear localisation signal), and a ligand binding domain (LBD; exons 5-8) [19]. The search of a microtubule binding domain (MBD) in AR has shown that there are likely many regions in the DBD, hinge region, and LBD which contribute to AR binding to microtubules [20-21].

The LBD and DBD show significant homology among steroid hormone receptors (e.g. progesterone receptor, glucocorticoid receptor), in both sequence and structure, while the NTD sequence is not conserved [22].

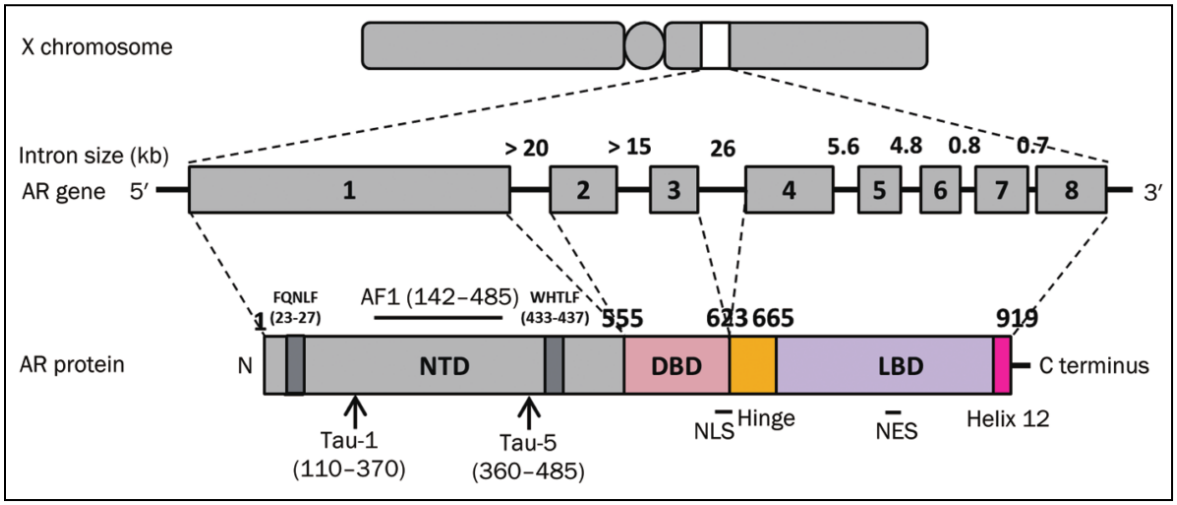

Figure 3: AR gene and protein domain. Adapted from Tan et al., 2015 [19].

The NTD of AR contains the Activation Function 1 domain (AF-1; aa 142-485), while the LBD contains the AF-2 domain (exact residues not defined; C-terminal residues of LDB, including helix 12). These domains are important for transcriptional activation of AR. AF-1 is ligand-independent (constitutively active) and is required for maximal transcriptional activity, whereas AF-2 is ligand-dependent and is important for coregulator binding [19, 23]. Two regions of AF-1 necessary for transcriptional activation have been identified by deletion analysis and point mutations: Tau1 (aa 101–370) and Tau5 (aa 360–485) [24-26].

When there is no stimulation by androgens, AR is inactive in the cytoplasm, bound by HSP90 (heat shock protein 90) (Fig. 4). When testosterone diffuses into prostate cells, it is converted to DHT by 5α-reductase. However, both testosterone and DHT can activate AR, although DHT has a higher affinity and is therefore more biologically active [19]. DHT or testosterone binding to the LBD of AR causes a conformational change which releases AR from HSP90, followed by its translocation to the nucleus. In the nucleus, AR forms a homodimer, enabling binding to androgen response elements (AREs; 6 bp palindromic sequences separated

by 3 bps) on stretches of DNA located in the promoter region of target genes. AR acts as a transcription factor (TF) upon binding to coactivators (or corepressors) and the transcriptional machinery, thus regulating the transcription of androgen mediated AR target genes necessary for homeostasis and function of the prostate [16].

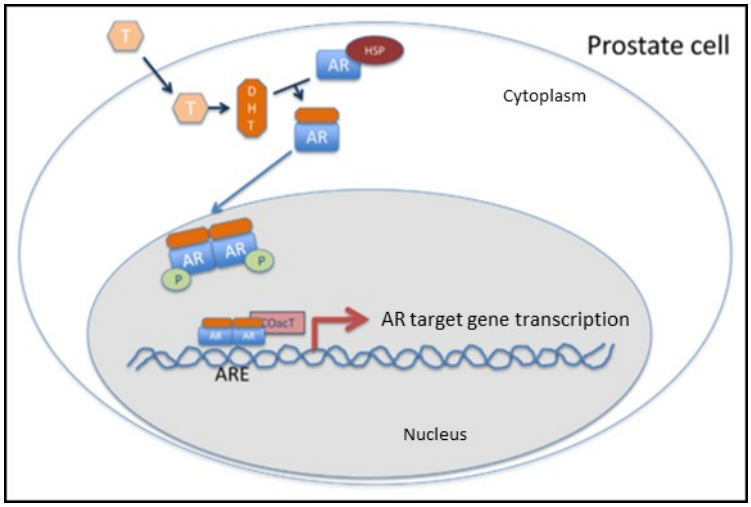

Figure 4: Canonical androgen/AR axis. Adapted from Quero et al., 2015 [15].

The androgenic regulation of the prostate was first shown by the team of Huggins et al., who demonstrated that androgen deprivation by surgical castration causes its regression in dogs [27]. This was followed by surgical castration in PCa patients at advanced stage of disease, significantly improving their symptoms [28]. These findings led to the concept of the androgen-dependency of PCa, which is now often referred to as androgen-sensitivity. Most prostatic tumor cells, especially at an earlier stage of disease (and before hormone treatment), are sensitive to androgen-mediated AR signaling controlling tumor growth and differentiation [3].

4. CRPC and AR Reactivation

AR is the main therapeutic target for advanced disease, but new methods of inhibiting its action need to be developed. Different alterations of AR (overexpression, point mutations leading to promiscuous ligand binding, AR splice variants) or androgen-independent AR

reactivation downstream of signaling pathways upregulated in CRPC often play a role in resistance against currently available treatments and result in progression to the castration-resistant state (Table 1) [29] [19].

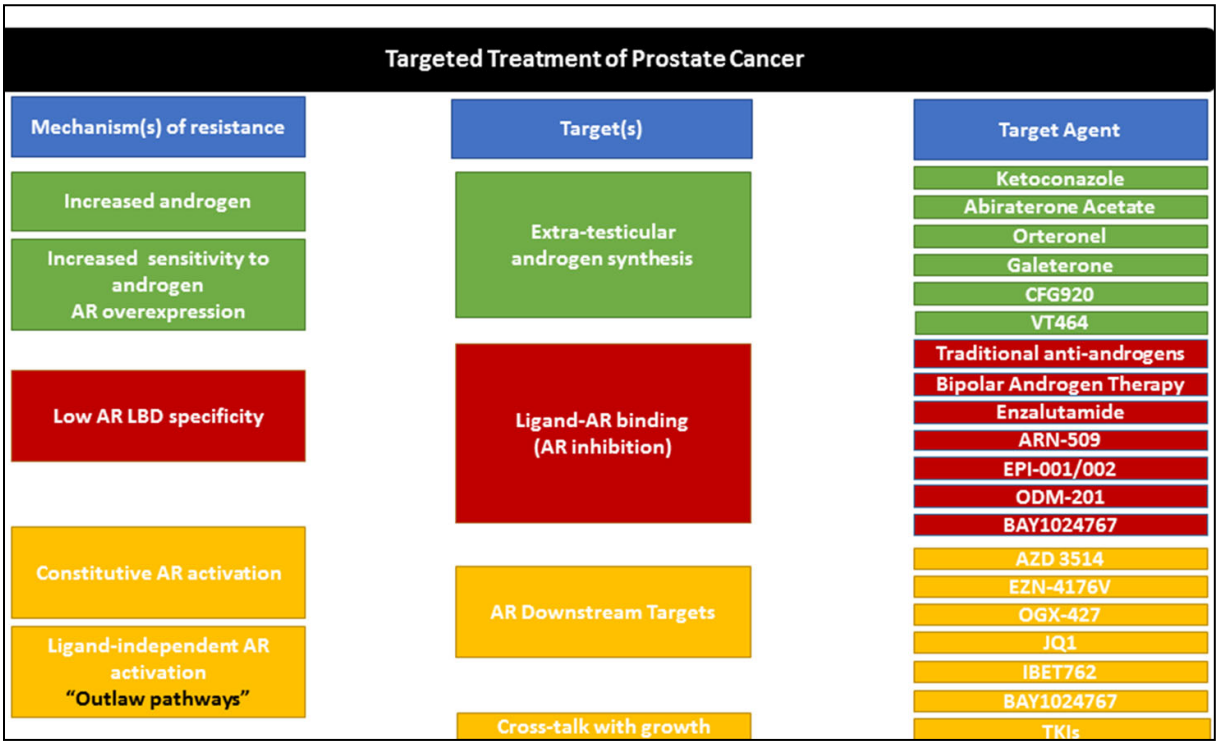

Table 1: Mechanisms of AR dependent resistance and relevant drug targets. Adapted from Pelenakou et al., 2016 [30].

a. AR Variants

One way by which AR is reactivated in CRPC is through the expression of constitutively active AR variants (AR-Vs). Most variants lack part (or all) of the C-terminal domain (Fig. 5), which consists of the LBD (exons 5-8) and the hinge region (HR; exon 4) and contains the NLS. AR-Vs may then explain the resistance to drugs targeting the AR LBD. It has been difficult to study the role or clinical significance of different AR-Vs in PCa because of the unavailability of specific antibodies against them (except for AR-V7). Inconsistent detection methods seem to be responsible for part of the recently reported discrepancies [31].

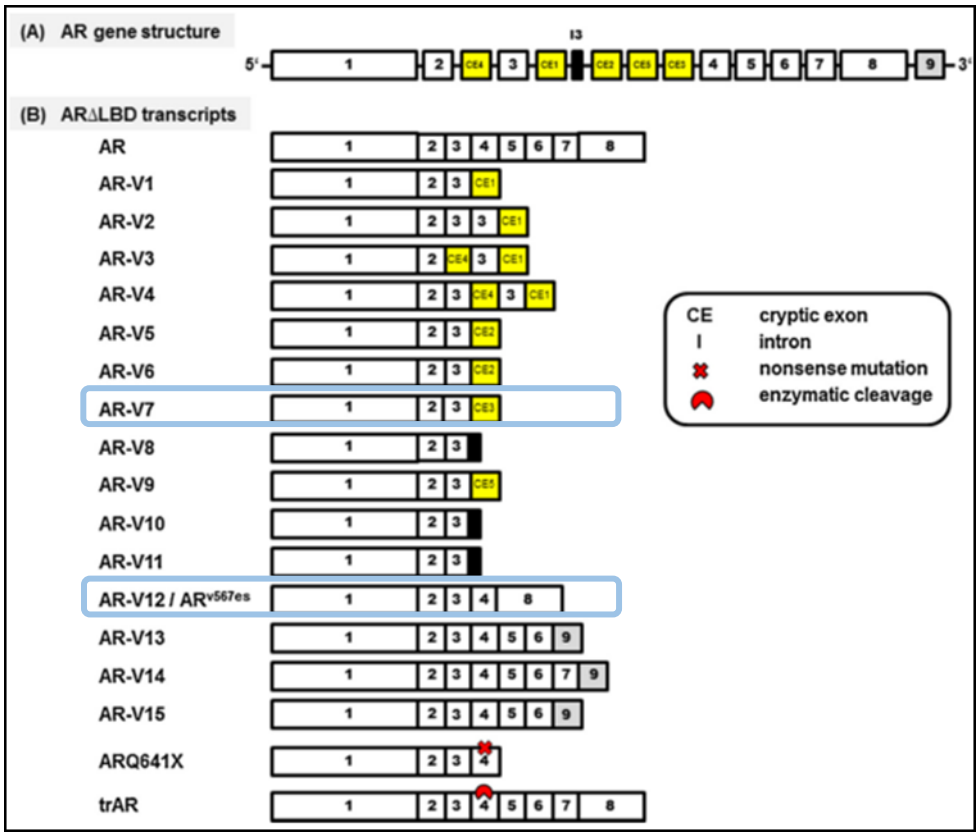

Figure 5: AR and its splice variants. Adapted from Azoitei et al., 2016 [32].

AR-V7 and AR-V12 (also known as ARv567es) are the most commonly studied AR-Vs. AR-V7 consists of the NTD and DBD, while AR-V12 has the NTD, DBD, the hinge region, and part of the LBD. Some of the mechanisms by which AR-Vs mediate gene regulation have been elucidated by showing that AR-V7 and AR-V12 form homo- and heterodimers with each other, as well as with the full-length AR (AR-FL) in PC3 cells transfected with these variants. The aforementioned dimers were thus detected in the absence of androgens, and levels were diminished upon DHT treatment, in which case AR-FL homodimers increased. Interestingly, AR-V7/AR-FL dimers were still detected upon DHT treatment when the LBD of AR-FL was mutated (A596T/S597T) to inhibit its homodimerization. Heterodimer formation can thus compete with AR-FL homodimerization. AR-V7/AR-V7 and AR-V7/AR-FL complexes were primarily nuclear in these experiments, while AR-V7/AR-V12, AR-V12/AR-V12, and AR-V12/AR-FL were detected in both the cytoplasm and nucleus of PCa cells. This suggests that

AR-V7 allows more robust transcriptional activation of genes, while AR-V12 may not be directly linked to transcription [33].

In the CRPC cell line 22RV1 which expresses many forms of AR including AR-V7 and AR-FL, enzalutamide (inhibitor of androgen binding to the AR LBD) had no significant effect on growth in the presence or absence of DHT. AR-FL knock-down had no effect, while knocking-down of AR-V7 rendered their growth androgen-dependent, controlled by AR-FL [34]. Furthermore, gene expression profiling experiments showed similarities in the transcriptional program of AR-Vs, representing a subset of the genes regulated by AR-FL, while others have shown that the AR-V transcriptional program is distinct from that of androgen-independent AR signaling [34, 150]. This explains how AR-V7 can mediate resistance to drugs such as abiraterone (inhibitor of steroid synthesis) or enzalutamide by activating AR signaling independently of androgens and in the presence of antiandrogens [34]. Some AR-Vs can thus replace ligand-activated AR, being active and regulating a similar set of genes.

Comparison of AR-V7 expression by immunohistochemistry (IHC) in primary, metastatic, and CRPC tumors revealed that AR-V7 is most highly expressed in PCa tissue from CRPC patients; it correlates with development of CRPC and cancer specific survival, and can be used as a prognostic factor for CRPC patient, as well as a predictive marker for CRPC development [35]. Antonarakis et al. showed that the presence of AR-V7 mRNA in circulating tumor cells (CTCs) of mCRPC patients predicts resistance to enzalutamide and abiraterone, but not to taxane-derived chemotherapeutics (anti-mitotics; docetaxel and cabazitaxel) [36, 37]. Since AR needs to interact with microtubules to translocate into the nucleus, taxane-derived chemotherapy appears as means to inhibit AR translocation and subsequent transcriptional activity. This also supports the above findings of AR-V7 mediated transcription replacing the androgen/AR axis when activation by ligand binding is inhibited. Nevertheless, AR-V7 mRNA detection in CTCs could be used to determine which therapy might be optimal for a patient.

b. AR Crosstalks with Signaling Pathways

AR reactivation can also result from aberrant activation or alterations of pathways controlling survival and growth of PCa cells. Because of tumor heterogeneity in CRPC and the

diverse growth factors and cytokines present in the tumor microenvironment, progression can occur through additional factors triggering signaling and leading to crosstalks between pathways, including the canonical androgen/AR axis. Some of the factors that can lead to ligand-independent AR activation via the MAPK pathway are interleukin-6 (IL-6), insulin-like growth factor 1 (IGF-1), epithelial growth factor (EGF), and bombesin, a skin frog peptide corresponding to the active sequence of the human gastrin-releasing peptide (GRP) [15, 23, 38, 124].

5. AR Genomic Reprogramming in CRPC

Sharma et al. have shown through gene patterns obtained in an AR chromatin immunoprecipitation sequencing (ChIP-seq) study on nuclear extracts from human prostate tissues from CRPC patients that there is a shift of AR binding from known AREs to DNA motifs associated to STATs, E2Fs, and Myc. This was in contrast with results in cell lines (LNCaP and VCaP) treated or not with R1881 (a synthetic androgen), showing that Forkhead and NF-1 sites were predominant [39, 40]. Furthermore, gene set enrichment analysis (GSEA) showed that Myc and E2F targets were higher in mCRPC compared to primary tumors [41].

Such shifts of AR binding to other DNA motifs might be due to novel interactions between TFs, arising from post-translational modifications (PTMs) of AR or its interactors, as well as aberrant AR activation downstream of upregulated or altered signaling pathways. Indeed, it has been reported that over 100 different proteins, including TFs, coregulators, and DNA repair proteins, form complexes with AR and that these complexes can be altered as the cancer progresses [42].

a. Signal Transducer and Activator of Transcription (STATs)

The STAT family of TFs consists of 7 proteins: STAT1, STAT2, STAT3, STAT4, STAT5a, STAT5b, and STAT6. Downstream of growth factor and cytokine signaling pathways, they mediate cellular proliferation, apoptosis, and differentiation, as well as immunity [43]. In the context of PCa, STAT3 deserves particular attention.

STAT3 is the main TF downstream of the IL-6 (interleukin 6) pathway. It is an 85 kDa (770 aa) TF consisting of an N-terminal coiled-coil domain (CCD), a DNA binding domain (DBD), a SH2 (Src homology 2) domain, and a C-terminal transactivation domain (TAD) which includes the Y705 activation site (Fig. 6). SH2 domains consist of about 100 amino acids involved in non-covalent binding to specific pY-motifs on proteins. The 3 to 7 C-terminal amino acids of the pY-motif are important for recognition by SH2 domains [44].

Figure 6: STAT3 functional domains. CCD (aa 130-320); DBD (aa 320-494); SH2: (aa 580-670); TAD (aa 570-770). Prepared as an adaptation of Zouein et al., 2015 [45].

IL-6 is a pleiotropic cytokine normally involved in regulation of immune reactions, as well as cell growth, proliferation, and differentiation [46]. In the canonical pathway (Fig. 7), IL-6 binds to the α subunit of the IL-6 receptor at the cell surface, leading to the activation of the signaling receptor, gp130 (β subunit), by tyrosine (Y) phosphorylation through the action of Jak1/Jak2 (Janus kinases 1/2). The pY-motif on gp130 then serves as a docking site for the STAT3 SH2 domain. STAT3 is next phosphorylated on Y705 by the Jaks. This activation of STAT3 is necessary for its homodimer formation (reciprocal interaction between pY705 of one STAT3 with the SH2 domain of the other). This allows translocation to the nucleus where the dimers bind to IL-6 response elements (IL-6RE) in the promoters of genes involved in inflammatory responses [47].

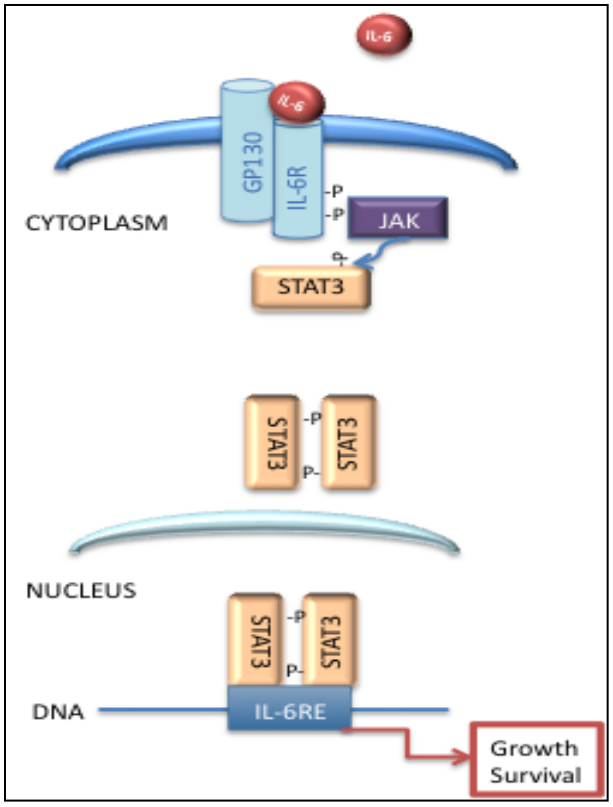

Figure 7: IL-6/STAT3 canonical pathway. Adapted from Rocha et al., 2013 [48].

STAT3 expression (as opposed to its activation) in PCa tissues has not been well studied. One group have found that STAT3 is increased in PCa compared to BPH [49]; another has reported high (3+) STAT3 expression in PCa tissues, and also studied STAT3 activation showing a correlation with tumor stage, grade, and extraprostatic extension [50]. IL-6 is also often increased in PCa and is a serum marker for CRPC [51]. High levels of both pY705 STAT3 (pSTAT3) and IL-6 correlate with CRPC and poor outcome [52]. *In vitro*, PCa cell lines express STAT3 and pSTAT3; IL-6 is a paracrine growth factor for LNCaP cells, but autocrine for PC3 and DU145 [53]. Furthermore, inhibition of STAT3 signaling in DU145 cells induces apoptosis [54].

The IL-6/STAT3 pathway leads to activation of genes involved in prostate carcinogenesis, PCa cell growth, migration, as well as neuroendocrine (NE) differentiation and

progression to CRPC [46]. It is involved in resistance to enzalutamide and radiation. IL-6 has also been linked to AR transcriptional activation, for which pSTAT3 is required [55-57].

b. c-Myc

c-Myc is a 48kDa member of the basic helix-loop-helix-leucine zipper (bHLHZ) family of TFs. It is a proto-oncogene overexpressed in most human tumors due to genomic amplification, including PCa [58]. It is involved in both the initiation and progression of many cancers.

The canonical TF partner of c-Myc is MAX (Myc-associated protein X) [59]. *Myc* transcription is regulated downstream of various growth-promoting signaling pathways, such as WNT, TGF-β (transforming growth factor β), and ERK/MAPK (extracellular signal-regulated kinase/mitogen-activated protein kinase) (Fig. 8) [60-63]. In normal cells, c-Myc controls cell growth, senescence, and apoptosis, while in malignant cells it promotes cell growth and angiogenesis, and allows cancer cells to bypass senescence and apoptosis [58]. Activation of c-Myc also leads to genomic instability due to DNA damage caused by replication stress [64, 65].

In PCa, copy number gain of 8q, which includes the *Myc* gene locus, is one of the most common copy number alterations, with more frequent amplification in metastases and CRPC [66-68]. Genomic gain in primary tumors is a predictor of BCR [67]. Conversely, *Myc* sequence mutations are not common [66].

Myc mRNA expression is significantly higher in tumors vs benign tissues and is an independent predictor of BCR [69]. c-Myc protein nuclear staining is strongly positive in PIN and PCa compared to the matched normal epithelium [70]. Increase in nuclear c-Myc correlates with tumor stage, presence of metastases, and two year overall survival [71]. This shows that nuclear c-Myc overexpression is involved in both PCa initiation and progression [70, 71]. A positive correlation between c-Myc protein expression in PCa and the presence of extraprostatic extension and high pathologic stage has also been shown [72].

Myc transcription is directly regulated by AR in a ligand-independent manner in PCa, and their mRNA levels correlate with each other in soft tissue metastases of CRPC patients, as shown

by microarray analysis [73]. The suppression of either c-Myc or AR inhibits cell growth in the absence of ligand, while c-Myc overexpression negates the effects of AR suppression [73]. On the other hand, R1881 treatment of AR-dependent PCa cell lines reduces c-Myc mRNA and protein levels [74]. Androgen-independent AR activation of c-Myc expression thus promotes growth of androgen-independent PCa cells.

Targeting c-Myc has led to the development of drugs interfering with c-Myc action or expression through different mechanisms: upstream inhibition (activation, stabilization, degradation), inhibition of MAX interaction, antisense oligodeoxynucleotides or miRNAs to decrease c-Myc levels [75, 76]. Many of these drugs have entered clinical trials, but none have yet been approved for clinical use [77]. Although c-Myc is potentially a major target for treating PCa and many other cancers, it remains difficult to target as a TF.

N-Myc is another interesting member of this TF family. It drives NE differentiation of PCa, in which NE markers are expressed, while AR and PSA are not [78-82].

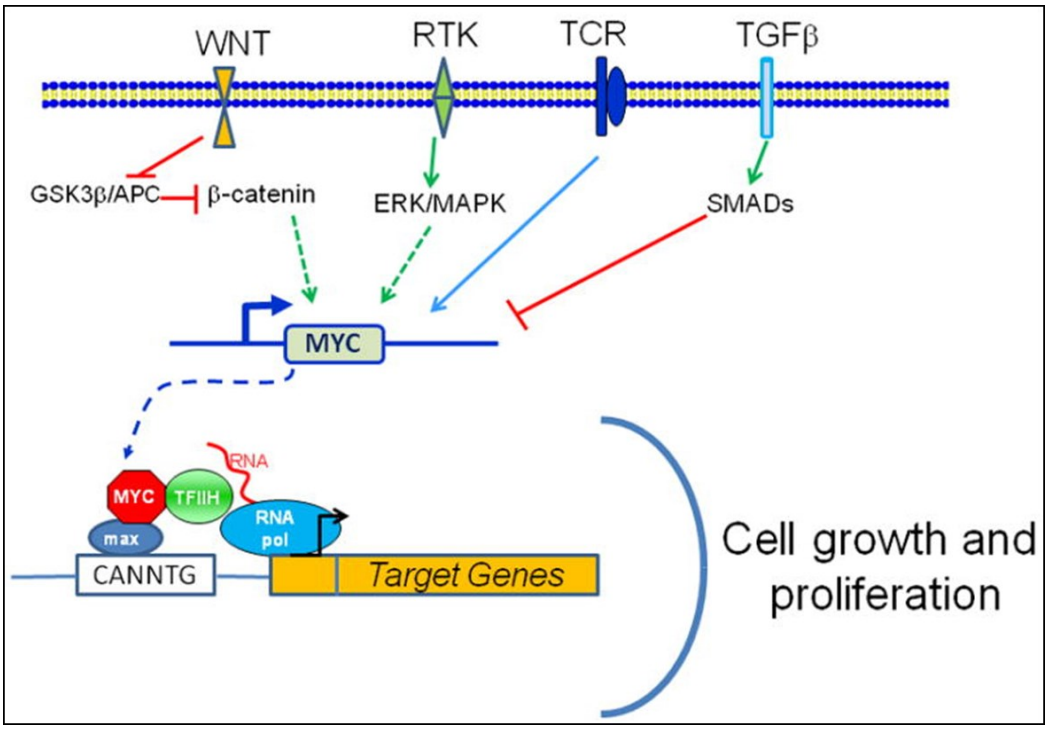

Figure 8: Regulation of Myc transcription downstream of various signaling pathways. *Myc* expression is positively regulated downstream of WNT, ERK/MAPK,

and TCR, and negatively regulated downstream of TGF-β. Adapted from Dang et al, 2012 [60].

c. E2F1

The E2F family of TFs (E2F1-E2F8) is involved in DNA synthesis and cell cycle regulation, acting on development, apoptosis, and cell proliferation. This family of TFs is divided into two groups: activators (E2Fs 1-3) and suppressors (E2Fs 4-8).

E2F1 is a 47kDa transcriptional activator of genes involved in checkpoint control (G1/S), DNA synthesis and apoptosis, as well as in cell differentiation. Its implication in the cell cycle is illustrated in Figure 9, along with its partners. E2F1 plays many different, often opposing roles in various cancers, having both pro-survival and proapoptotic effects. Nevertheless, its implication depends on an increase in its expression, promoting invasion and metastases. It has an N-terminal DNA binding domain (DBD), followed by a homo- and hetero-dimerization domain (important for binding to its TF partner: DP1), and a C-terminal transactivation domain (TAD) [83].

E2F1 expression is low in benign or localized PCa of hormone-naïve patients, but shows increased intensity in metastatic tumors of CRPC patients [87]. Its expression correlates with GS, pathological stage, and early BCR after surgery [88, 89].

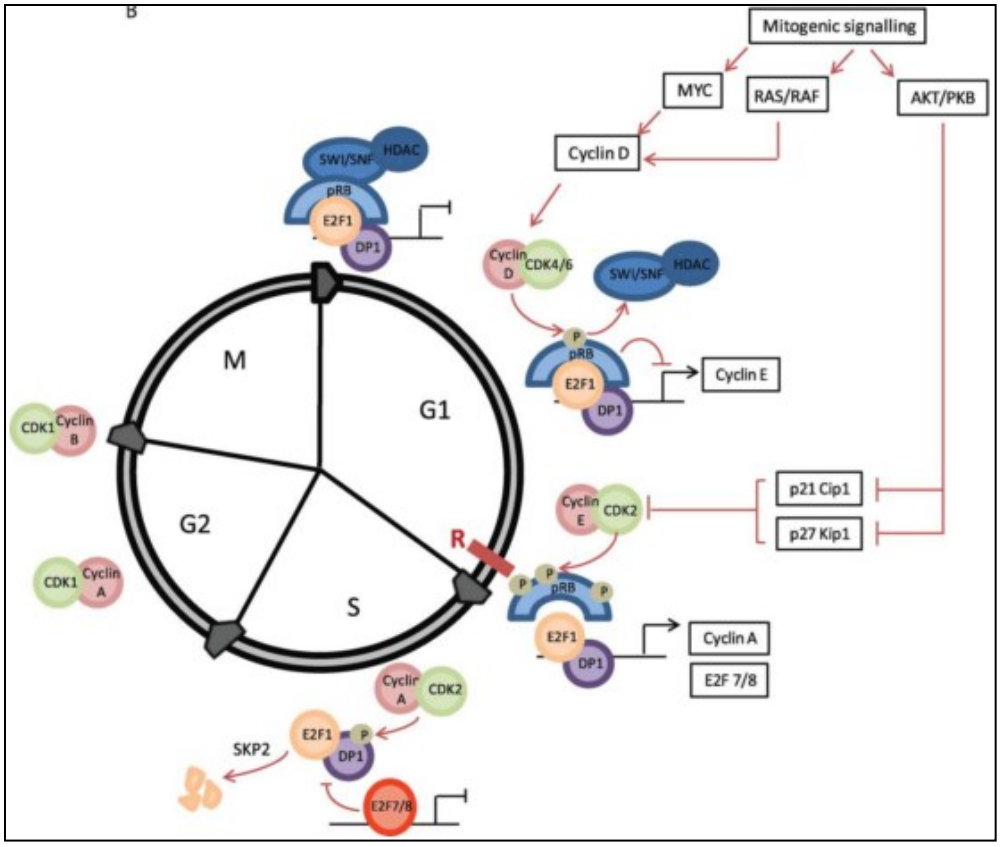

Figure 9: Regulation of E2F1 transcriptional activity. Adapted from Roworth et al, 2015 [90]

In various PCa cell lines, E2F1 has been shown to enhance cell cycle progression, migration, and invasion, as well as epithelial to mesenchymal transition (EMT) and tumor growth in xenograft models [89, 91]. E2F1 overexpression in androgen-sensitive LNCaP cells was reported to deregulate growth, prevent differentiation, and enhance apoptosis [92]. On the other hand, overexpression of E2F1 sensitizes androgen-sensitive and insensitive cell lines to radiation by increasing apoptosis, as shown in cell lines and in tumor xenografts [93, 94].

Through whole exome sequencing and RNA transcript profiling, it has been demonstrated that there is an inverse correlation between AR activity vs E2F1 expression and cell cycle progression in primary and metastatic tumors of CRPC patients, looking at 21 known AR-regulated genes [95]. E2F1 has also been shown to inhibit AR mRNA transcription and its androgen-dependent transcriptional activity in LNCaP cells [87, 96].

Certain genes involved in tumor development have been found to have binding sites for both AR and E2F1. Their transcription is dependent on the expression of AR and E2F1, as well as on exposure to androgens. A physical interaction between E2F1 and AR was also detected, but the nature of the complex formed (direct vs indirect; involvement of coactivators) was not established [97]. PEG10, a protein involved in placental development but also expressed in NE PCa, is differentially regulated at the transcript level by both AR upon R1881 stimulation (negatively) and E2F1 (positively) [98].

E2F3 is also an E2F family TF implicated in PCa. It is known to be involved in PCa development and cellular proliferation [99, 100]. Its overexpression has been found predictive of clinical outcome, and its transcript levels has also been studied as a potential PCa biomarker in blood [101, 102]. E2F3 activity has not been linked to AR.

6. Protein Tyrosine Kinases and Tyrosine Phosphorylation in CRPC

Protein Y-phosphorylation, controlled by the balance between the action of protein tyrosine kinases (TKs) and protein tyrosine phosphatases (PTPs), plays a major role in most cytokine, growth factor, and NE product mediated signalling pathways. If this balance is modified, it can lead to cancer initiation or progression. For instance, this may occur through activating mutations or overexpression of TKs, or through complete or partial loss of expression or inactivating mutations in PTPs.

Amplifications or mutations of TK genes are rare in PCa. Nonetheless, CRPC cases show an increase in Y-phosphorylation, with an average intensity more than twice as high as compared to benign prostate or hormone naïve PCa cases. This increase of Y-phosphorylation is observed in 50% of CRPC cases [103].

Inhibitors of many TKs found to be involved in mCRPC, such as EGFR, VEGFR, PDGFR, Src, and c-Met, have gone to clinical trials, although none have shown promising results [144]. This is partly because TK inhibitors are likely to work on a subset of patients according to their specific molecular characteristics, while clinical trials were carried out without necessarily taking into consideration which patients would be more likely to benefit from these

treatments. Tumor cell heterogeneity may also enter into play. Many other TKs have also been found to be activated in metastatic tumors from CRPC patients, such as Fak, TYK2, and Jak2, as well as the PTPs PTPN6 and PTPN11 [145].

7. Previous Work Done in the Host Lab:

a. Search for TKs in PCa

The host lab found that there is enhanced Y-phosphorylation and TK activity in dog prostate basal epithelial cell hyperplasia and metaplasia, as well as in extracts from human PCa tissues, but not in benign prostates [104, 105]. This was also observed when immature canine prostate basal cells were cultured in primary monolayers, whereas no (or minimal) activation was observed in normal prostate or in freshly isolated epithelial cells [106]. In order to identify TKs that might be important in androgen-independent prostate growth in the dog and in human PCa, a *cDNA* expression library was produced from dividing androgen-insensitive dog prostate cells, which was then expressed in bacteria and probed for expressed pY-proteins to identify active TKs. Among the several TKs identified, the most prominent was Fer (Fps/Fes Related) TK, with high homology to its human counterpart [107].

b. Fer Tyrosine Kinase in PCa

Fer is a 94 kDa (816 amino acids) non-receptor TK of the Fes/Fps family. It consists of (Fig. 10) an N-terminal F-BAR/FX domain known to allow protein-protein interactions, including Fer oligomerization, and phospholipid binding at the membrane [108]. It also contains a SH2 domain, a protein tyrosine kinase (PTK) domain containing its activation site, (Y714), and a NLS.

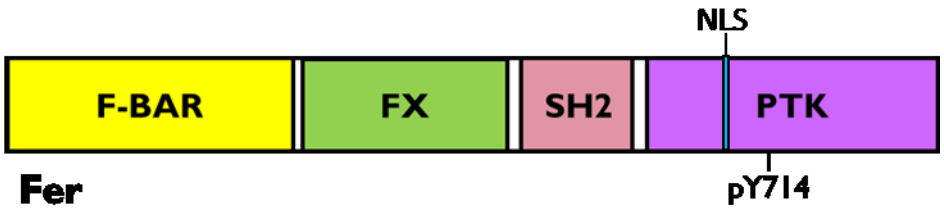

Figure 10: Fer functional domains. F-BAR: Fes/CIP4 homology-Bin/Amphiphysin/Rvs domain (aa 1-259); FX: F-BAR extension (aa 270-445); SH2 (aa 460-550); PTK (aa 563-816); NLS (aa 650-659). Prepared as an adaptation of Liu et al., 2015 and Greer et al., 2002 [108, 109].

The exact function of Fer is unclear, although it is known to act downstream of the epidermal growth factor receptor (EGFR) and platelet-derived growth factor receptor (PDGFR) and is involved in cell adhesion, migration, and chemotaxis [110-112]. It is also involved in the reorganization of the actin cytoskeleton through interactions with cortactin and p120Cas, and in regulating cell-cell adhesion through interactions with β-catenin [107]. The host lab reported that these known Fer interactions in fibroblasts do not specifically apply in the human PC3 cells known as an aggressive androgen-independent and AR-negative (-) PCa cell line with high metastatic potential [107].

Furthermore, the host lab found that Fer is overexpressed in PCa vs normal or BPH tissues, and that it is also expressed in different PCa cell lines. Fer knock down in PC3 cells resulted in a reduction of growth rate and colony formation in soft agar in cells expressing low levels of Fer. Despite several attempts, no Fer null clones were obtained. These findings supporting a role of Fer in PCa cell survival and proliferation suggested that it may represent a novel biomarker and potential drug target for this disease [107].

While the host lab searched for a pathway in which Fer might be involved in PCa, a paper was published showing that co-expression of Fer and STAT3 in COS cells led to activation of STAT3 by phosphorylation on Y705 [113]. Since STAT3 is the canonical TF downstream of IL-6, this pathway became the focus of a PhD thesis (Zoubeidi A).

c. Fer and STAT3 in the IL-6 Pathway (AR- Model)

Zoubeidi et al. reported that Fer is required for IL-6 signaling through STAT3 in PC3 cells. Short term exposure to IL-6 leads to rapid gp130 and Fer Y-phosphorylation, and complex formation between Fer and gp130. Fer then directly phosphorylates STAT3 on Y705 and binds to this pY-motif through its SH2 domain, as validated by *in vitro* kinase assays with recombinant Fer and pull down experiments with the Fer-SH2 domain. Fer and pSTAT3 then colocalize to the nucleus [114]. Fer downregulation in PC3 cells inhibits IL-6 mediated PC3 cell growth, as well as STAT3 activation, nuclear translocation, and transcriptional activity. Conversely, Fer overexpression leads to IL-6 enhanced growth via increased levels of pSTAT3 and Fer/pSTAT3 nuclear complexes. Both Fer and pSTAT3 show nuclear and cytoplasmic expression in PCa tissues compared to benign or normal prostate, with highest nuclear levels in more aggressive cases [114]. Collectively, these findings on the role of Fer in IL-6 mediated androgen-independent PCa cell growth in AR negative cells suggest that in tumors, this mechanism may allow the selection of subsets of AR negative cells to grow under ADT.

d. Fer and AR in the IL-6 Pathway (AR+ Model)

IL-6 is known to drive AR to the PSA gene in a process requiring pSTAT3 [115]. LNCaP cells made to overexpress IL-6 or constitutively active STAT3 show resistance to enzalutamide treatment, compared to parental LNCaP cells. Overexpression of IL-6 also enhances the transcriptional activity of both STAT3 and AR. Inhibition of both pathways might therefore help to avoid resistance mechanisms against certain antiandrogens, and control growth of AR- PCa cells (issued from such a trans-differentiation process) [56].

Because Fer is necessary for STAT3 activation, the host lab next investigated the relationship between Fer, STAT3, and AR, and the role of Fer in IL-6 driven AR transactivation in the AR+ and androgen-sensitive LNCaP model.

First, they showed that in LNCaP cells, Fer activates STAT3 and binds to its pY705 motif via its SH2 domain, as seen in AR- cells. Next, they showed that Fer also phosphorylates AR on Y223 (part of Tau1 domain of AF-1 important for transcriptional activation) and binds to this

pY-motif via its SH2 domain. This was demonstrated first by immunoprecipitation (IP) experiments, then by *in vitro* kinase and binding assays in the presence of short AR phosphor-peptides for different sites as competitors for Fer, as well as in pull-down assays using the Fer-SH2 domain.

Fer knockdown inhibited IL-6 mediated cell growth, while also decreasing mRNA and protein levels of PSA. AR, pSTAT3, and Fer co-localize to the nucleus in IL-6 treated LNCaP cells, as well as in human PCa tissues from CRPC patients. Fer therefore leads to, and is necessary for, AR transcriptional activation downstream of the IL-6/STAT3 pathway [116]. Altogether, these findings support the involvement of Fer in androgen-insensitive progression of CRPC due to its role in enhancing and integrating the IL-6 signal between the AR axis and pSTAT3 pathway, thereby allowing AR+ cell adaptation to treatment.

e. The Role of Fer in Androgen Activation of AR

Androgens can be present at low levels in the tumor microenvironment even after androgen deprivation, as they can be produced intratumorally [117]. Since Fer plays a key role in IL-6 mediated STAT3/AR crosstalks, its role in the androgen/AR pathway was studied in LNCaP cells exposed to R1881.

Upon R1881 exposure, Fer was found to phosphorylate AR on Y223 and bind this motif via its SH2 domain, as it does upon IL-6 exposure. Loss of Fer abolishes AR Y223 phosphorylation and reduces R1881-mediated cell growth and PSA expression. Finally, mutation of the Y223 site of AR led to a decrease in transcription of known AR target genes, such as PSA. Therefore, AR Y223 phosphorylation enhances AR transcriptional activity in both IL-6 and R1881 treated cells. On the other hand, androgens did not induce STAT3 phosphorylation, despite Fer activation [48]. Altogether these novel findings demonstrate that Fer is a key player in aberrant IL-6 and R1881 pathways turned on in metastatic PCa cells and involving two key TFs, AR and STAT3.

HYPOTHESIS AND OBJECTIVES

Previous reports by the host lab revealed IL-6 mediated Fer-dependent AR and STAT3 activation and co-localization in the nucleus of both primary tumor cells in prostate tissues from CRPC patients and PCa cell lines. This leads to IL-6 induced crosstalks between two key pathways known to be involved in CRPC.

As mentioned, AR ChIP-seq data on human PCa tissues from CRPC patients revealed a reorientation of AR DNA binding from known AREs to motifs associated with STATs, Myc, and E2Fs.

Accordingly, we propose that AR may form activated complexes with this set of TFs. More specifically, activation of AR by TKs like Fer would lead to AR interactions with STAT3, c-Myc, and E2F1 in the nucleus, allowing an integration of signals emanating from different upregulated pathways in advanced PCa.

Objectives were to:

1) Further explore AR Y223 phosphorylation and its interaction with STAT3, including full-length AR and its AR-V7 variant;

2) Determine whether AR forms complexes with c-Myc and E2F1;

3) Investigate the Y-phosphorylation of c-Myc and E2F1;

4) Ascertain the clinical significance of STAT3 and c-Myc expression in human PCa.

CHAPTER 2: Materials and Methods

1. PCa Cell Lines and Cell Culture

LNCaP and PC3 human PCa cell lines were purchased from American Type Culture Collection. 22RV1 cells were generously provided by Dr. M. Tremblay (Goodman Cancer Center, McGill University, Montreal, Canada). LNCaP cells (AR positive) are derived from human metastatic prostate carcinoma to the lymph nodes. PC3 cells (AR negative) are derived from human metastatic prostate adenocarcinoma to the bone. 22RV1 cells (AR and AR-V7 positive) are derived from the parental human prostate carcinoma cells line, CWR22 (androgen dependent) following serial propagation in mice after castration-induced regression and relapse. Cells were cultured in RPMI 1640 supplemented with 10% fetal bovine serum (FBS) and 1% penicillin-streptomycin (Wisent, Inc.).

For all experiments, cells were cultured to 70-80% confluence and starved in serum-free phenol red-free media for 24 hours before any of the subsequent 90 minute exposures: 100 ng/mL IL-6 (Peprotech, Inc.), 10 nM R1881 (generously provided by Dr. V. Giguère (Goodman Cancer Center, McGill University, Montreal, Canada)), 10% FBS (Wisent, Inc.), or 100 μM pervanadate (pV). pV was freshly prepared prior to use by mixing equimolar concentrations of sodium orthovanadate (New England Biolabs, Inc.) and hydrogen peroxide, diluting to 10 mM in phosphate buffered saline (PBS), and incubating at room temperature for 10 minutes.

2. Antibodies (Abs)

The following commercial Abs were used: STAT3 (#124H6, Cell Signaling, Inc.), pSTAT3 (#9145, Cell Signaling, Inc.), c-Myc (#9402, Cell Signaling, Inc.), c-Myc (for IHC; ab32072, Abcam, Inc.), E2F1 (#3742, Cell Signaling, Inc.), AR N-terminal (Clone 411, Santa Cruz, Inc.), AR-V7 (ab198394, Abcam, Inc.), pY (#9417, Cell Signaling, Inc.), and HA (#2367, Cell Signaling, Inc.).

Fer-SH2 Abs had been produced in the host lab as previously reported [114]. To produce pY223AR and pY714Fer Abs, 17 amino acid (aa) peptides from the AR and Fer sequences were coupled to Keyhole Limpet Hemocyanin (KLH) (Sheldon Biotech Center) and used as antigens (2mg of peptide) injected subcutaneously into rabbits, followed by boosts at two week intervals. Antiserum reactivity was monitored by ELISA using the antigenic peptides and was also ascertained with uncoupled smaller p-peptides (6aa) until the titer reached over 1 million. The antiserum was aliquoted and stored at -80°C until needed. Abs were purified first to obtain immunoglobulins (IgGs) using protein-A Sepharose beads, and next by affinity using short 6-7 aa long pY223AR and pY714Fer peptides coupled to Sepharose beads via cyanogen bromide. Their specificities for the pY223AR and pY714Fer proteins was demonstrated by in vitro kinase assays using the recombinant human Fer catalytic domain and human recombinant proteins, as previously reported for STAT3 [114] and AR [116].

Of note, the AR (N-terminal) and pY223AR Abs may detect two bands at ~105 kDa and 110kDa, according to duration of electrophoresis.

3. Constructs For Cell Transfection

Cells were transfected with various plasmids (cDNA) 24hours prior to stimulation, using Polyplus jetPRIME reagent according to the manufacturer's instructions (Polyplus, Inc.).

AR-His, and *ARY223F-His* plasmids were generated as previously reported [114]; *STAT3-HA* was a gift from Dr. A. Koromilas (McGill University, Lady Davis Institute, Montreal, Canada); *408 pSG5L HA E2F1* was a gift from William Sellers (Addgene plasmid # 10736) [118]; and *pCDNA3-HA-HA-humanCMYC* was a gift from Martine Roussel (Addgene plasmid # 74164) [119].

4. Protein Extraction, Immunoprecipitation (IP), and Western Blotting (ID)

After exposure to stimuli, cells were washed with ice-cold PBS containing 1mM sodium orthovanadate for 15 minutes on ice, then lysed in RIPA buffer containing 50 mmol/L Tris–HCl

(pH 7.4), 150 mmol/L NaCl, 1mmol/L EDTA (pH 8), 1% NP40, 0.25% sodium deoxycholate, protease inhibitor cocktail (1 tablet/10mL; Sigma Aldrich, Inc.), and 1mM sodium orthovanadate.

For IP, 750µg proteins were incubated with 3µg Abs (vs control IgG) overnight at 4°C. Samples were then incubated 1 hour at 4°C with Protein G-Sepharose, and immune complexes were collected by centrifugation after washing three times with RIPA buffer. Samples were boiled in Laemmli buffer and resolved by SDS-PAGE (10% gel) alongside 75µg proteins from whole cell lysates (WL).

For ID, proteins were transferred to a nitrocellulose membrane and incubated with primary Abs at 4°C overnight according to manufacturer's recommendations or optimized conditions for each Ab. HRP-conjugated goat anti-mouse or anti-rabbit Abs were used (Life Technologies, Inc.), followed by detection with chemiluminescent HRP antibody detection reagent (Denville Scientific, Inc.).

Band intensities were determined using ImageJ gel analysis tools; the data analysis toolpack on Excel was used for statistical analysis (F-test for variances, followed by the corresponding t-Test). Data were graphed as mean value for n experiments; error bars show standard deviation.

5. Pull-Down Assay (PD)

STAT3-SH2-GST plasmid was a generous gift from Dr. M. Tremblay (Goodman Cancer Center, McGill University, Montreal, Canada). The fusion proteins Fer-SH2-GST and STAT3-SH2-GST were produced, as described previously [114]. For pull-downs, 750 µg proteins from cell lysates were incubated with 10 µg of STAT3-SH2-GST or Fer-SH2-GST fusion proteins overnight at 4°C. For competition reactions, 15 µg of AR peptides (ARY223, ARpY223, ARpY534) were added for 5 minutes to reaction mixtures as competitors before the addition of the fusion SH2 domains for PD. Glutathione Sepharose beads were added for one hour at 4°C to recover complexes by centrifugation after washing three times with PBS. Samples solubilized by

boiling in Laemmli buffer were resolved by SDS-PAGE (10% gel) along with 75µg of proteins from WL and submitted to western blotting.

6. *In Vitro* Fer Kinase Assay

Recombinant human Fer kinase catalytic domain (Life Technologies, Inc.) was used in kinase assays with recombinant human c-Myc (ab84132, Abcam, Inc.), E2F1 (ab82207, Abcam, Inc.), and AR (Calbiochem, Inc.). Assays consisted of 50ng enzyme (Fer) and varying concentrations of substrates (AR, c-Myc, and E2F1), up to 100ng, in commercial kinase buffer (Invitrogen, Inc.). DTT (dithiothreitol; Bio Basic Canada, Inc.; 2.5mM final concentration) and ATP (Adenosine triphosphate; Invitrogen, Inc.; 200µM final concentration) were added to start the reaction (total volume 25µL). Controls with enzyme alone or substrate alone were included. After a 30-minute incubation at 30°C, samples were cooled for 10 minutes on ice before adding Laemmli buffer and boiling. Samples were then submitted to SDS-PAGE and western blotting using Abs for pY, pY714Fer, Fer, and the candidate substrates (AR/pY223AR, c-Myc, and E2F1).

7. Immunofluorescence (IF)

For IF, 8000 cells were seeded onto poly-lysine coated 8-well plastic chamber slides and cultured for 24 hours, followed by 24-hour incubation in serum-free phenol red-free media prior to treatment. Cells were then fixed with 3.7% paraformaldehyde for 5 minutes, incubated with 50 mM NH_4Cl for 10 minutes, permeabilized with 0.5% Triton X-100 in PBS for 15 minutes, and blocked with 0.5% BSA in PBS for 1 hour before overnight incubation with primary Abs at 4°C. Anti-rabbit and anti-mouse secondary Abs coupled to either Alexa Fluor 488 or Cy3 were used (Invitrogen, Inc.). Nuclei were stained with DAPI (4',6-diamidino-2-phenylindole).

8. Immunohistochemistry (IHC)

IHC for STAT3 and c-Myc was performed on sections from formalin-fixed and paraffin-embedded PCa blocks (for optimization) and tissue microarrays (TMAs) from Dr. Saad at the Centre Hospitalier de l'Université de Montréal (CHUM). Briefly, sections (4 μm) were rehydrated with alcohol, followed by antigen retrieval in 10mM sodium citrate buffer pH 6.0, permeabilization in 0.025% Triton X-100 for 30 minutes, followed by a 30 minute peroxidase block (EMD Millipore kit used throughout the procedure). Next, sections were incubated in the provided blocking solution for 30 minutes (to reduce non-specific binding of Abs) before overnight incubation with the primary Abs at 4°C. Sections were incubated with biotinylated secondary Abs for 45 minutes, and streptavidin-peroxidase conjugate to amplify the signal. Staining was revealed using N-Histofine DAB (3,3-diaminobenzidine tetrahydrochloride; Cedarlane, Inc.). Hematoxylin was used as a counterstain, and sections were dehydrated and mounted. Slides were scanned using an Aperio Scanscope slide scanner and staining intensity (0, 1+, 2+, 3+) was scored blindly by two examiners (the second reviewing 10% of cores if readings are not different) using the ImageScope software. The H score (HS) [120] for each core was calculated $\{0\times(\%\ 0^{+}) + 1\times(\%\ 1^{+}) + 2\times(\%\ 2^{+}) + 3\times(\%\ 3^{+})\}$ and used for subsequent analysis.

Cutoffs for each marker were determined using the web application Cutoff Finder version 2.1 (http://molpath.charite.de/cutoff/) to determine the most significant values [121]. For cutoffs that are too low or too high, 1st and 3rd quartiles were used respectively, in order to include at least 25% of cases in each group. Statistical analysis was done using the IBM SPSS Statistics software (Kaplan-Meier survival curves, uni/multivariate Cox tests, and ROC curves).

CHAPTER 3: AR Activation by Y223 Phosphorylation

The host lab demonstrated that AR is phosphorylated by Fer on Y223 upon PCa cell (LNCaP) exposure to IL-6 or R1881 [48], allowing its nuclear translocation and transcriptional activation [116]. To further explore the role of pY223AR in these pathways, our lab produced and characterized specific pY223AR Abs. Since Fer activation implies its Y-phosphorylation, pY714Fer Abs were also produced to further investigate its role [122]. These Abs were tested for specificity after affinity purification, using cell lysates, specific phosphor-peptides vs non-phosphorylated peptides, and *in vitro* Fer kinase assays.

1. Characterization of pY223AR and pY714 Abs

The *in vitro* Fer kinase assays were repeated to confirm specificity following the purification of new batches of antiserum. First, kinase assays were carried out using recombinant human AR and recombinant human Fer catalytic domain (Fig. 11A). Anti-pY Abs (*panel 1*) show that the experiment was successful (i.e. AR was Y-phosphorylated by activated Fer). The detection of pYAR by pY223AR Abs (*panel 2*) confirmed that this phosphorylation implies the Y223 motif, while AR (*panel 3*) and Fer (*panel 4*) Abs show bands at their exact molecular weights, confirming the presence of these proteins in each sample. pY223AR Abs detect AR (112kDa) in samples containing both Fer (60kDa) and AR (i.e. when AR is phosphorylated on Y223), but not when Fer is omitted (negative control), while AR is detected in both samples. Fer-SH2 Abs (generated against the SH2 domain of Fer: aa 460-550) also detected the recombinant Fer catalytic domain, because it contains the last 10 amino acids of the SH2 domain (aa 541-882; overlap of aa 541-550).

Kinase assays testing pY714Fer Abs consisted of Fer being incubated in the presence of ATP to show its autophosphorylation, along with a negative control containing Fer but no ATP (Fig. 11B). Fer-SH2 Abs detect the presence of catalytic Fer domain in both samples, while pY714Fer Abs detect activated Fer only in the samples containing ATP. The results confirm that pY223AR and pY714Fer Abs specifically detect the phosphorylated forms of AR (Y223) and Fer (Y714), respectively.

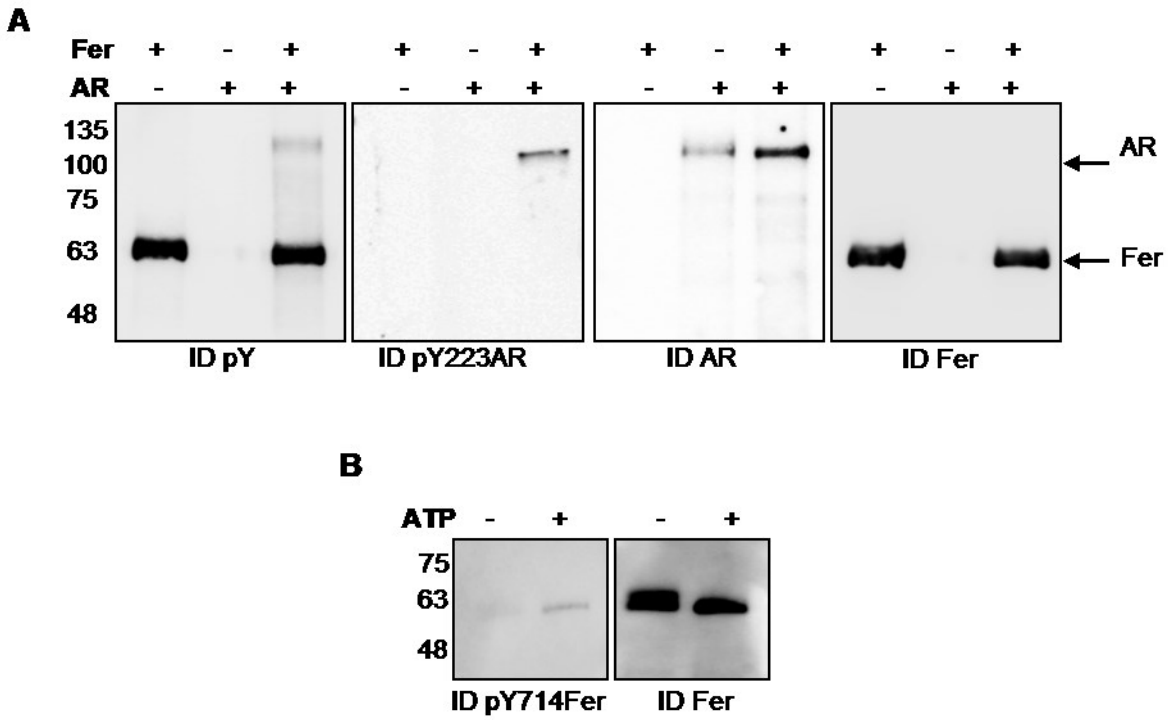

Figure 11: Testing specificity of pY223AR and pY714Fer Abs.

(**A**) Fer catalytic domain was incubated with recombinant AR in the presence of ATP. Controls of Fer alone and AR alone were included. Samples submitted to SDS-PAGE were western blotted with anti-pY, pY223AR, AR, and Fer Abs. (**B**) Fer catalytic domain was incubated with or without ATP, submitted to SDS-PAGE, and western blotted with pY714Fer and Fer Abs.

2. **AR Activation by IL-6 vs R1881 in LNCaP and 22RV1 Cells**

Based on the above findings, the pY223AR and pY714Fer Abs were used as tools for studying Fer and AR activation in human PCa. This was done in cell lines in this project, while their clinical relevance was demonstrated by studies in prostate tumors from patients (Altaylouni, T.; pY223AR in MSC thesis 2018 and pY714Fer, unpublished data).

The pY223AR Abs were used first to determine the levels of AR phosphorylation on Y223 in LNCaP cells exposed to IL-6, R1881, or their combination. The N-terminal AR Abs were used in parallel to detect all forms of AR.

As shown in western blots of AR and pY223AR (detected at 110kDa) (Fig. 12A), IL-6 increases AR Y223 phosphorylation to a higher extent than R1881, while their combination leads to a pY223 band intensity similar to that observed for IL-6 exposure. These findings were reproduced in several experiments (n=4). Experiments were carried out with short term exposure to IL-6, R1881, or IL-6+R1881 to allow the phosphorylation, nuclear translocation, and interactions of transcription factors prior to changes in transcriptional activity. The 90 minute time-point was selected based on IF results showing an increase in Fer/pY714Fer and STAT3/pSTAT3 nuclear accumulation at 90 vs 30 minutes (data not shown). The intensity of each band was quantified using ImageJ and normalized relative to the intensity of the corresponding proteins observed in untreated cells. The increase in AR Y223 phosphorylation upon treatment was significant ($p<0.05$): 2.7-fold by IL-6 or IL-6+R1881 treated cells, and 1.7-fold for R1881 alone.

AR levels seem lowered in the 90 minute IL-6 exposure in LNCaP cells. There have been contradictory reports regrading the IL-6 effect on AR protein levels in LNCaP cells. Some have reported an increase [146, 147], no change [48, 148], or a decrease [149]. The cause of these discrepancies has not been explained, but it is speculated to be dependent on the number of passages the cells have gone through. Time of exposure in minutes vs hours or days may also matter, as well as variable accessibility of the solubilized protein during IP. Nonetheless, the AR band intensity was used to quantify interactions and express the data, whenever applicable.

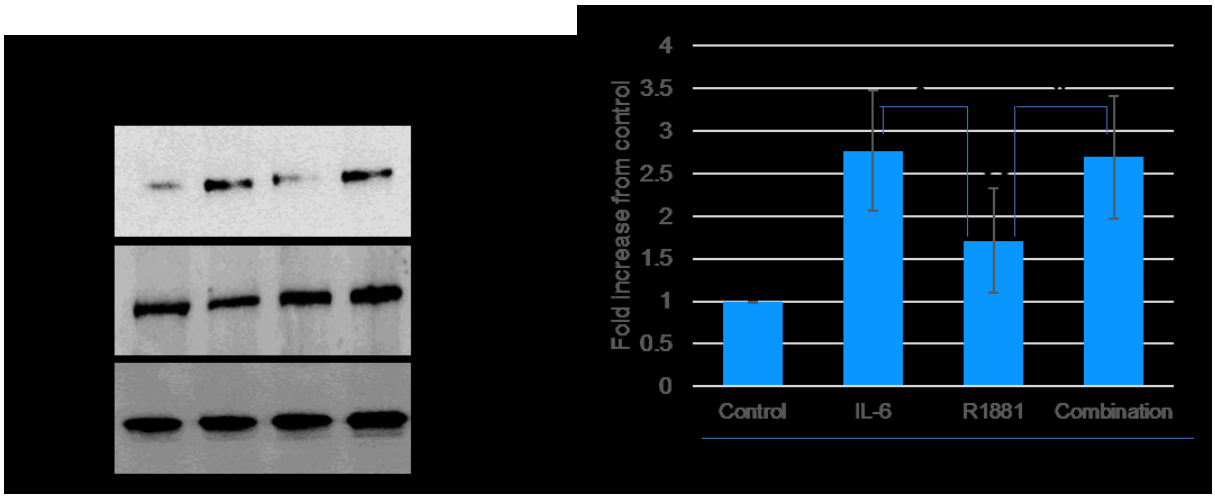

Figure 12: AR activation in LNCaP cells.

Whole lysates of LNCaP cells treated or not with IL-6, R1881, or IL-6+R1881 (90 minutes) were subjected to SDS-PAGE and western blotting. Abs against pY223AR and AR (N-terminal epitope) were used, along with actin as a loading control. Statistical significance ($p<0.05$) between different treatments is denoted by an asterisk, and difference between control vs treatments are denoted by two asterisks. Error bars represent the mean ± standard deviation for each condition (n=4).

Similar experiments were carried out in 22RV1 cells to verify whether full-length AR and AR-V7, an AR variant (75kDa) associated with CRPC, are also phosphorylated on Y223 in the same conditions. The AR N-terminal Abs used can detect most AR variants (including AR-V7), since they contain the AR NTD.

Western blotting of 22RV1 cell lysates (Fig. 13A) with AR Abs revealed a minor and a major band at the molecular weight of full-length AR (110kDa) and AR-V7 (75kDa) respectively, independently of treatments. The pY223AR Abs also revealed both bands in relative proportions similar to bands detected by AR Abs, thereby supporting activation of both the variant and full-length AR proteins.

To determine the levels of pY223AR and pY223AR-V7, the intensities of bands detected by pY223AR Abs were determined and normalized against the levels of AR and AR-V7. Figure

13A shows that AR and AR-V7 are activated even in non-treated 22RV1 cells, and there is no significant difference in pY223AR or pY223AR-V7 levels in any condition tested ($p>0.05$ for all, n=4). Levels of AR-V7 activation by Y223 phosphorylation yielded similar results whether the intensity was normalized against the 75kDa band detected by AR N-terminal Abs or the band detected by AR-V7 Abs (data not shown).

To determine whether constitutive phosphorylation of AR and AR-V7 in 22RV1 cells reflects Fer activation, levels of pY714Fer were determined in these cells, as well as Fer levels. Figure 13B shows that Fer and pY714Fer Abs revealed bands at the 94kDa position expected for Fer. Of note, Fer Abs detect only the 94kDa band in LNCaP cells, whereas in 22RV1 another band is seen in the 65kDa range, as we also observed in PC3 cells (data not shown). This band is of the same molecular weight as a Fer variant described in differentiating adipocytes *in vitro* [123]. Fer activation, as shown by pY714Fer detection, is present in all conditions, including untreated cells.

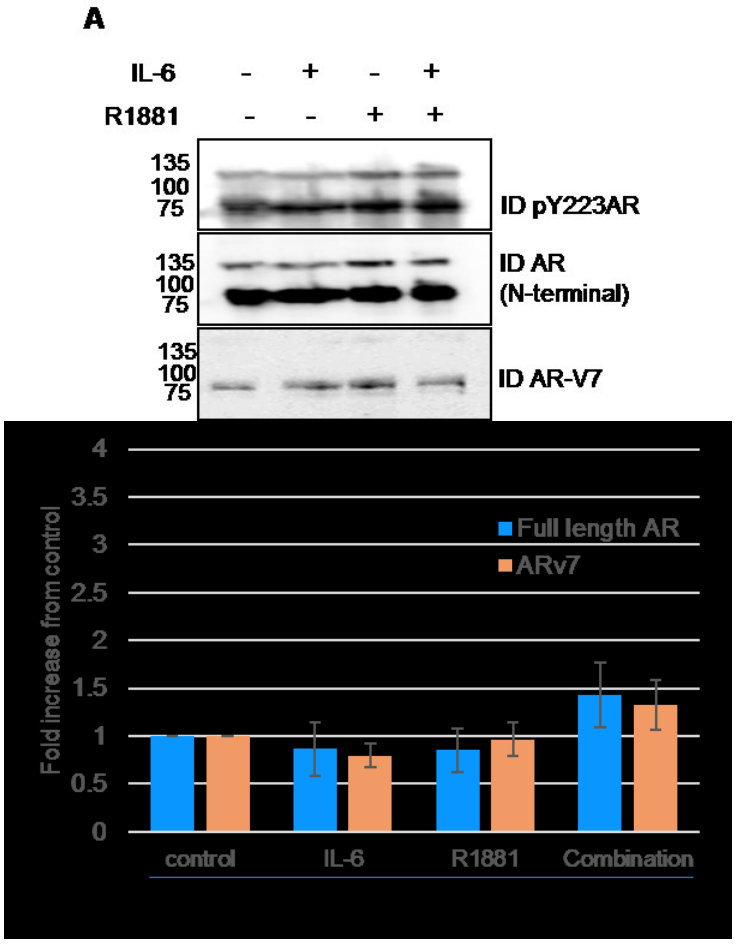

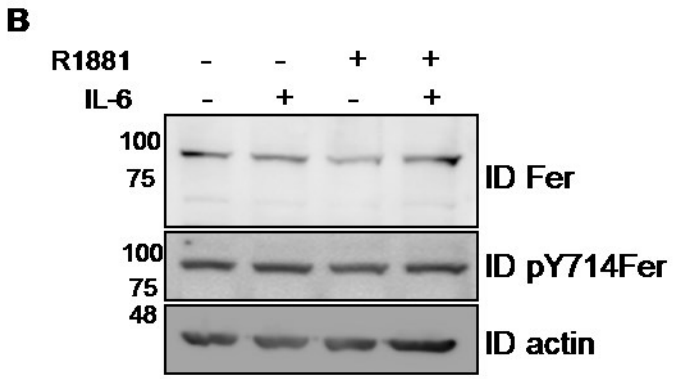

Figure 13: AR and AR-V7 Y223 phosphorylation and Fer activation in 22RV1 cells.

Whole lysates of 22RV1 cells treated or not with IL-6, R1881, or IL-6+R1881 (90 minutes) were subjected to SDS-PAGE and western blotting. Abs against (**A**) pY223AR, AR (N-terminal epitope), and AR-V7 and (**B**) pY714Fer and Fer-SH2 were used, along with actin as a loading control. Statistical significance ($p<0.05$) between different conditions is denoted by an asterisk. Error bars represent the mean ± standard deviation for each condition (**A**: n=4; **B**: n=3).

Thus, in LNCaP cells, Fer and AR are activated upon treatment with IL-6, R1881, or their combination, while in 22RV1 cells pY223AR, pY223AR-V7, and pY714Fer are constitutively phosphorylated and present at same levels, with no effect of IL-6 or R1881 exposure or their combination.

CHAPTER 4: AR Interaction with STAT3

AR has been found to bind to DNA motifs associated to STATs in human PCa tissues from CRPC patients; this was not found in LNCaP cells exposed to androgens [39]. In vitro, IL-6 mediated AR transcriptional activation is dependent on activation of STAT3 [115]. AR was reported to interact with STAT3 via its AF-1 domain, more specifically the aa 234-558 of the protein [124]. Since in LNCaP cells both AR and STAT3 are activated by Fer in the IL-6 pathway, we asked whether the interaction between these TFs may be related to AR phosphorylation and involve a direct interaction mediated by the SH2 domain of STAT3, resulting in changes in AR DNA binding. R1881 was also tested, as it leads to the activation of Fer and AR, but, to our knowledge, its effect on STAT3 phosphorylation has not been reported.

1. Cellular Localization of STAT3 and AR in IL-6 or R1881

First, the activation of STAT3 by Y705 phosphorylation was assessed in IL-6 or R1881 treated LNCaP cells (Fig. 14A). Western blots of STAT3 and pSTAT3 showed its detection at the 88kDa position. STAT3 activation is absent in non-treated cells. STAT3 is phosphorylated upon IL-6 exposure of LNCaP cells as expected. Interestingly, it is not phosphorylated in R1881 treated LNCaP cells, even though Fer is activated and can AR. These findings are in agreement with earlier unpublished data [48].

In parallel, we assessed the distribution of AR and STAT3 (Fig. 14B) and their activation (Fig. 14C) in these cells by IF upon R1881 and IL-6 exposure, knowing that AR, Fer, and pSTAT3 co-localize to the nucleus of IL-6 treated LNCaP cells and tumor cells from PCa tissues of CRPC patients [116]. AR and STAT3 are cytoplasmic in the absence of treatment (Fig. 14B; *left*). Upon R1881 exposure (*middle*), AR translocates to the nucleus, but STAT3 remains cytoplasmic (as it is not activated). In IL-6 (*right*), both AR and STAT3 are primarily nuclear, as expected.

The cellular localization of pY223AR by IF (Fig. 14C; *top*) revealed minimal or low levels in non-treated cells. There is an increase of AR activation in both the cytoplasm and the

nucleus upon R1881 or IL-6 exposure, with higher activation by IL-6. In contrast, pSTAT3 (Fig. 14C; *bottom*) remained non-detectable under R1881 exposure, but was activated and nuclear upon IL-6 exposure. This is in line with results of AR and STAT3 activation (shown by western blotting) and cellular localization, showing that both proteins are activated and nuclear upon IL-6 exposure, while R1881 only activates AR.

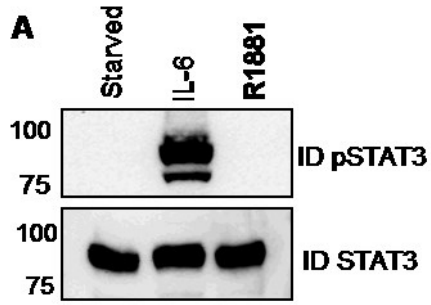

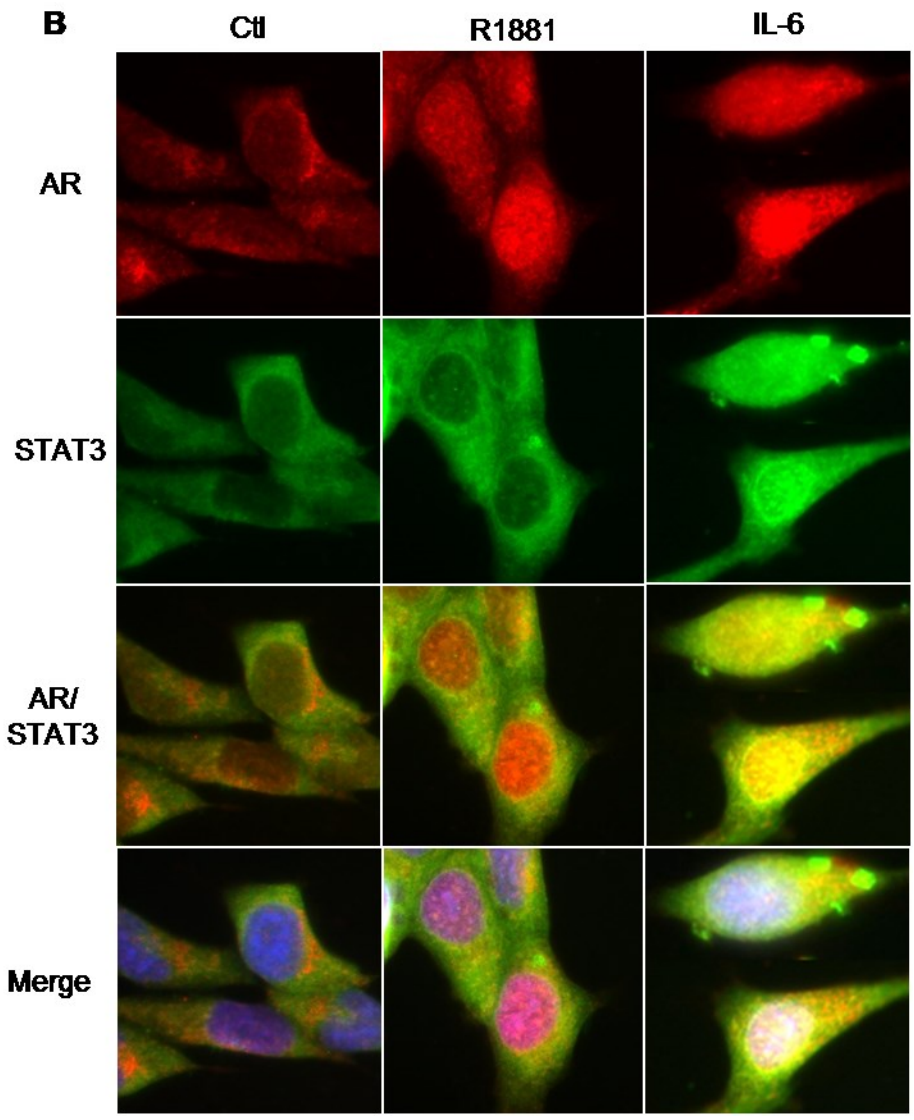
B
Ctl
R1881
IL-6
AR
STAT3
AR/
STAT3
Merge

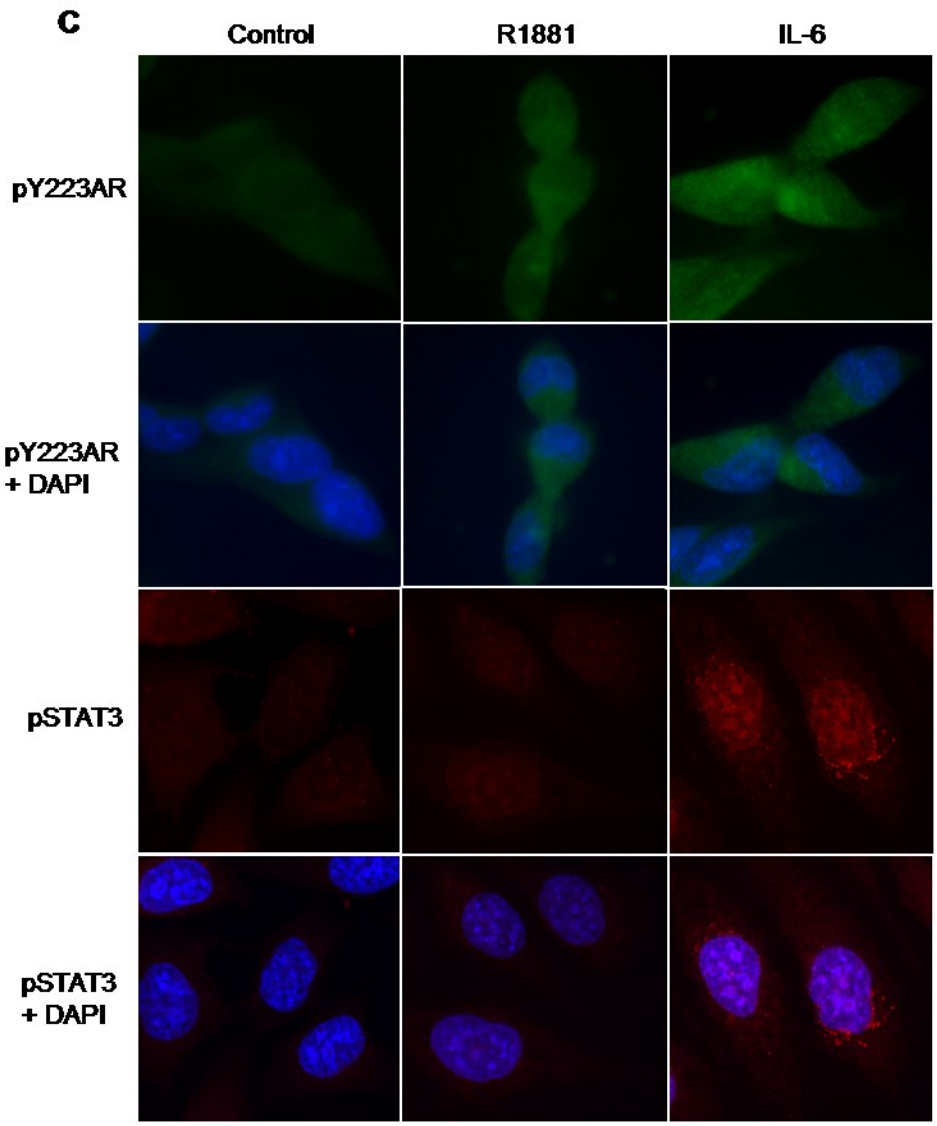

Figure 14: Subcellular localization of AR and STAT3

(A) Lysates of LNCaP cells exposed or not to IL-6 or R1881 (90 minutes) were blotted for pSTAT3 and STAT3. (**B**) IF staining of LNCaP cells exposed or not to IL-6 or R1881 (90 minutes) showing AR (red) and STAT3 (green) with DAPI nuclear stain (blue). Images were merged to show overlap between AR and STAT3, with (*4th row*) or without (*3rd row*) DAPI staining. (**C**) IF staining of LNCaP cells exposed or not to IL-6 or R1881 (90 minutes) showing staining for either pY223AR (green) or pSTAT3 (red) with DAPI nuclear staining (blue).

2. Characterization of AR/STAT3 Interaction in LNCaP Cells

As mentioned, AR ChIP studies on PCa tissues from CRPC patients did not show AR binding to AREs (expected for androgen activation of AR) [39]. We showed above that STAT3 is not activated or nuclear upon R1881 treatment of LNCaP cells, whereas both are activated by Fer and become nuclear under IL-6. Accordingly, we studied the interaction between AR and STAT3 to test the hypothesis that their interaction may be direct and mediated by the STAT3 SH2 domain binding to the pY223 motif of AR.

Pull-down experiments using the STAT3 SH2 domain were carried out on lysates of LNCaP cells exposed or not to IL-6 or R1881. We observed in Figure 15 that pY223AR (at 110kDa) was pulled-down by the STAT3 SH2 domain upon IL-6 or R1881 exposure of cells. pSTAT3 (88kDa) is also pulled down by the STAT3 SH2 domain upon IL-6 exposure, as expected for pSTAT3 homodimers in the canonical IL-6 pathway. STAT3 does not interact with its SH2 domain in R1881 treated cells, where it remains unphosphorylated. Although STAT3 is not activated by R1881, activated AR can physically interact with the STAT3 SH2 domain in cell lysates. However, this would not be possible *in vivo* in cells, since R1881-mediated activated AR is nuclear, while non-activated STAT3 remains in the cytoplasm.

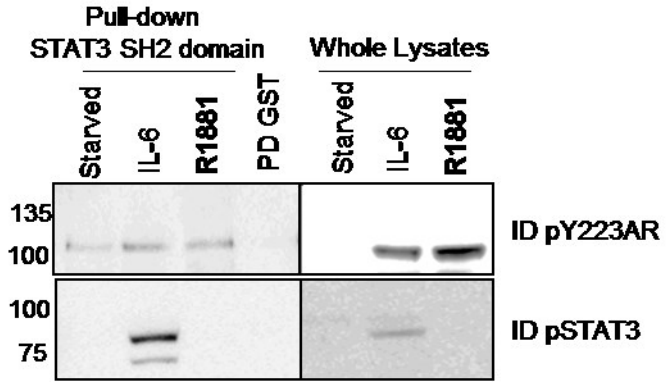

Figure 15: The SH2 domain of STAT3 interacts with pY223AR.

LNCaP cells were treated or not with IL-6 or R1881 (90 minutes). Proteins were pulled down using the STAT3 SH2 domain (pull-down with GST on IL-6 treated samples: negative control). Samples were submitted to SDS-PAGE and western blotted for pY223AR and pSTAT3 (n=3).

In line with these findings, since both IL-6 and R1881 lead to AR Y223 phosphorylation and binding to the recombinant STAT3 SH2 domain, we investigated whether the pY223 motif of AR is involved in the AR/STAT3 interaction. For this purpose, site directed mutagenesis of Y223 in AR to phenylalanine (F) was performed prior to transfection in AR- PC3 cells.

Results on the formation of pY223AR/STAT3 complexes are shown in Figure 16 A. PC3 cells were co-transfected with *HA*-tagged *STAT3* and *His*-tagged *AR* cDNAs, either wild-type *AR* or *ARY223F*, before IL-6 treatment. STAT3 was IPed with HA Abs, followed by western blotting with AR Abs, controlling for IPed STAT3 with HA Abs. Whole lysates show that AR-His and ARY223F-His were detected at 110kDa by AR Abs, while STAT3-HA was detected at 90kDa by HA Abs. IP of HA (STAT3) showed an interaction between STAT3 and WT AR, which was not present for ARY223F. The Y223 of AR is therefore necessary for STAT3 binding in the IL-6 pathway.

Next, lysates of these co-transfected cells were used in competition with short AR peptides (Y223, pY223, and pY534) before pull-down experiments, in order to determine their effect on STAT3 SH2 binding to pY223AR (Fig. 16B). The pre-incubation of cell lysates with the pY223AR peptide is the most potent for reducing the level of pY223AR retained by STAT3-SH2. 73% decrease in pY223AR binding to STAT3 SH2 was observed in the presence of the pY223 AR peptide, as opposed to 9% decrease for the pY534 peptide and 33% for Y223. The difference was significant ($p<0.01$) between all conditions ($n=2$). None of the peptides affect the quantity of STAT3 binding to the SH2 domain of STAT3. These findings support that the pY223 peptide displaces AR and that this motif binds the STAT3 SH2 domain. Taken together, these results show that, upon IL-6 exposure, STAT3 binds to the pY223 motif of AR via its SH2 domain in LNCaP cells.

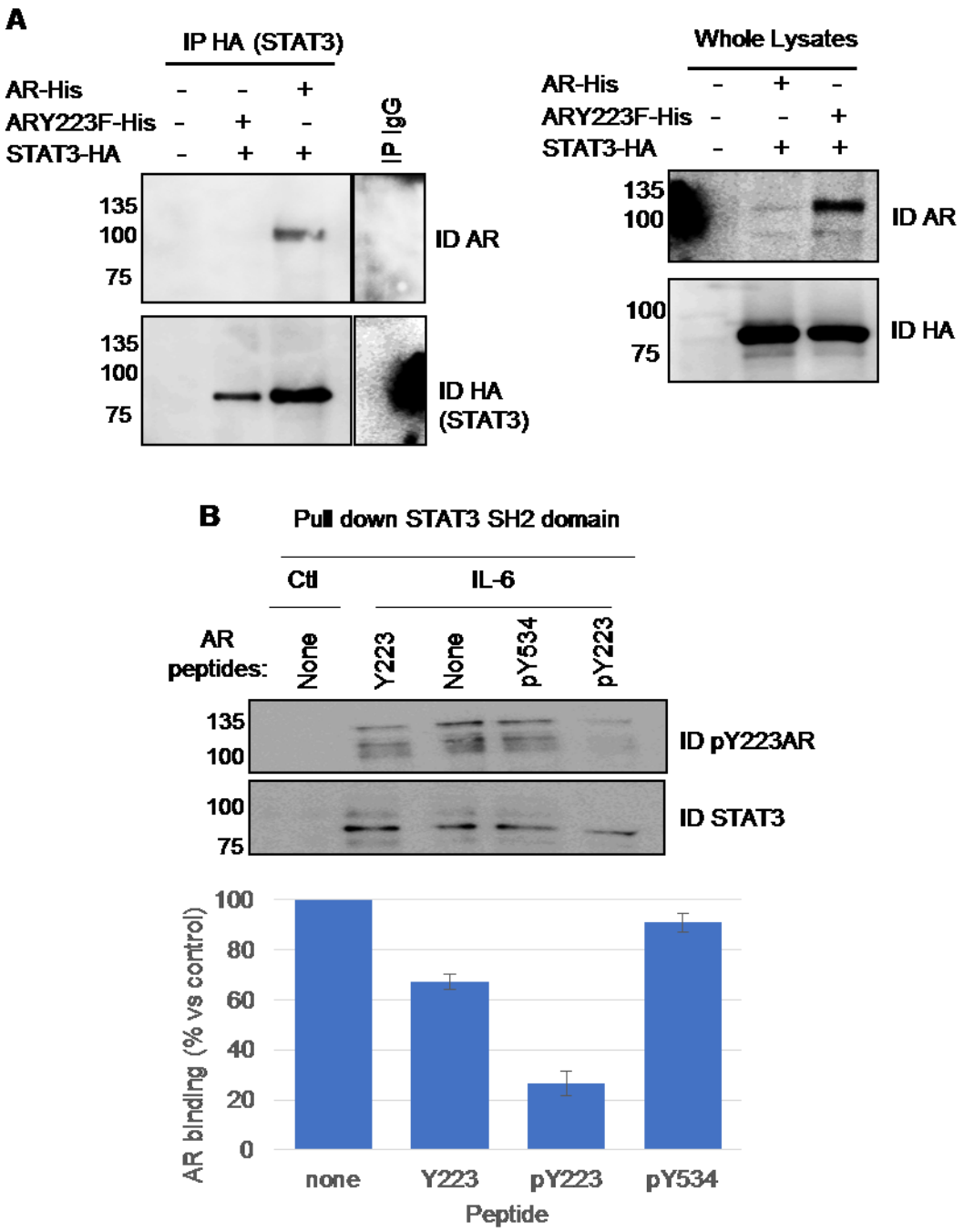

Figure 16: The pY223 motif of AR directly interacts with the STAT3 SH2 domain

(**A**) PC3 cells were co-transfected with *STAT3-HA* cDNA and either *ARY223F-His* or *AR-His* cDNAs before IL-6 exposure (90 minutes). Cell lysates were IPed using HA (STAT3) Abs before SDS-PAGE (alongside IP IgG on lysates from *STAT3-HA/AR-His* transfected cells as negative control) and whole lysates. This was followed by western

blotting using AR and HA Abs. (n=2). (**B**) PC3 cells were co-transfected with *AR-His* and *STAT3-HA* and treated or not with IL-6 (90 minutes). Proteins were pulled down using the STAT3 SH2 domain after competition with different AR short peptides: Y223, pY223, and pY534. Samples were submitted to SDS-PAGE and western blotted for pY223AR and STAT3. AR was quantified using ImageJ and changes were calculated as a percentage of pY223AR pulled down in the absence of peptide (100%). Error bars represent the mean ± standard deviation (n=2).

3. AR-V7 Interacts With STAT3

Since the interaction between AR and STAT3 is mediated by the SH2 domain of STAT3 binding to the pY223 motif of AR, and AR-V7 is activated by phosphorylation of Y223, we explored in 22RV1 cells whether AR-V7 can also interact with STAT3. First, the pY-status of STAT3 was tested in 22RV1 cells treated or not with IL-6 or R1881 (Fig. 17). STAT3 and pSTAT3 were detected at 88kDa by their respective Abs. Interestingly, STAT3 was found to be activated by phosphorylation on Y705 upon IL-6 exposure, but not in untreated or R1881 treated cells (as we see in LNCaP cells). However, this is in contrast with results of activated pY223AR and pY714Fer in 22RV1 cells, which were activated even in basal conditions (Fig. 13). In localization experiments (by IF), STAT3 was mainly cytoplasmic in untreated cells, with some nuclear accumulation upon IL-6 treatment of 22RV1 cells (not shown).

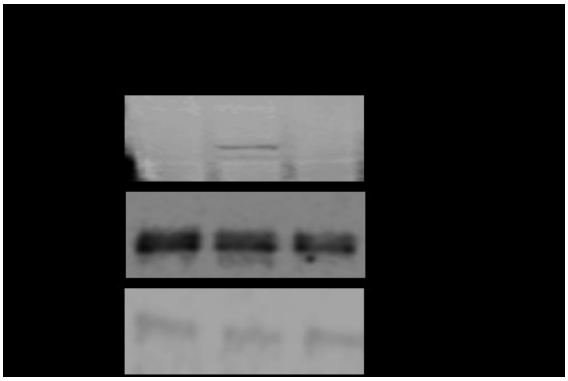

Figure 17: STAT3 phosphorylation in IL-6 or R1881 treated 22RV1 cells

Protein lysates of 22RV1 cells exposed or not to IL-6 or R1881 (90 minutes) were submitted to SDS-PAGE and western blotting using pSTAT3, STAT3, and actin Abs.

To determine whether STAT3 can interact with AR-V7, IP experiments were performed using AR-V7 Abs on lysates of 22RV1 cells treated or not with IL-6. Results in Figure 18 show the detection of pSTAT3 (88kDa) binding to AR-V7 (75kDa) in IL-6 treated 22RV1 cells, but not in untreated cells. This is in line with results obtained above on IL-6 mediated AR/STAT3 interactions in LNCaP cells and PC3 cells transfected with AR (Figs 15, 16). This demonstrates that AR-V7 interacts with STAT3 upon IL-6 exposure, i.e. only when both are Y-phosphorylated, further showing the importance and the scope of STAT3 complexes with AR and its variants in tumor cells, as drugs targeting full length AR, and not N-terminal variants, would not necessarily inhibit crosstalks between the androgen/AR axis and the IL-6 signaling pathway.

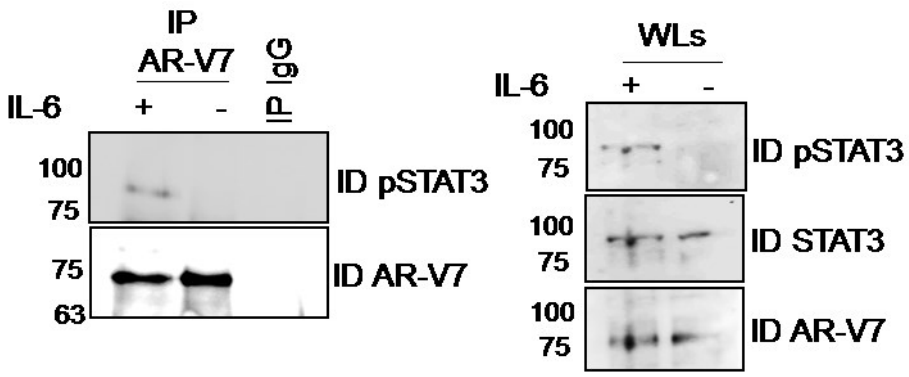

Figure 18: AR-V7 interacts with pSTAT3

Protein lysates of 22RV1 cells exposed or not to IL-6 (90 minutes) were subjected to IP using AR-V7 Abs (with IP IgG on IL-6 treated samples), followed by SDS-PAGE and western blotting using pSTAT3, STAT3, and AR-V7 Abs.

CHAPTER 5: Interactions of AR with c-Myc and E2F1

Our results showing pY223AR/pSTAT3 nuclear complexes upon IL-6 exposure, as well as reports of AR transcriptional reprogramming in CRPC leading to AR binding to DNA sites associated with STATs, Myc, and E2Fs, led us to explore whether IL-6 allows AR or pY223AR to form complexes with specific members of these TF families known to be involved in CRPC. Expression levels of c-Myc correlate with AR levels in mCRPC patients [73], while N-Myc rather drives NE cell differentiation, a subtype in which AR and PSA are believed not to be expressed [78-82]. Of the E2F family of TFs, E2F1 and E2F3 have been studied in PCa [99-102]. Here, we study E2F1 as AR and E2F1 were reported to interact in the LNCaP model and share binding sites for certain androgen-regulated genes involved in prostate tumor development [97]. To date, no studies have characterized these TFs in relation to AR in androgen-independent signaling pathways.

1. Subcellular Localization of c-Myc and E2F1 in IL-6 or R1881 Treated LNCaP Cells

First, we questioned the localization (cytoplasmic vs nuclear) of c-Myc and E2F1. This was assessed, in parallel with AR, by IF in LNCaP cells upon IL-6 or R1881 treatment (Fig. 19). As expected, AR (Fig 19A/B; row *1*) was cytoplasmic in untreated cells, while some nuclear translocation was observed upon IL-6 or R1881 treatment.

The c-Myc protein (Fig. 19A; *row 2*) was observed in both the nuclear and cytoplasmic compartments in untreated cells and remained so in all conditions tested. Some overlap between AR and c-Myc staining (*rows 3-4;* merge images) was observed in the cytoplasm of untreated cells, while their co-localization was observed in both the nuclei and cytoplasm of IL-6 and R1881 treated cells.

The E2F1 and AR localization is shown in Figure 19B. E2F1 (*row 2*) is cytoplasmic and nuclear in untreated and IL-6 treated cells. More nuclear E2F1 is observed in cells exposed to R1881. There is overlap between nuclear E2F1 and AR staining (*rows 3-4*) mainly in the R1881 series. Co-localization is observed in both the cytoplasm (peri-nuclear) and the nucleus of

untreated cells and under IL-6. These findings indicate close proximity of these TFs in the two compartments.

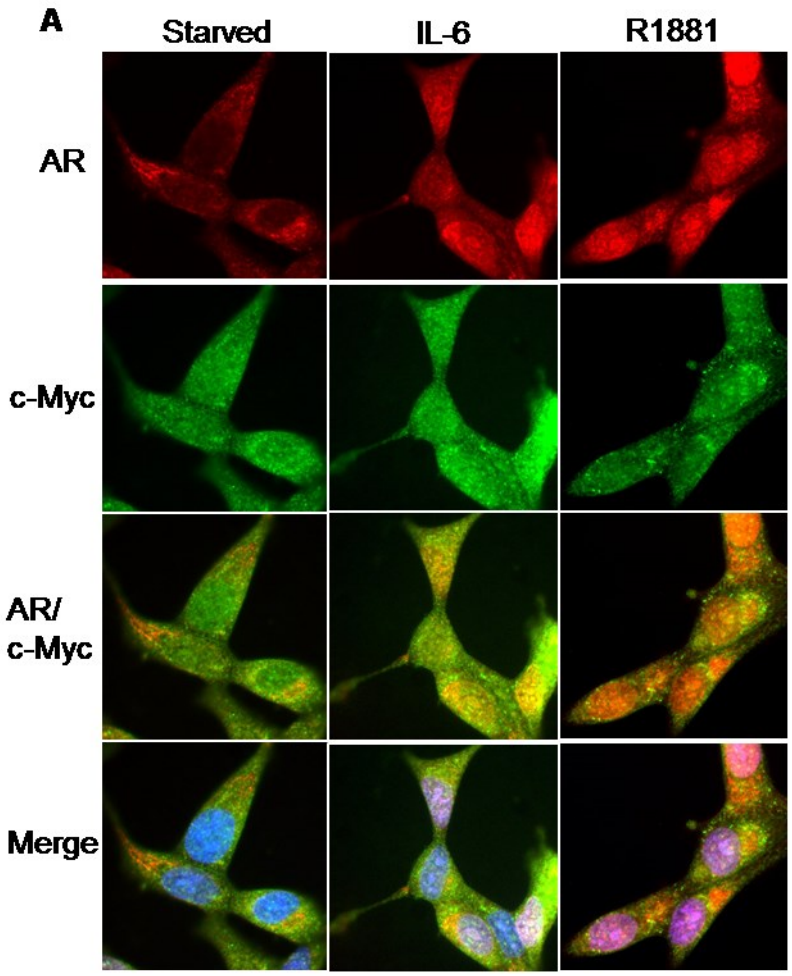

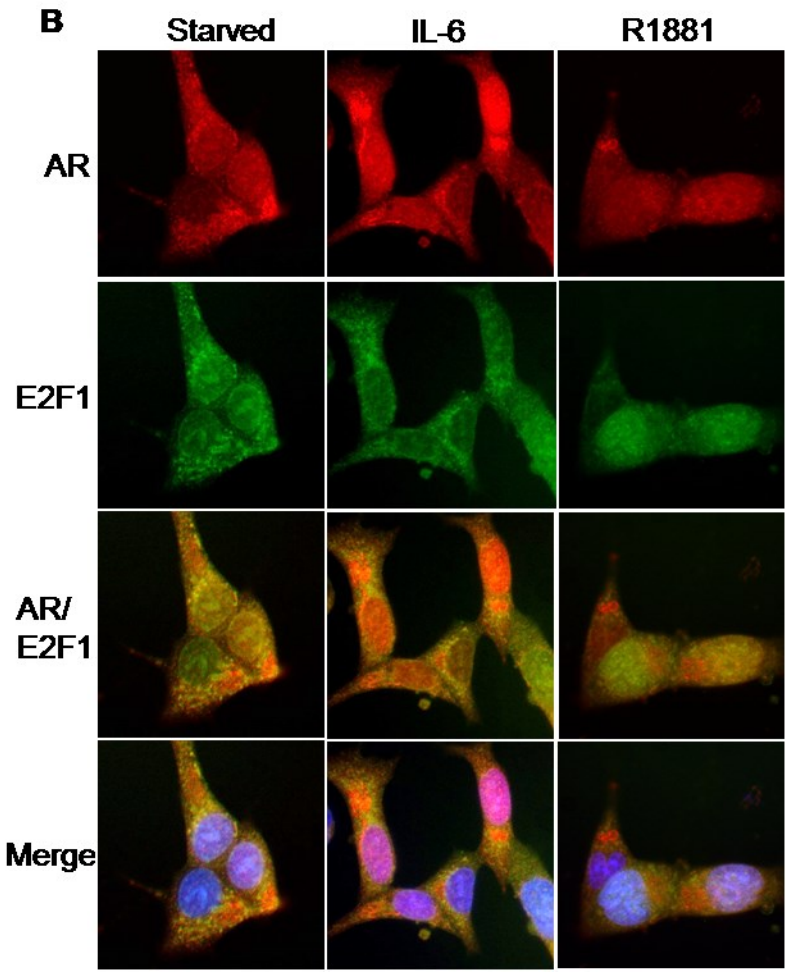

Figure 19: Subcellular localization of c-Myc, E2F1, and AR upon exposure to IL-6 or R1881

IF staining of LNCaP cells exposed or not to IL-6 or R1881 (90 minutes) showing AR (red; *row 1*) with (**A**) c-Myc or (**B**) E2F1 (green; *row 2*), and DAPI nuclear staining (blue). Images were merged to show overlap with or without DAPI (*rows 3 and 4*).

2. Interactions of c-Myc and E2F1 with AR

Since IF staining of these TFs showed some nuclear co-localization in IL-6 or R1881 treated LNCaP cells, we tested possible interactions of AR with c-Myc and included E2F1 as well because it was already shown to be an AR partner in an androgenic (R1881) context. This was done by AR IP and western blotting experiments of c-Myc and E2F1 in LNCaP cells treated

with IL-6 or R1881 (Fig. 20). Abs revealed AR bands at 105 and 110kDa, c-Myc at 63kDa, and E2F1 at 60kDa.

For c-Myc, there was already an interaction present in untreated cells, seen also upon treatment. For E2F1, minimal interaction was observed in untreated cells, while more complexes were observed upon treatment with IL-6 or R1881.

For quantification of interaction levels, the intensities of all bands were measured (reproduced in several experiments). Bands of interest were normalized to those of the IPed protein and graphed as an increase in interaction levels in lysates from non-treated (control) cells. When AR Abs show two bands, normalization was done using either one or both bands, giving very similar results. AR complexes with c-Myc increased by 2-fold upon IL-6 exposure ($p<0.05$), while R1881 exposure made no difference. AR/E2F1 complexes increased by 2.7-fold upon IL-6 exposure ($p<0.01$), and 1.5-fold upon R1881 exposure ($p<0.05$). Levels of AR complexes with c-Myc and E2F1 also significantly differ between IL-6 and R1881 treatment ($p<0.05$ for c-Myc; $p<0.01$ for E2F1), being highest in IL-6.

We also verified if there was an interaction between c-Myc and E2F1 in these samples but found none (not shown). Converse IP experiments of c-Myc or E2F1 and western blotting for AR yielded similar results (not shown).

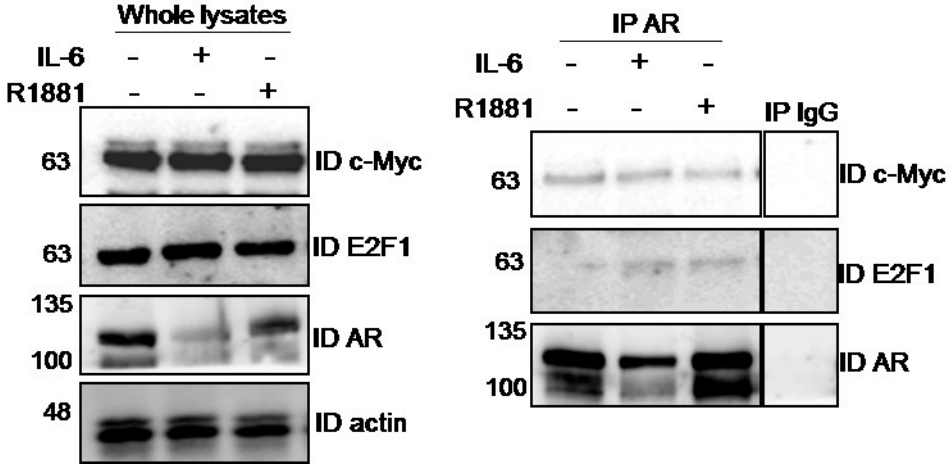

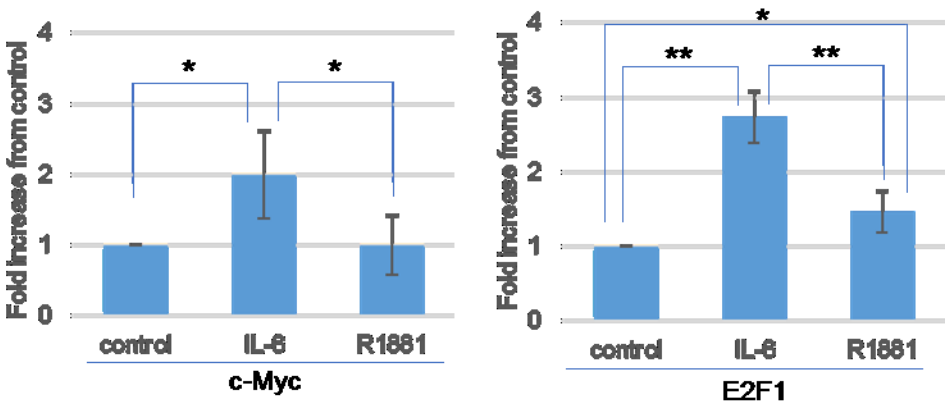

Figure 20: AR complexes with c-Myc and E2F1 in LNCaP cells.

Protein lysates of LNCaP cells treated or not with IL-6 or R1881 (90 minutes) were subjected to IP using AR Abs, followed by SDS-PAGE and western blotting using AR, c-Myc, and E2F1 Abs (IP IgG negative control using IL-6 treated lysates). Intensities of all bands were determined using ImageJ to calculate interaction levels, next normalized to those in non-treated (control) lysates. Statistically significant differences in levels of interacting proteins ($p<0.05$) between conditions are denoted by an asterisk; ($p<0.01$) by two asterisks. Error bars represent the mean ± standard deviation. (c-Myc n=5; E2F1 n=4).

To further validate these findings, similar experiments were performed in PC3 cells (AR negative) co-transfected with either *c-Myc-HA* or *E2F1-HA* cDNAs with *AR-His* and treated with IL-6. HA Abs were used for IP, followed by AR detection by western blotting. AR Abs showed bands at 110kDa, while anti-HA showed bands at 63kDa for c-Myc-HA and 60kDa for E2F1-HA. In Figure 21A, IP HA (c-Myc) revealed an interaction between c-Myc and AR. Similarly, IP HA (E2F1) in Figure 21B showed an interaction between E2F1 and AR. These transfections results confirm that AR forms complexes with each of these TFs in IL-6 treated cells.

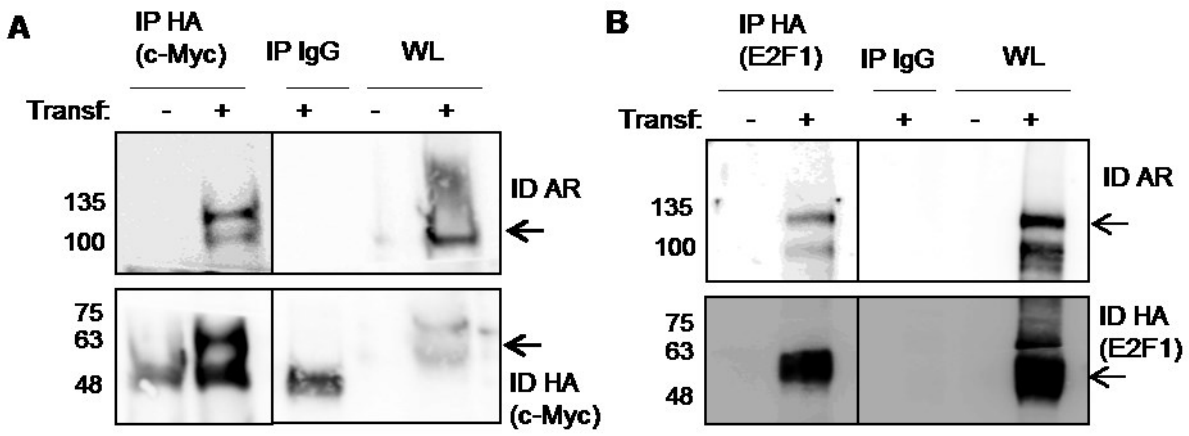

Figure 21: Validation of AR/c-Myc and AR/E2F1 complexes

PC3 cells co-transfected with *AR-His* and either (**A**) *c-Myc-HA* or (**B**) *E2F1-HA* cDNAs were exposed to IL-6 (90 minutes). Proteins lysates were submitted to IP using anti-HA Abs, SDS-PAGE, and western blotting using anti-AR and HA Abs. Non-transfected cells were used as a negative control, along with IP IgG of transfected lysates.

Taken together, results in LNCaP or PC3 (co-transfections) support the presence of c-Myc/AR and E2F1/AR nuclear complexes in prostate tumor cells, found at highest levels in androgen-independent (IL-6) conditions. These findings are in line with AR ChIP data showing AR binding to Myc and E2F related motifs on DNA of PCa tissues from CRPC patients, but not in R1881 treated LNCaP cells [39]. Accordingly, IL-6 or other cytokines and growth factors (as opposed to androgens) in the tumor microenvironment may, as in advanced cancer, allow new partnerships between TFs in the nucleus, resulting in genomic reprogramming.

Because the interactions between AR and these TFs were found under conditions leading to AR Y223 phosphorylation, we questioned whether AR is phosphorylated in these complexes. First, we repeated experiments as above, with IP of c-Myc and E2F1 from IL-6 or R1881 treated LNCaP cells, looking for bound pY223AR. In whole lysates (Fig. 22), Abs revealed a c-Myc band at 63kDa, E2F1 at 60kDa, and AR at 110kDa, along with pY223AR which confirmed activation under IL-6 and R1881.

pY223AR Abs showed an interaction with c-Myc, as detected in IP c-Myc in all conditions. Interaction levels were measured using intensities of pY223AR bands normalized to those of the IPed protein and graphed as an increase from control (untreated) cells.

Quantification showed increased pY223AR/c-Myc complexes upon IL-6 exposure (2.7-fold; $p<0.05$) while R1881 showed no significant increase ($p=0.2$). Complexes with activated AR were also found for E2F1. Quantification showed a slight (1.5-fold) increase upon IL-6 exposure but did not reach significance ($p=0.09$), whereas levels were lowest (less than in controls) in the R1881 context. These pY223AR/E2F1 interactions thus tended to increase upon IL-6 treatment, where we found AR to be most highly activated.

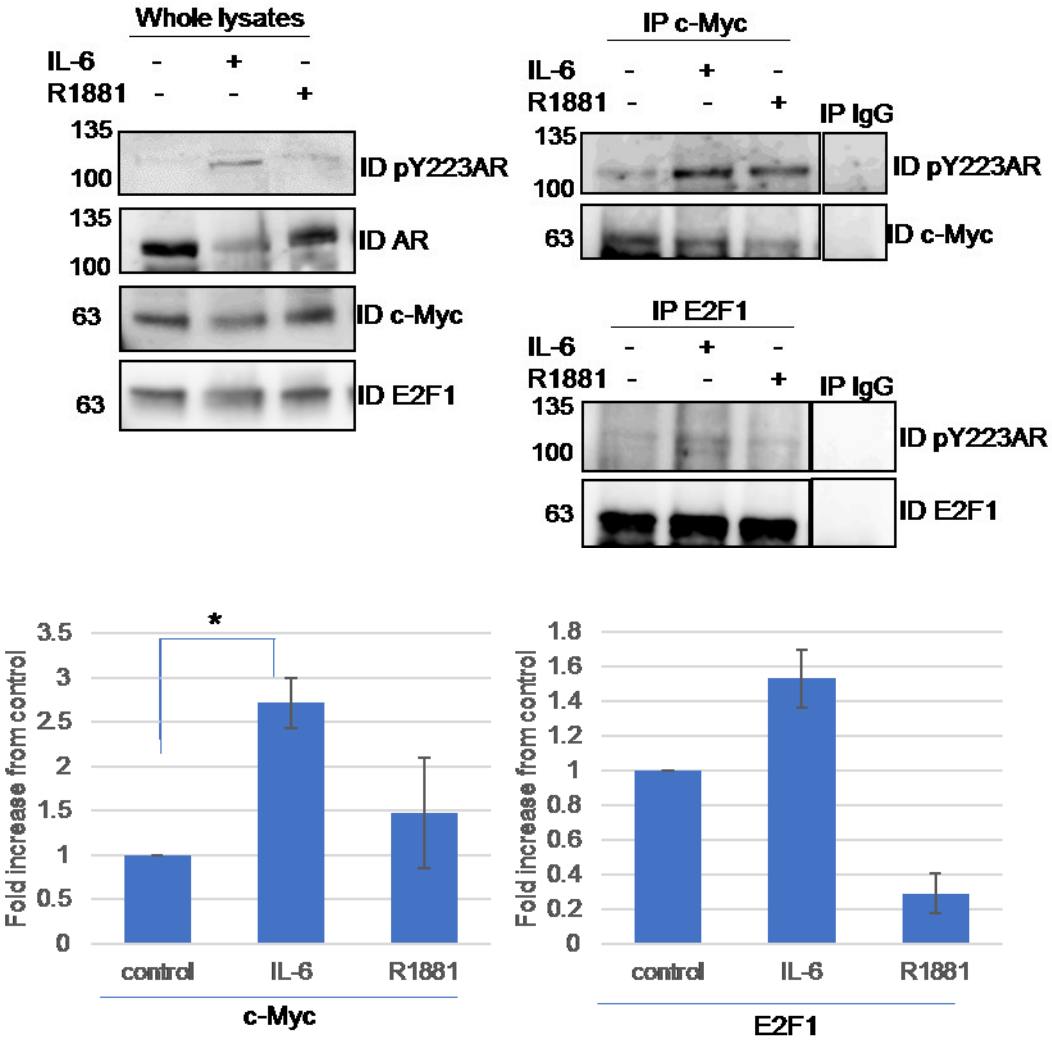

Figure 22: c-Myc and E2F1 interact with pY223AR

Protein lysates from LNCaP cells treated or not with IL-6 or R1881 (90 minutes) were subjected to IP using c-Myc (*top*) or E2F1 (*bottom*) Abs (IP IgG negative control using IL-6 treated lysates), followed by SDS-PAGE and western blotting using Abs for pY223AR, c-Myc, and E2F1, along with AR in blots for whole lysates. Intensities of all bands were used to calculate interaction levels, next normalized to those in untreated (control) lysates. Statistically significant differences in levels of interacting proteins ($p<0.05$) between conditions are denoted by an asterisk. Error bars represent the mean ± standard deviation (n=2).

Next, to determine whether AR Y223 phosphorylation is necessary for c-Myc or E2F1 binding, PC3 cells co-transfected with *c-Myc-HA* or *E2F1-HA* cDNAs and either *WT AR-His* or *ARY223F-His* cDNAs before IL-6 treatment were used in similar IP/ID experiments (Fig. 23). Anti-HA Abs revealed bands at 63kDa for c-Myc-HA and 60kDa for E2F1-HA. Anti-AR revealed bands at 110kDa for WT and mutant AR.

For c-Myc (Fig. 23A), no interaction with WT AR was detected in untreated cells. Complexes were detected upon IL-6 exposure in cells co-transfected with WT AR, but not ARY223F. For E2F1 (Fig. 23B), there was some interaction with WT AR in untreated cells, which increased upon IL-6 exposure. There is an important decrease in levels of complexes between E2F1 and mutant AR under IL-6.

These findings support that Y223 phosphorylation of AR is necessary for formation of complexes with c-Myc, and also contributes to interactions with E2F1. Therefore, IL-6, which activates Fer and AR, also leads to interactions of pY223AR with c-Myc and E2F1. We showed that the pY223 motif of AR is important for the formation of these complexes, although c-Myc and E2F1 are not known to contain SH2 or phosphotyrosine-binding (PTB) domains.

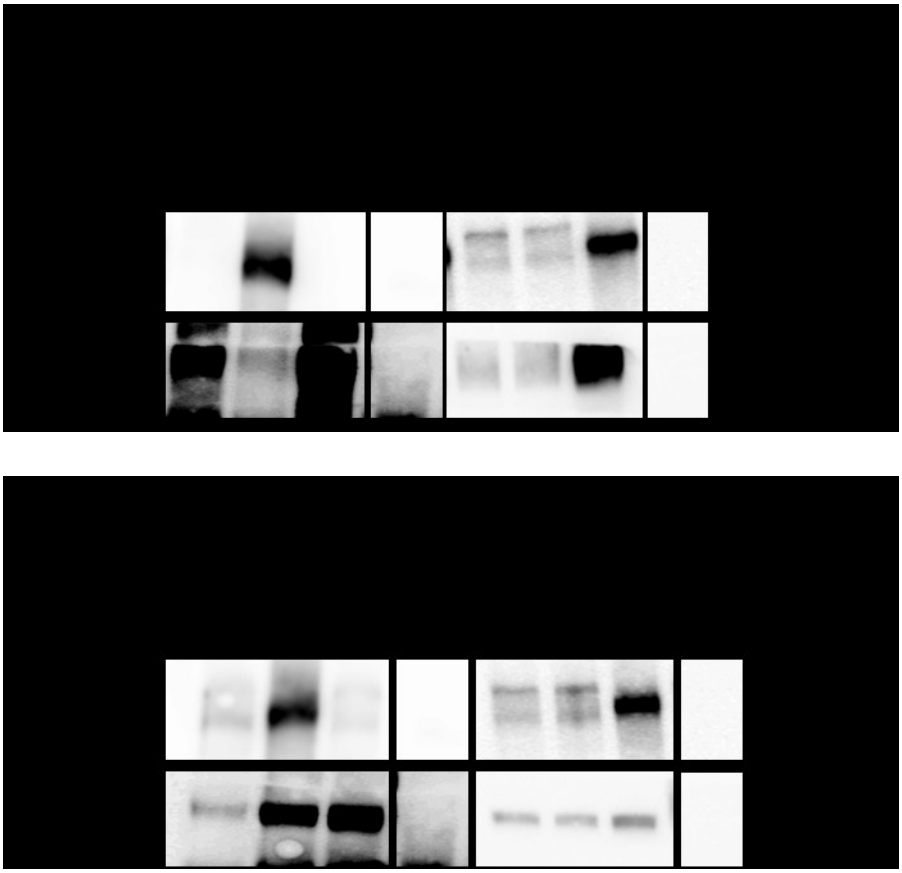

Figure 23: Importance of Y223AR in AR/c-Myc and AR/E2F1 complexes

PC3 cells were co-transfected with cDNAs of either *AR-His* or *ARY223F-His*, with (**A**) *c-Myc-HA* or (**B**) *E2F1-HA,* and analyzed along with non-transfected controls. Cells were then treated or not with IL-6 (90 minutes), IPed using anti-HA Abs (IP IgG negative control on IL-6 treated *AR-His* lysates) and subjected to SDS-PAGE and western blotting with AR and HA Abs (n=2).

3. AR-V7 Interaction with c-Myc and E2F1

Because the pY223 motif of AR is important for binding to c-Myc and E2F1, we asked whether these TFs would also interact with AR-V7, which is constitutively activated on Y223 in 22RV1 cells. IP experiments of c-Myc and E2F1 on IL-6 or R1881 treated (vs untreated) 22RV1 cells were carried out to analyze activated AR and AR-V7 by western blots.

Figure 24 shows that pY223AR Abs detect multiple bands, notably at the positions of full length AR and in the 75-85kDa range (*panel 1*). However, AR-V7 Abs reveal no interaction of AR-V7 with c-Myc or E2F1 in any of the conditions tested (*panel 2*). Converse experiments (IP AR-V7; ID c-Myc/E2F1) gave the same negative results (not shown).

Taken together, these findings imply that in PCa cells expressing AR full length and its variants including AR-V7, their activation takes place, and leads to interactions of activated AR-V7 with STAT3, but not with c-Myc and E2F1.

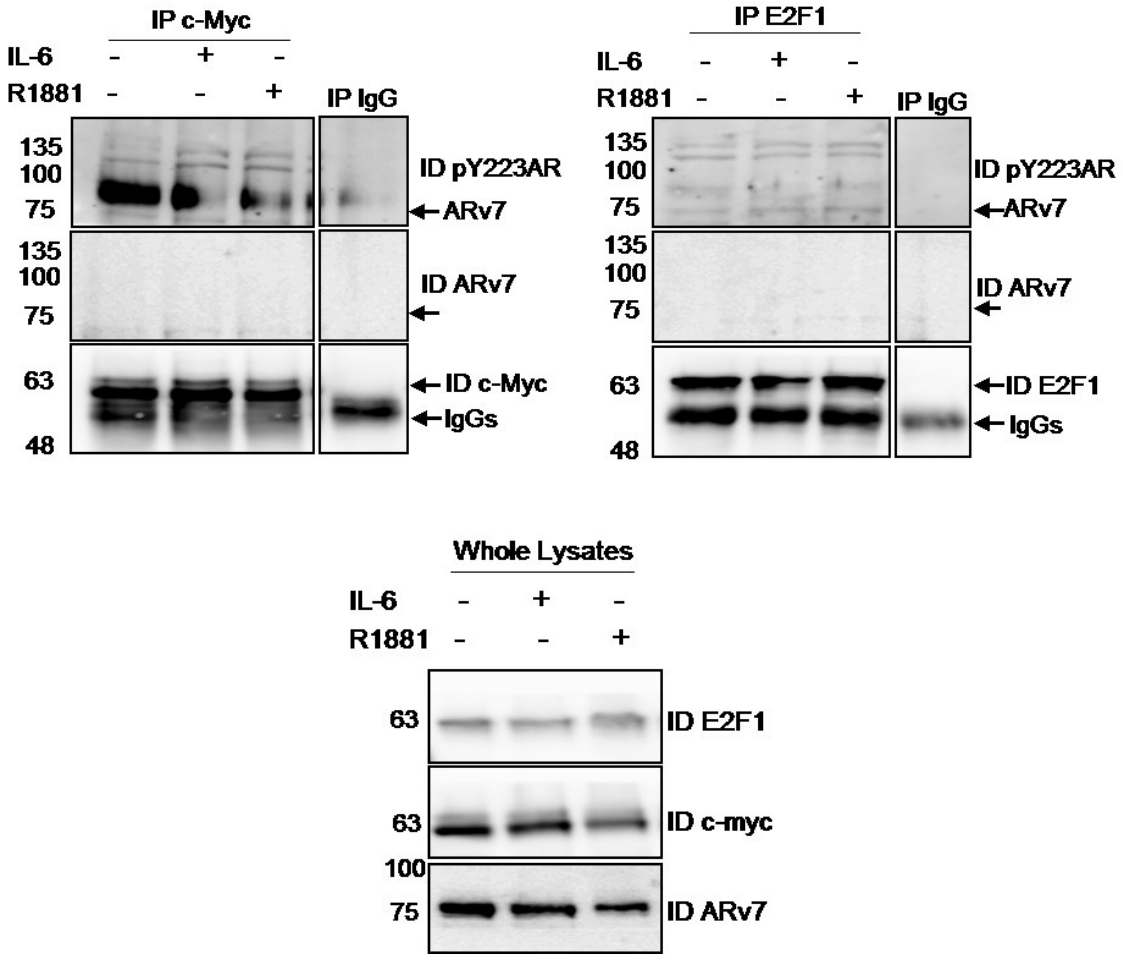

Figure 24: AR-V7 does not interact with c-Myc or E2F1

Protein lysates of 22RV1 cells exposed or not to IL-6 and R1881 (90 minutes) were subjected to IP using c-Myc (*left*) or E2F1 (*right*) Abs (IP IgG negative control on IL-6

treated lysates), before SDS-PAGE and western blotting using pY223AR, AR-V7, c-Myc, and E2F1 Abs (n=3).

CHAPTER 6: Y-phosphorylation of c-Myc and E2F1

Increase in Y-phosphorylation levels is important in progression to CRPC [103]. The Fer TK controls both AR (Y223) and STAT3 (Y705) phosphorylation and transcriptional activation in the IL-6 pathway, translating in increased cell growth [116]. We found that the direct interaction of AR with STAT3 also depends on AR Y-phosphorylation. We questioned whether c-Myc and E2F1, both related to CRPC, are Y-phosphorylated, which may lead to aberrant transcriptional activity. The c-Myc phosphorylation on Y74 has been reported in breast and ovarian cancer cell lines and tumors (cytoplasmic staining), but its role has not been elucidated [125]. To our knowledge, E2F1 Y-phosphorylation has not been reported.

The pY-status of c-Myc (Fig. 25) and E2F1 (Fig. 26) were examined by IP/western blotting experiments in LNCaP and PC3 cells. The stimuli used were: IL-6, R1881 (LNCaP only), FBS and pervanadate (pV), vs non-treated controls. pV is a reagent known to irreversibly inhibit PTPs by oxidation of the thiol groups of their catalytic cysteine residues, thus leading to increased levels of Y-phosphorylation [126].

For c-Myc in LNCaP cells (Fig. 25A), we performed IP of Y-phosphorylated proteins with pY Abs, followed by blotting for c-Myc (*top*). The c-Myc band was observed in all conditions, with a slight increase upon IL-6 or R1881 exposure. In the converse experiments (*bottom*), IPed c-Myc was blotted with anti-pY Abs, which revealed bands in the 63kDa range (c-Myc position) and multiple other bands. These were seen in all conditions, with a marked increase upon pV exposure. The bands revealed clearly in all experiments were at: 53, **63**, 71, 79, 88, and 99 kDa.

In PC3 cells, pY IP followed by blotting for c-Myc (Fig. 25B; *top*), showed that c-Myc is detected in all conditions, with an increase upon FBS or pV exposure. In the converse experiment, IP c-Myc followed by western blots with anti-pY Abs (*bottom*) revealed multiple bands upon pV treatment, including at the position of c-Myc, but not in other conditions. The bands revealed clearly in at least two equivalent experiments (n=3) were at: 36, 53, **63**, 73, 79, 88, 97, 109, and 124 kDa.

Several pY-proteins interacting with c-Myc were common to both cell lines: 53, ~71/73, 79, 88, and ~97/99 kDa. To our knowledge, Y-phosphorylated partners of c-Myc have not been identified. These results support the Y-phosphorylation of c-Myc in PCa cells, in agreement with reports on breast and ovarian cancer cell lines and tumors, and identifies c-Myc interactions with several common pY-proteins in the two PCa cell models tested.

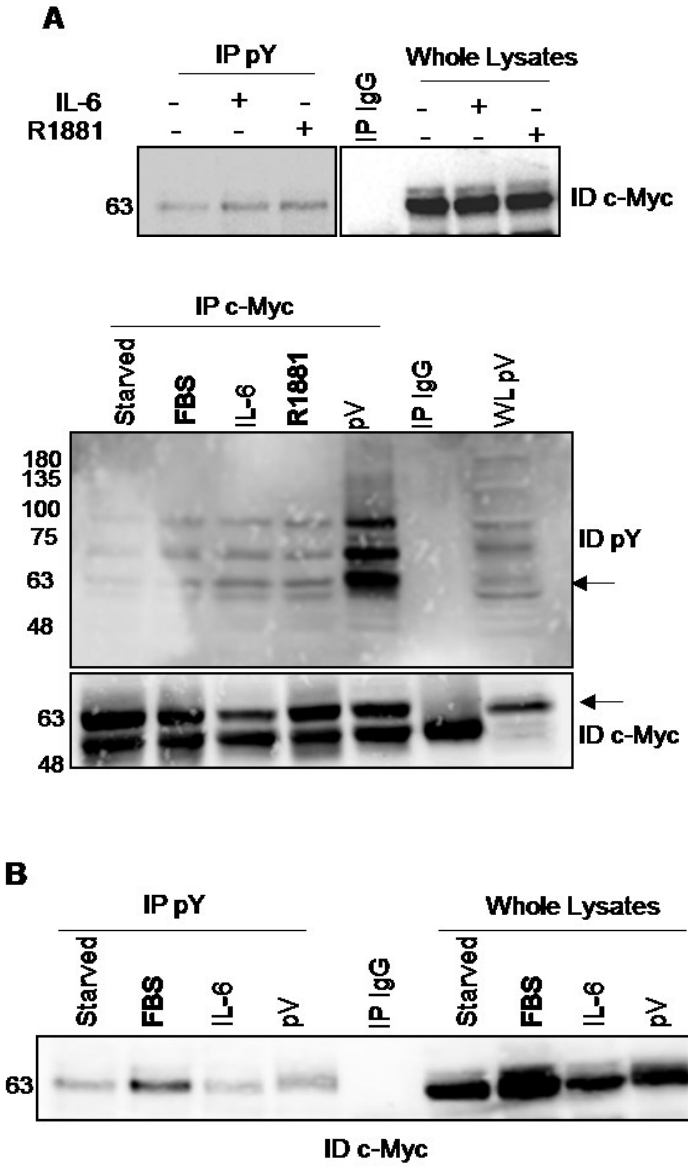

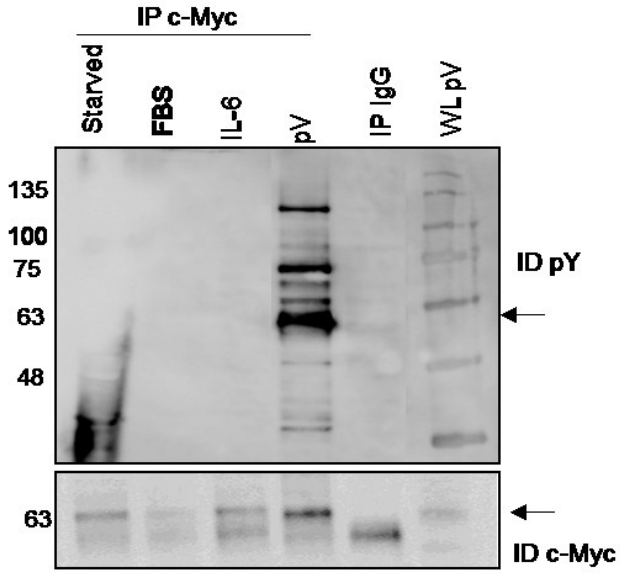

Figure 25: c-Myc Y-phosphorylation in LNCaP and PC3 cells.

(A) LNCaP cells were exposed to IL-6, R1881, FBS, or pV (90 minutes) before IP with pY or c-Myc Abs, followed by SDS-PAGE and western blotting using these same Abs (n=2). (**B**) Similar experiments were performed in PC3 cells exposed to FBS, IL-6, or pV (90 minutes) (n=3).

The analysis of E2F1 activation in LNCaP and PC3 cell lines also suggests its Y-phosphorylation. In LNCaP cells (Fig. 26A), IP pY Abs followed by blotting for E2F1 (*top*) revealed no E2F1 band. The converse experiment (IP E2F1/ID pY; *bottom*) shows several pY-proteins associated with E2F1 (**60**, 70, 78, 83, 95, 105, 114 kDa) solely upon pV exposure, including at the E2F1 position (60 kDa).

For E2F1 in PC3 cells (Fig. 26B), IP pY and blot for E2F1 (*top*) showed a faint band for E2F1 only upon pV exposure. The converse experiment (*bottom*) showed a band at 60kDa, the E2F1 position, and other pY-proteins (38, **60**, 78, 85, 93, and 114 kDa), again solely upon pV exposure.

Several pY-proteins interacting with E2F1 were common to both cell lines: 78, ~83/85, ~93/95, and 114 kDa. To our knowledge, and as mentioned, the Y-phosphorylation of E2F1 and

pY-partners of E2F1 has not been reported. These results in two PCa cell models support that E2F1 may be Y-phosphorylated upon pV exposure, and that it interacts with several pY-proteins common to both cell lines.

Therefore, Y-phosphorylation in various conditions appears as potential new mechanism of activating these TFs in PCa cell lines. The underlying mechanisms require further investigation. Mass spectrometry would be needed to confirm the Y-phosphorylation of each of these TFs and allow the identification of their pY-partners.

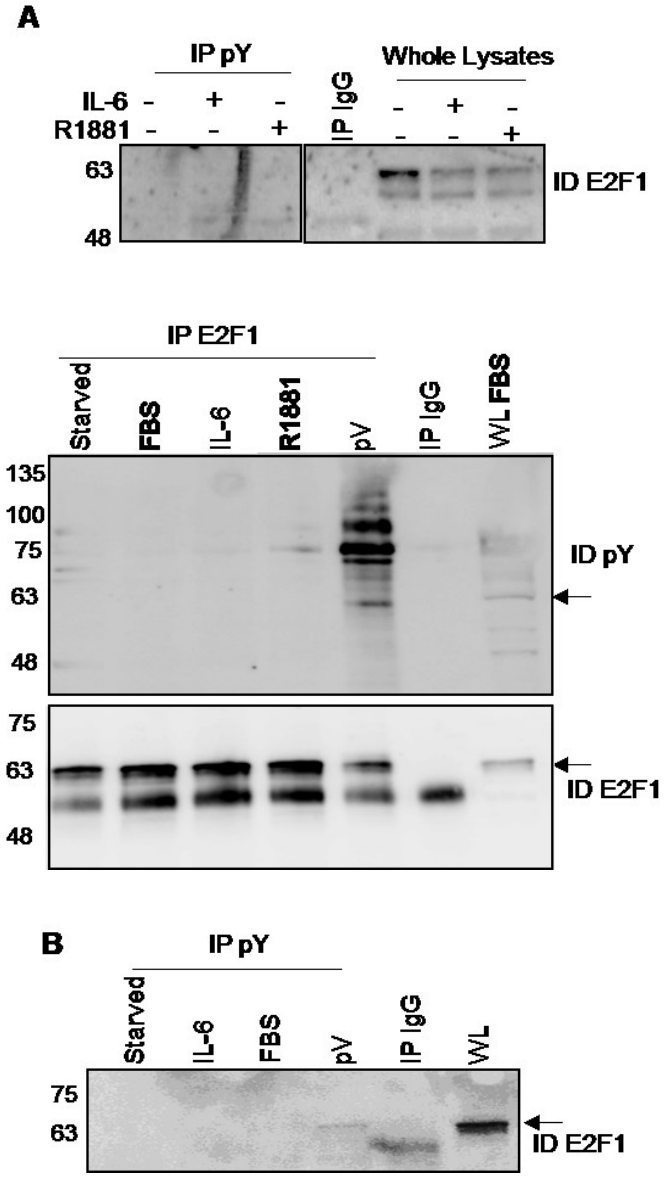

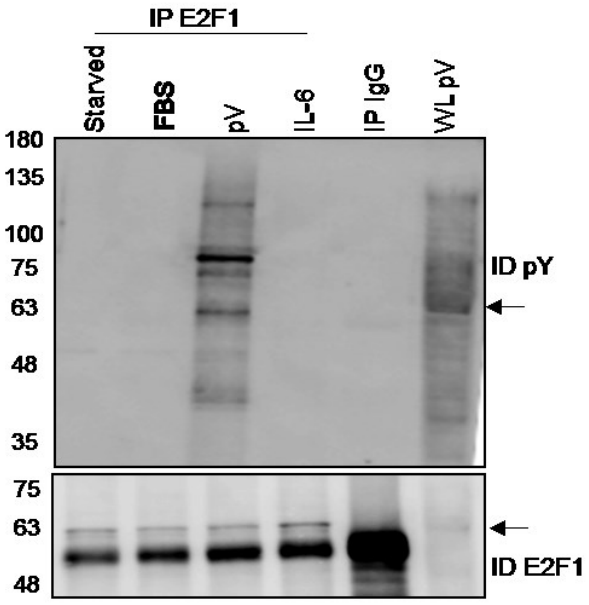

Figure 26: E2F1 Y-phosphorylation in LNCaP and PC3 cells.

(A) LNCaP cells were exposed to IL-6, R1881, FBS, or pV (90 minutes) before IP with pY or E2F1 Abs, followed by SDS-PAGE and western blotting using these same Abs (n=2). (**B**) Similar experiments were performed in PC3 cells exposed to FBS, IL-6, or pV (90 minutes) (n=3).

Since we find that both TFs are potentially Y-phosphorylated in PCa cell lines, we tested whether Fer may be involved directly. Although IL-6 treatment does not seem to induce phosphorylation of E2F1, we know that other growth factors, such as EGF and IGF-1, can activate Fer (although to a lesser extent) [48]. Moreover, Fer activity on its two identified substrates in PCa cell lines, AR and STAT3, depends on the stimulus (i.e. Fer induced AR activation, but not that of STAT3 upon exposure to androgens, as shown in Fig. 14 and by Rocha, J; PhD thesis 2013 [48]).

In vitro Fer kinase assays were performed using human recombinant c-Myc (65kDa) and E2F1 (64kDa). Each of the recombinant proteins alone was used in parallel as a negative control, with the human recombinant Fer catalytic domain alone (60kDa) as a positive control for Fer Y714 activation. Initial experiments conducted in conditions reported by the host lab for Fer

activity on STAT3 and AR did not allow a distinction between the Fer band and the potential substrates tested (similar molecular sizes) (Fig. 27A) [114, 116]. However, when conditions were modified (i.e. lower Fer levels, range of substrate concentrations, longer duration of electrophoresis), the separation of the two activated substrates was possible, although larger bands were observed due to diffusion in gels.

Figure 27B shows the results in optimized conditions. Western blots were performed with anti-pY Abs (*panel 1*) to detect phosphorylation of each protein, as well as for the substrates (c-Myc and E2F1; *panel 2*) and the enzyme (Fer; *panel 3*) to show the exact molecular weight of each protein. Interestingly, c-Myc, but not E2F1, is found phosphorylated by Fer, with an increase of pY detected (at the level of c-Myc) with increasing concentrations of c-Myc.

These findings imply that c-Myc can be directly phosphorylated by Fer, whereas another TK (or several) would allow E2F1 Y-phosphorylation in PCa cells. This would occur in conditions allowing hyperactivation of kinases with minimal activity of phosphatases on pY-levels of c-Myc and E2F1. This raises questions on whether such activation may change their binding partners in cancer cells and their transcriptional activity, resulting in genomic reprogramming

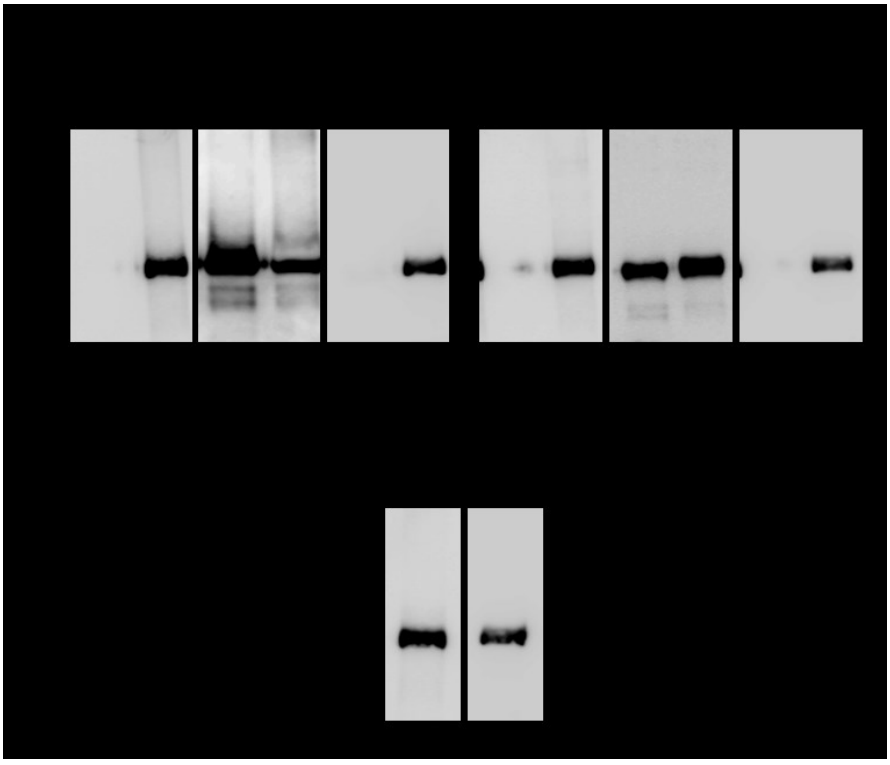

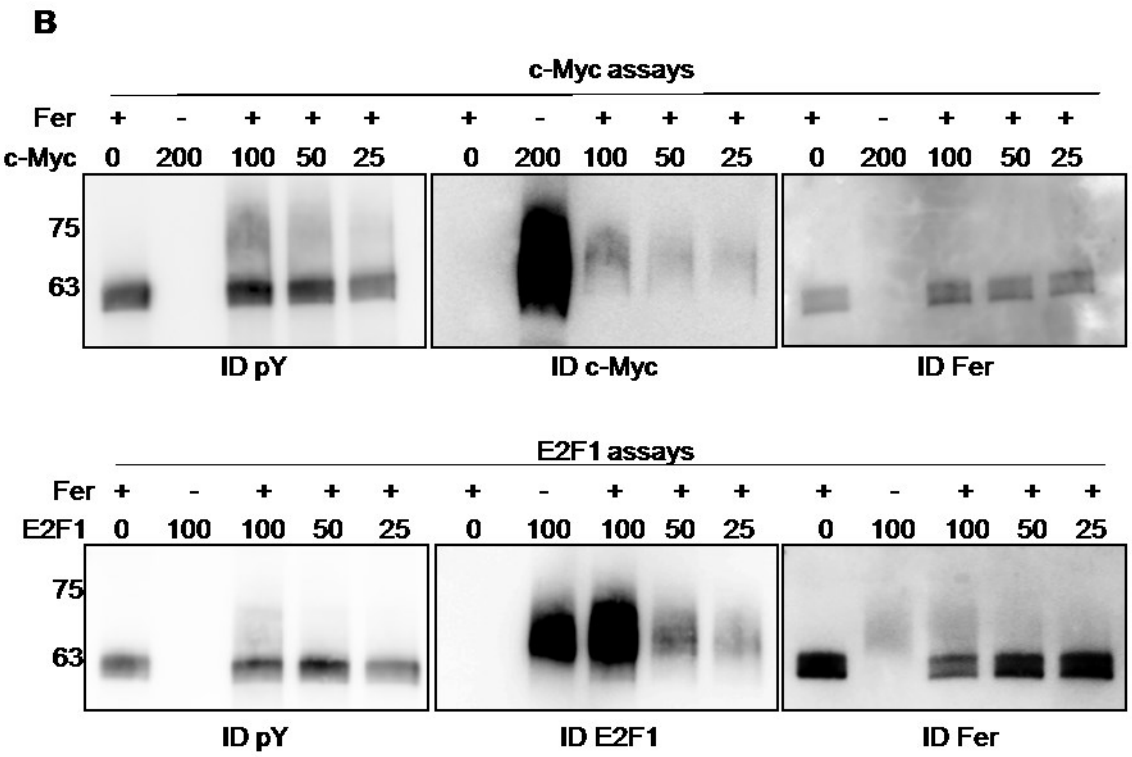

Figure 27: In vitro Fer kinase assays for c-Myc and E2F1.

(**A**) *In vitro* Fer kinase assays were performed using the catalytic domain of Fer (100 ng) and recombinant c-Myc and E2F1 (50 ng), alongside Fer alone (positive control for phosphorylation) and c-Myc and E2F1 alone (negative controls). Samples were submitted to SDS-PAGE and western blotting using anti-pY, Fer, c-Myc, and E2F1 Abs (n=2) (**B**) Similar experiments were performed using 50 ng of Fer and varying concentrations of recombinant human c-Myc and E2F1 (25 to 200 ng) (n=3).

CHAPTER 7: Clinical Significance of STAT3 and c-Myc Expression

To follow on observations made *in vitro* on Fer and its substrates STAT3 and AR, both activated in the IL-6 signaling pathway, the host lab studied all three proteins and their activated forms, i.e. Fer and pY714 Fer, AR and pY223AR, and STAT3 and pY705STAT3 in human prostate samples. This was done in diverse McGill cohorts representing all stages of disease, and clinical significance was found. As part of an international project initiated by Movember (through Prostate Cancer Canada), it was proposed that several investigators would validate markers of their choice in an additional cohort of patients shared by all teams. Dr. Saad at Centre Hospitalier de l'Université de Montréal (CHUM) offered a tissue microarray (TMA) built from his RP cohort. In line with *in vitro* data in cell lines, I investigated STAT3 and c-Myc expression by IHC. For this study, the protocol BMD-10-1160 was amended and approved by the ethics board of the research institute.

1. Cohort Characteristics

The cohort, described in Table 2, consists of 243 PCa patients who underwent RP. The median age was 62 years old, with a median clinical follow-up of 128 months. The mean PSA was 8.3 ng/mL at diagnosis. The majority of patients had a GS of ≤6 (55%) or 3+4 (32%), with few patients at GS 4+3 or ≥8. 77% of patients had a pathological tumor stage of T2 (localized to the prostate) and 21% at T3 (spread to adjacent structures) with no positive lymph node (N0) or distant metastases (M0). 4 patients had metastases to lymph nodes, 10 to bones, and only 1 to soft organs. 72 showed BCR (described as PSA of 0.2 and rising), and 30 have died (7 PCa specific death).

Total number of cases	243
Median followup (months)	128
Median age (years)	63 ± 5.5
Median pre-operative PSA (ng/mL)	8.3 ± 5.3
Extraprostatic extension	52 (21.4%)
Seminal vesicle invasion	5 (2.1%)
LN invasion (n=177)	4
Bone metastases	10 (4.1%)
Soft organ metastases (n=241)	1
Death	30 (12.3%)
PCa specific death	7 (2.9%)
Biochemical recurrence	72 (29.6%)
Gleason score (n=241)	
≤ 6	132 (54.8%)
7 (3+4)	78 (32.4%)
7 (4+3)	12 (5.0%)
≥ 8	19 (7.9%)
Pathological stage	
T2 (N0 M0)	187 (77.0%)
T3 (N0 M0)	51 (21.0%)
T2/3 N1 or M1	5 (2.0%)

Table 2: Cohort descriptive features.

Kaplan-Meier survival curves show the probability of an outcome at a given time, for subsets of a cohort (e.g. low vs high PSA) [127]. Established clinical parameters (pre-operative PSA, GS, and pTNM) were tested by Kaplan-Meier analysis to confirm that they are predictive of outcome (Fig. 28).

Figure 28A shows that high PSA (≥10ng/mL) was predictive of BCR and bone metastases, but not of death or PCa specific death. In Figure 28B, high GS was predictive of BCR, bone metastases, and PCa specific death, segregating between the lower (≤ 6 and 3+4) and higher (4+3 and ≥8) grades. The stage (pathological TNM) was predictive of BCR, bone

metastases, death, and PCa specific death (Fig. 28C). For bone metastases, death, and PCa death, patients with no metastases clustered together, while for BCR patients with a pathological stage of T3 clustered with those with metastases.

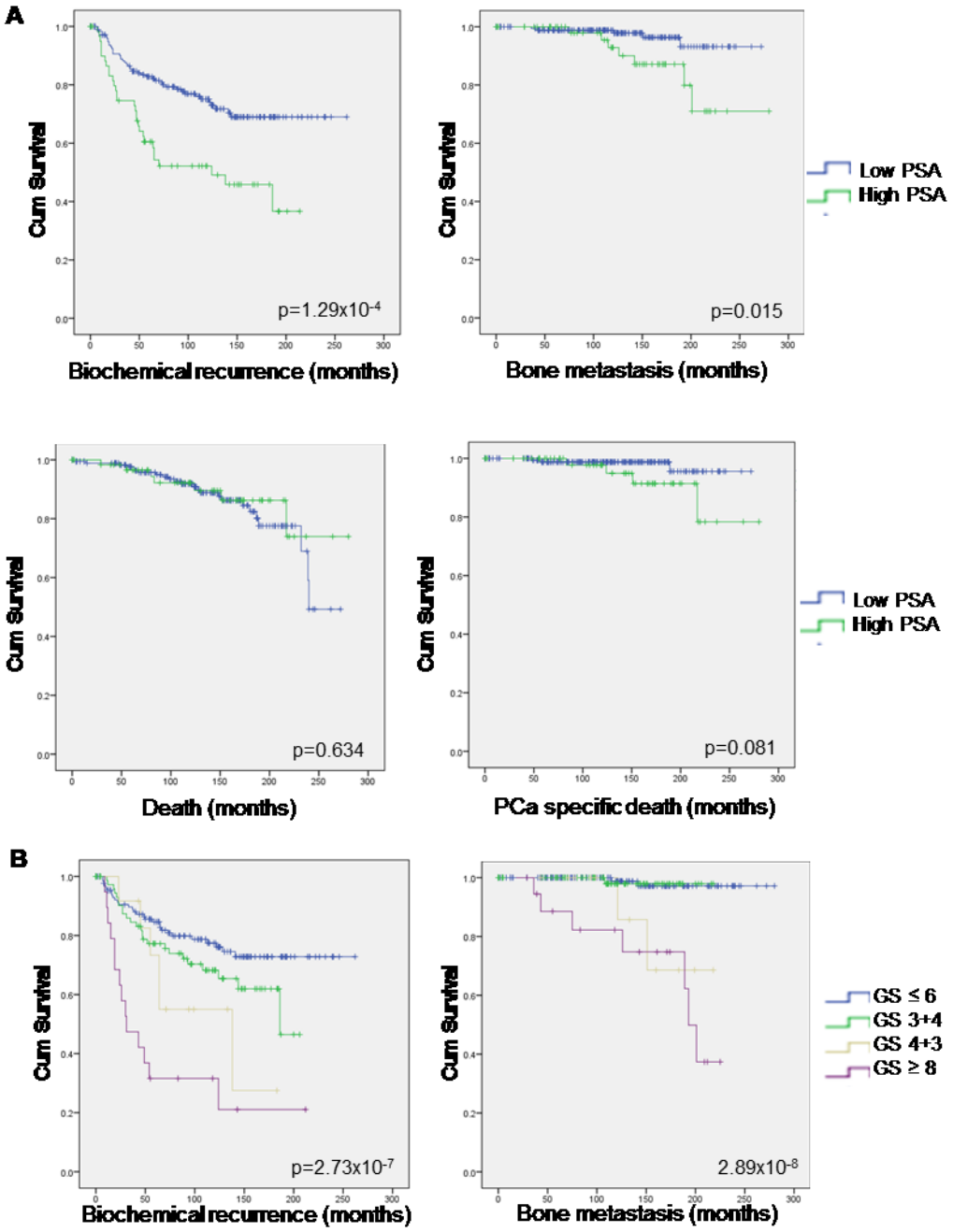

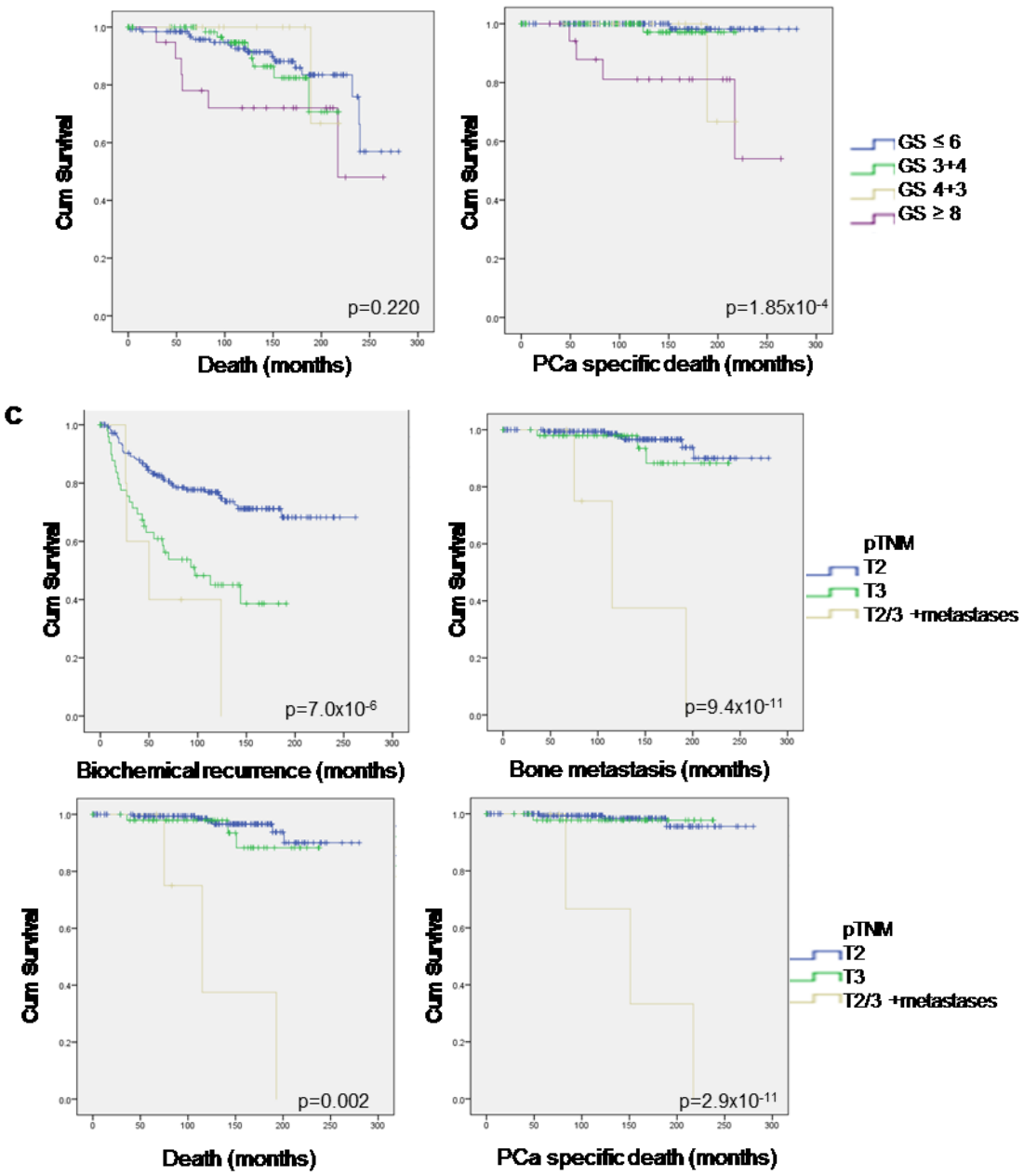

Figure 28: Kaplan-Meier survival analysis based on cohort clinical parameters. Kaplan Meier analysis was carried out for (**A**) PSA (≤10ng/mL), (**B**) GS (≤6, 3+4, 4+3, ≥8), and (**C**) pTNM (T2, T3, T2/3 with metastases). BCR, presence of bone metastases, overall death, and PCa specific death were tested.

2. STAT3 and c-Myc IHC on the CHUM TMA Cohort

First, STAT3 and c-Myc Abs were tested for specificity by western blotting of PCa cell line extracts, to reveal one band at the expected size (STAT3 at 88kDa; c-Myc at 63kDa) (Fig. 29). IHC conditions were next optimized on prostate tissues from advanced cases and applied to the test TMA from the CHUM to reveal a range of staining intensities with minimal background prior to the staining of the entire TMA.

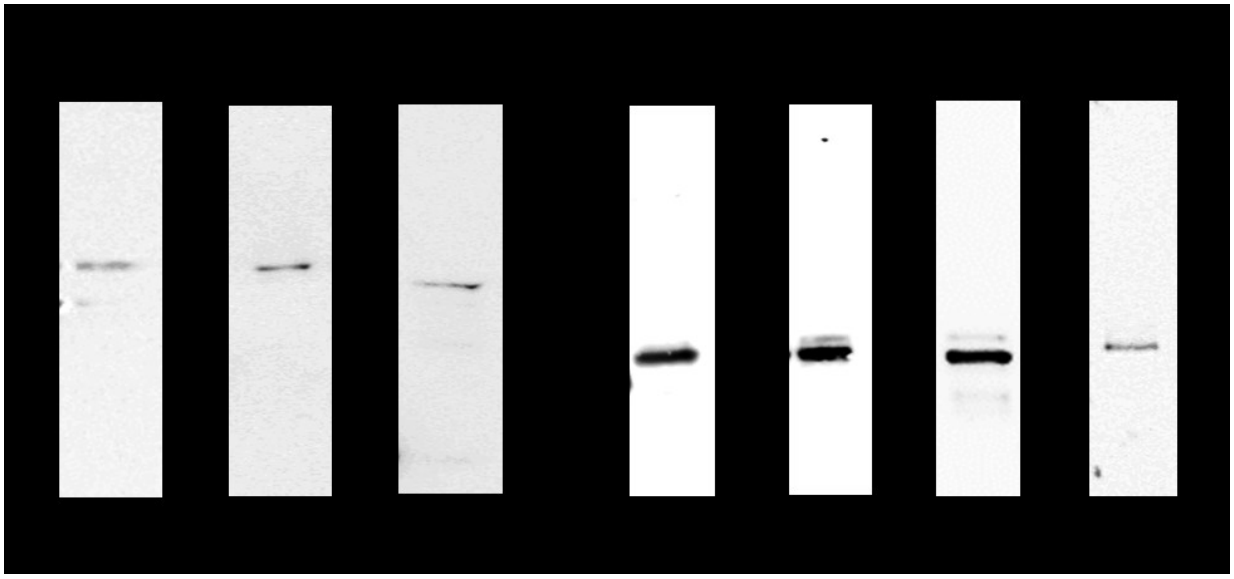

Figure 29: Testing STAT3 and c-Myc Abs using PCa cell lines.
Protein lysates (50µg) from LNCaP, 22RV1, and PC3 cell lines were submitted to SDS-PAGE followed by western blotting using (**A**) STAT3 or (**B**) c-Myc Abs. For c-Myc Abs, recombinant human c-Myc (25ng) was also included.

The staining of prostate tissues was analyzed in tumor foci and benign epithelium from the same cases. Figure 30A shows STAT3 nuclear staining at varying intensities in tumor foci, as well as in benign epithelium, with fainter staining in the cytoplasm. The c-Myc Abs showed nuclear staining at varying intensities (generally heterogeneous) in tumor foci, and negative or low staining in basal cells of benign foci (Fig. 30B). Cytoplasmic c-Myc was also observed, but at a lesser intensity compared to nuclei.

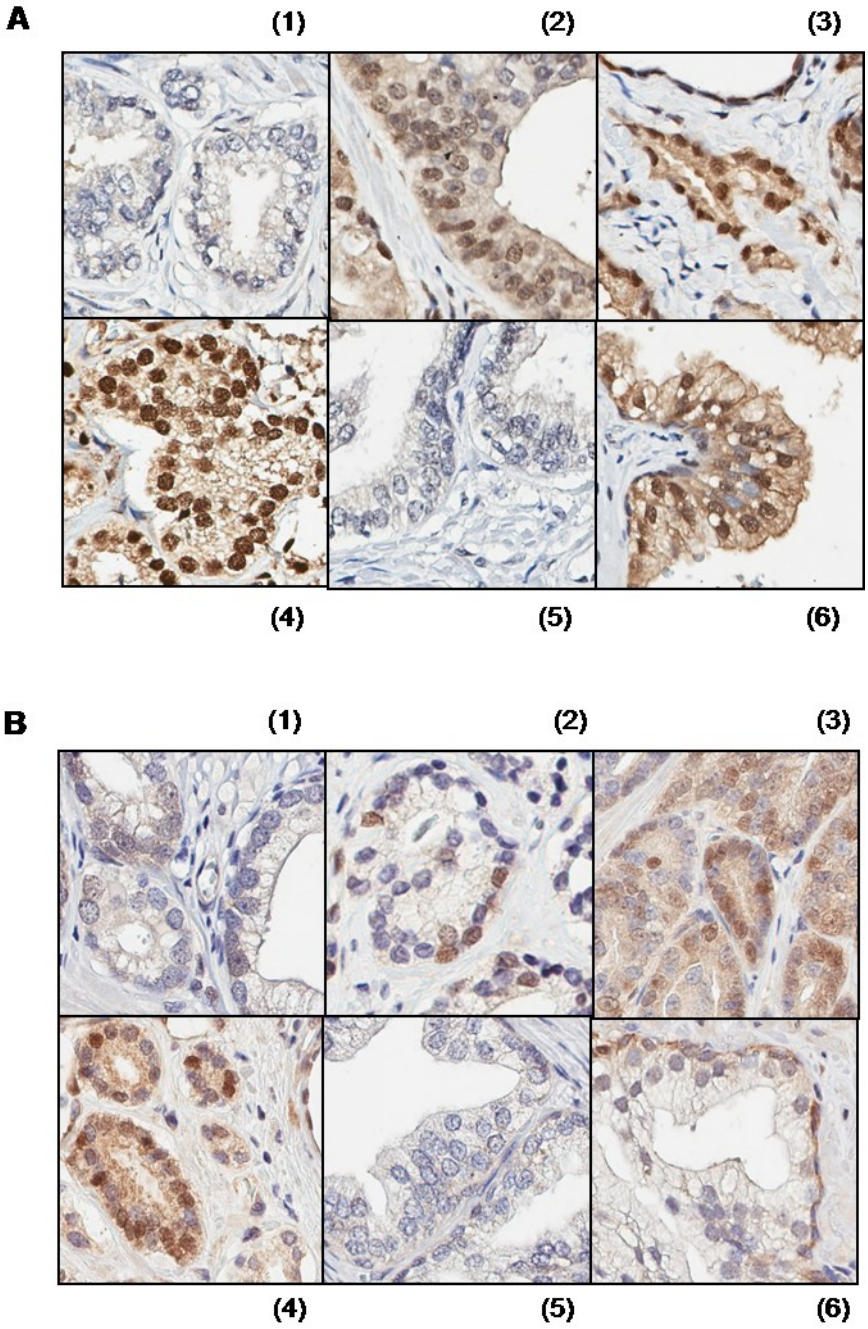

Figure 30: STAT3 and c-Myc expression in prostate tissues.

Cores of the CHUM TMA were stained according to optimal conditions. (**A**) Images of STAT3 in tumors: (*1*) negative, (*2*) heterogeneous, (*3*) moderate and (*4*) high intensity staining; in benign cores: (*5*) negative and (*6*) high intensity staining. (**B**) Images of c-

Myc in tumors: (*1*) negative, (*2*) heterogeneous, (*3*) moderate, and (*4*) high intensity staining; in basal cells of benign cores: (*5*) negative and (*6*) low intensity nuclear staining.

3. Statistical Analysis of STAT3 and c-Myc Expression in the CHUM TMA

STAT3 and c-Myc nuclear intensities (0, 1+, 2+, 3+ from negative to strong staining) were quantified in tumor cells using ImageScope software after optimization of the nuclear staining detection algorithm. H Scores (HS) were calculated from the staining intensities of nuclei in each cancer core.

In order to run statistical analysis, a cutoff for low vs high intensity staining for each marker was first selected using the web application Cutoff Finder, which identifies the most significant cutoff in a dataset [121]. These cutoffs were only used in our analysis if each group (low vs high) represented at least 25% of the cohort. HS of 46 was used as a cutoff for STAT3, and 35 for c-Myc. Clinical significance of low vs high STAT3 or c-Myc expression was then assessed using the statistical software SPSS.

Kaplan-Meier survival analysis was first performed for each marker to see whether they can predict the clinical outcome of patients (Fig. 31).

STAT3 (Fig. 31A) was found to be predictive of BCR, with high nuclear expression of STAT3 indicating earlier time to BCR ($p=0.043$). It was not predictive of bone metastases, death, or PCa specific death. This might be due, in this cohort, to very few patients having developed bone metastases (4%) or died of any cause (12%).

For c-Myc (Fig. 31B), we found that high nuclear c-Myc level predicts BCR ($p=0.026$), but none of the other outcomes tested, as seen with STAT3.

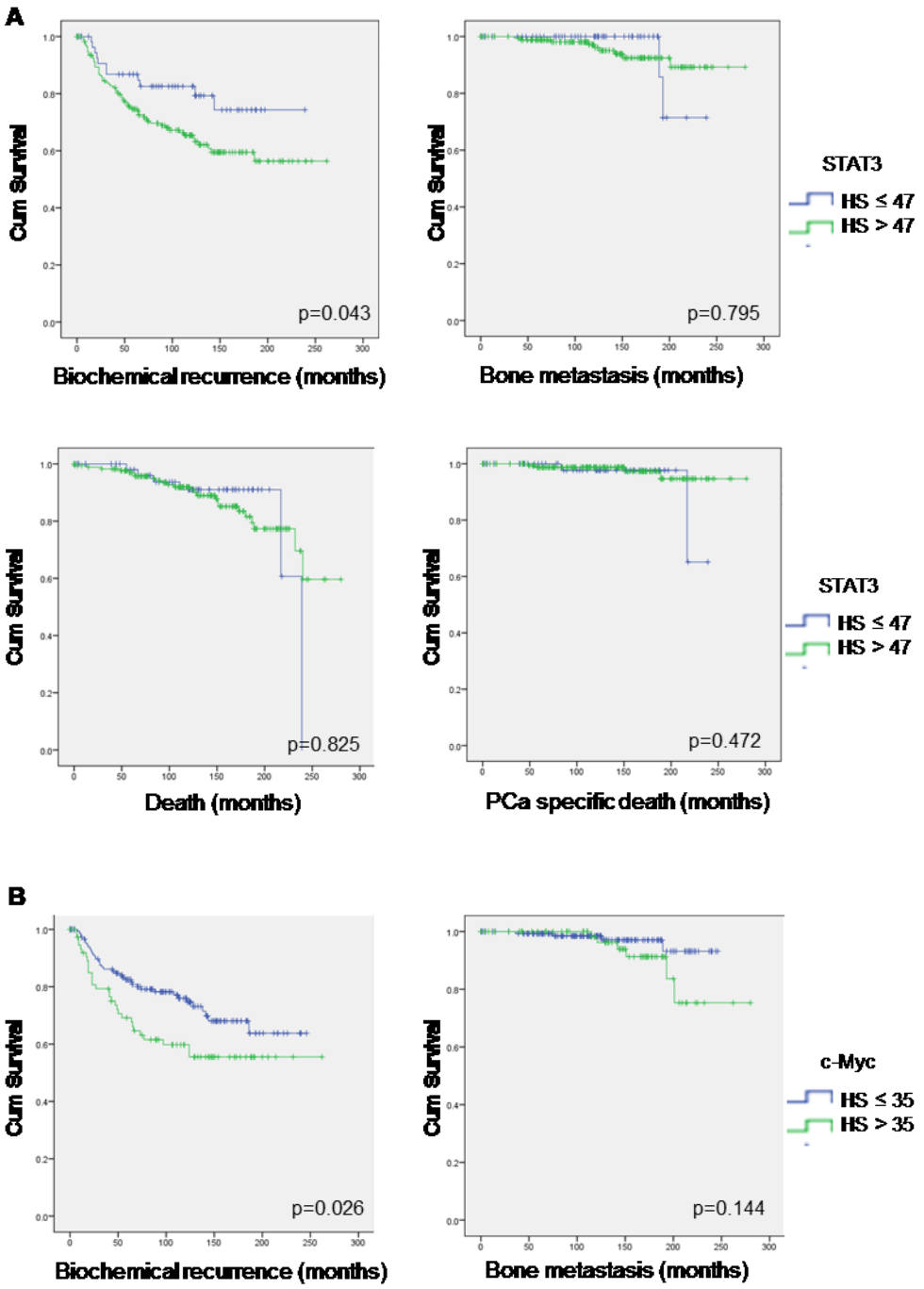
A
Cum Survival
p=0.043
Biochemical recurrence (months)
Cum Survival
p=0.795
Bone metastasis (months)
STAT3
HS ≤ 47
HS > 47
Cum Survival
p=0.825
Death (months)
Cum Survival
p=0.472
PCa specific death (months)
STAT3
HS ≤ 47
HS > 47
B
Cum Survival
p=0.026
Biochemical recurrence (months)
Cum Survival
p=0.144
Bone metastasis (months)
c-Myc
HS ≤ 35
HS > 35

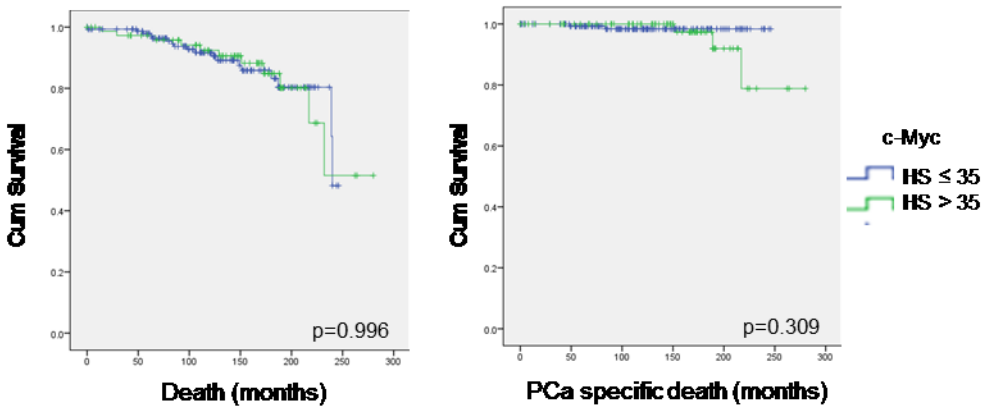

Figure 31: Kaplan-Meier survival analysis of STAT3 and c-Myc expression in PCa.

Kaplan Meier survival curves for (**A**) STAT3 (cutoff HS 47) and (**B**) c-Myc (cutoff HS 35). BCR, bone metastases, overall death, and PCa specific death were tested.

Because Kaplan-Meier analysis showed that both STAT3 and c-Myc are predictive of BCR, Cox analysis (proportional hazards regression) was next performed (Fig. 32). Cox analysis looks at the effect of a variable (STAT3 or c-Myc expression) on the time it takes for an event (BCR) to take place. The hazard ratio (HR) obtained from Cox analysis represents the relative rate of the event taking place, e.g. a HR of 2 for a given marker means that patients with high expression show twice the rate per unit time of an outcome taking place than those with low expression [128].

The analysis can be done as univariate or multivariate. In univariate Cox analysis, the predictive value of our markers is compared to those of parameters currently in use clinically (PSA, GS, and pTNM). Multivariate Cox analysis incorporates our markers with these clinical parameters as covariates to adjust for their impact, allowing a more clinically relevant assessment using multiple parameters.

STAT3 (Fig. 32A) univariate Cox analysis for BCR (*top*) shows a hazard ratio (HR) of 1.9. This is higher than the HR for PSA and GS, but not as high as that for pTNM (HR 2.5). The 95% confidence interval (CI) for STAT3 is also large (1.0-3.7). In multivariate analysis (*bottom*),

STAT3 performs better than all parameters tested (HR 2.6) and is more predictive than STAT3 in univariate analysis mentioned above.

For c-Myc (Fig. 32B), univariate analysis (*top*) gives a HR of 1.7, higher than PSA but lower than that for GS and pTNM. In multivariate analysis (*bottom*), it performs as well as the GS and pTNM (HR 1.5). STAT3 thus predict BCR better than other clinical parameters in multivariate analysis, while c-Myc performs as well as GS and pTNM.

A

Univariate Cox Analysis								
						Hazard	95.0% CI for Exp(B)	
	B	SE	Wald	df	Sig.	**Ratio**	Lower	Upper
STAT3	.652	.328	3.944	1	.047	1.919	1.009	3.650
PSA pre-op	.070	.016	20.195	1	.000	1.072	1.040	1.106
Gleason Score	.567	.111	26.263	1	.000	1.763	1.419	2.190
pTNM	.920	.188	23.899	1	.000	2.509	1.735	3.628
Multivariate Cox Analysis								
						Hazard	95.0% CI for Exp(B)	
	B	SE	Wald	df	Sig.	**Ratio**	Lower	Upper
STAT3	.955	.349	7.493	1	.006	2.599	1.312	5.151
PSA pre-op	.045	.019	5.787	1	.016	1.046	1.008	1.085
Gleason Score	.362	.124	8.455	1	.004	1.436	1.125	1.833
pTNM	.653	.212	9.485	1	.002	1.922	1.268	2.913

B

Univariate Cox Analysis								
						Hazard	95.0% CI for Exp(B)	
	B	SE	Wald	df	Sig.	**Ratio**	Lower	Upper
c-Myc	.536	.244	4.813	1	.028	1.709	1.059	2.759
PSA pre-op	.074	.015	22.919	1	.000	1.077	1.045	1.110
Gleason Score	.589	.114	26.563	1	.000	1.803	1.441	2.256
pTNM	.910	.192	22.466	1	.000	2.485	1.705	3.620
Multivariate Cox Analysis								
						Hazard	95.0% CI for Exp(B)	
	B	SE	Wald	df	Sig.	**Ratio**	Lower	Upper
c-Myc	.397	.251	2.490	1	.115	1.487	.908	2.435
PSA pre-op	.046	.020	5.379	1	.020	1.047	1.007	1.088
Gleason Score	.377	.135	7.818	1	.005	1.457	1.119	1.898
pTNM	.373	.225	2.765	1	.096	1.453	.935	2.256

Figure 32: Univariate and multivariate Cox analysis of STAT3 and c-Myc for BCR

Univariate (*top*) and multivariate (*bottom*) Cox analysis for BCR was carried out for (**A**) STAT3 and (**B**) c-Myc with clinical parameters: pre-operative PSA, GS, and pTNM.

The area under the curve (AUC) for the receiver operating characteristic (ROC) curve was used to show sensitivity (detection rate) and specificity (false positive rate) for STAT3 and c-Myc. Higher AUC (closer to 1) means a marker is very specific and sensitive, while low AUC (close to 0.5) is not as accurate. Neither STAT3 (Fig. 33A) nor c-Myc (Fig. 33B) performed better than PSA, GS, or pTNM, although the AUC was low for these as well.

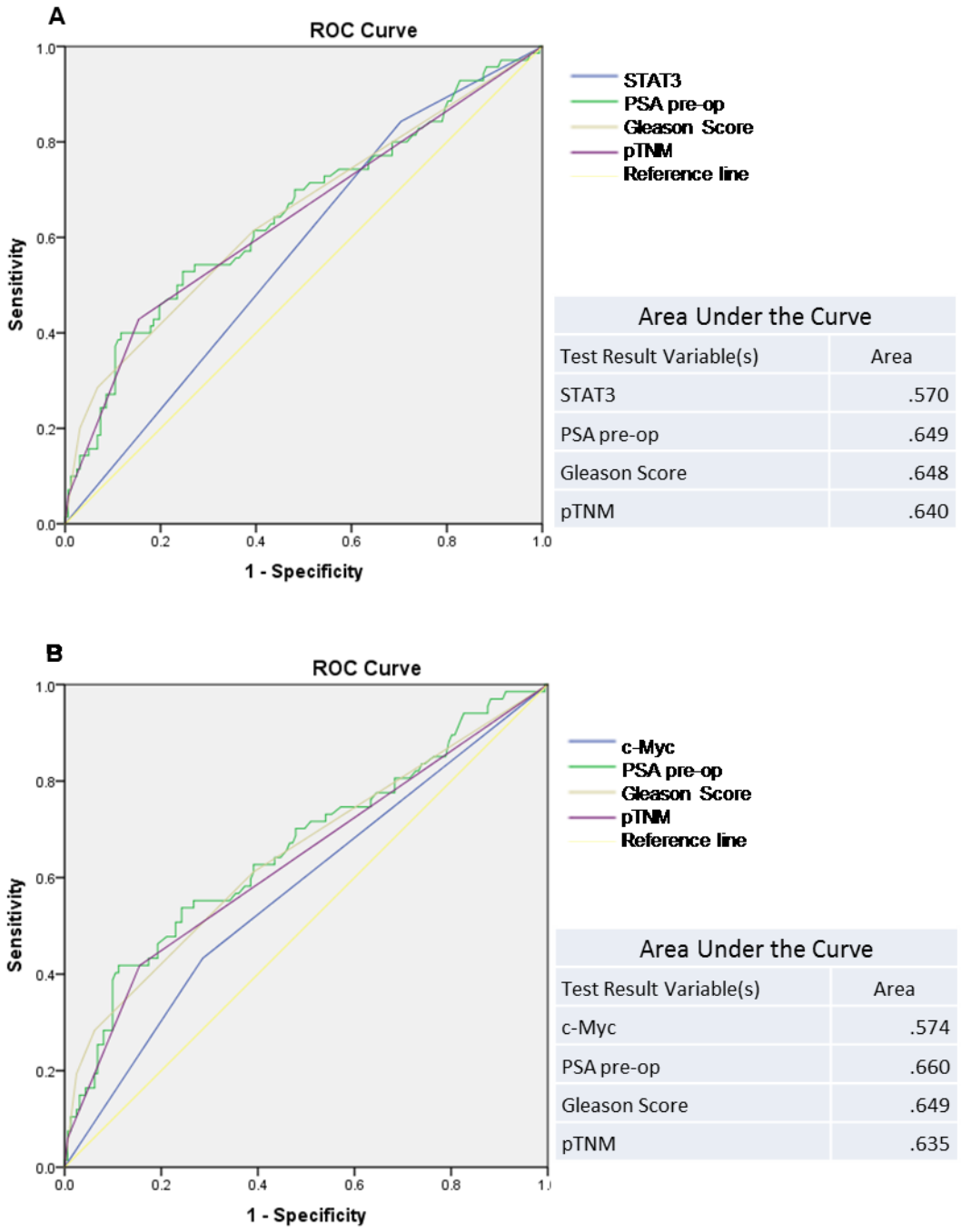

Area Under the Curve

Test Result Variable(s)	Area
STAT3	.570
PSA pre-op	.649
Gleason Score	.648
pTNM	.640

Area Under the Curve

Test Result Variable(s)	Area
c-Myc	.574
PSA pre-op	.660
Gleason Score	.649
pTNM	.635

Figure 33: Sensitivity and specificity of STAT3 and c-Myc

ROC curve and the area under the curve for (**A**) STAT3 and (**B**) c-Myc.

Analysis of STAT3 and c-Myc was also carried out in combination with pY223AR, Fer, and pY714Fer (results not shown). STAT3 increased the predictive power of each of these markers for BCR when used in combination, as revealed by Kaplan-Meier and Cox analysis. c-Myc and pY223AR performed better in combination as well. Therefore, although STAT3 and c-Myc are not sensitive/specific as shown by ROC curves, their use in combination with other markers could be useful in predicting early BCR.

CHAPTER 8: Discussion and Conclusions

1. AR Activation by Y223 Phosphorylation

Our team has previously reported on the phosphorylation of AR on Y223 by Fer in the IL-6 [116] and R1881 [48] pathways in LNCaP cells. The generation of specific pY223AR and pY714Fer Abs has been useful in pursuing our studies on crosstalks between these signaling pathways and investigating their clinical relevance.

pY223AR Abs were used to quantify the levels of AR activation in IL-6 or R1881 exposure of LNCaP cells. IL-6 treatment resulted in more robust AR activation than R1881. Furthermore, the combination of R1881 and IL-6 did not result in a further increase in AR phosphorylation levels. This could be because the activation levels reached are maximal in IL-6. The contribution of R1881 to AR activation is thus not discernable, but, as IL-6 and R1881 do not result in the same AR complexes (we showed that androgens do not activate STAT3), downstream signaling likely differentially affects AR transcriptional activity.

In more aggressive 22RV1 cells, full-length AR and AR-V7 appeared to be constitutively activated at a high level, unaffected by IL-6 or R1881 exposure. This is likely due to constitutive activation of Fer. This does not seem to be an effect of autocrine IL-6 production, since STAT3 is only activated in these cells upon IL-6 exposure, and all parts of the canonical IL-6/STAT3 signaling pathway (IL-6 receptor, Jak1/2) are expressed in 22RV1 cells [129]. On the other hand, they produce PDGF, which is known to activate Fer in fibroblasts and adipocytes [123, 130]. As the host lab reported that EGF and IGF-1 can also activate Fer in LNCaP cells, although to a lesser extent that IL-6, these growth factors could then activate AR Y223 phosphorylation [48]. The autocrine production of these growth factors has not been studied in 22RV1 cells [48, 131]. Testing diverse growth factors alone, in combination, or with the use of pV to create a more "oncogenic" milieu might help to understand the constitutive AR, AR-V7, and Fer activation in these cells. Fer knock-down would also be interesting, to investigate its implication on AR-V7 (vs AR) transcriptional activity and on growth, along with its effect on STAT3 activation and signaling, which we showed is regulated by IL-6.

2. IL-6 Mediated AR/STAT3 Interaction

To better understand crosstalks between the IL-6 and androgen pathways in PCa cells, we further studied the relation between STAT3 and AR. We showed that STAT3 is nuclear and phosphorylated (Y705) by IL-6, while it is unphosphorylated and cytoplasmic in R1881 treated LNCaP cells. The fact that both R1881 and IL-6 rapidly activate Fer (within 5-10 minutes), leading to phosphorylation of both TFs in the IL-6 pathway, while only AR, and not STAT3, is phosphorylated upon R1881 treatment, suggests that canonical pathways operate and lead to androgen/AR and IL-6/STAT3 transcriptional activation of distinct gene subsets. However, initial signaling events triggered by IL-6 and Fer would permit a merging of pathways via Fer/AR and Fer/STAT3 complexes formed up to the nucleus, as well as AR/STAT3 complexes. Fer was reported to regulate IL-6 mediated growth of PC3 (AR-) and LNCaP (AR+) cell lines.

Other TKs than Fer may intervene to regulate STAT3 activation in highly aggressive PCa, as exemplified in the 22RV1 model where STAT3 remains inactive in untreated cells while AR and Fer are activated. The strong inhibition of IL-6 mediated PC3 cell growth observed when each of Fer, Jak1, or Jak2 were knocked down (alone or in combination) supports a role of all three TKs in early activation kinetics of the IL-6/Fer/STAT3 pathway (unpublished results; Minho, C.). The fact that Fer directly phosphorylates STAT3 on Y705 *in vitro* and translocates to the nucleus [114] whereas Jaks remain in the cytoplasm support the intervention of Jaks prior to that of Fer. PTPs are also involved in the canonical IL-6 pathway, such as SHP2 (also known as PTPN11). SHP2 is also related to Fer in other contexts than PCa (Noonan syndrome, LEOPARD syndrome, vascular endothelial cells, and presynaptic development in the hippocampus) [132-134]. Further studies are required to understand how Fer may be coupled to Jaks and gp130 at the cell membrane and to other TKs or phosphatases controlling STAT3 activation.

Fer directly phosphorylates STAT3 and AR on Y705 and Y223 respectively and interacts with these motifs via its SH2 domain [114, 116]. We find that pY223AR and pSTAT3 also form a complex, which raised the question of whether pY223AR interacts with the SH2 domain of STAT3. However, prior to experiments, the likelihood of such an interaction was tested by several computational methods. Unfortunately, the NTD of AR has not been crystalized, and no good models could be produced because it is mostly disordered and has no homology with NTDs of other steroid hormone receptors [136]. The only SH2 domain known to bind the pY223 motif

of AR is that of Fer [116]. A BLASTp search showed no sequence similarity between the STAT3 and Fer SH2 domains [137]. We also compared by Scansite's Sequence Match and by BLASTp the STAT3 Y705 and AR Y223 motifs (since pY705 is bound by the STAT3 SH2 domain in homodimers), finding no similarity, even though both motifs can be bound by the Fer SH2 domain. Furthermore, Scansite's Motif Scan did not predict any SH2 domains binding to the AR pY223 site, although it did so for other sites, including Y534 (SH2 of PI3K regulatory subunit α); no SH2 domains were predicted to bind the STAT3 pY705 motif either, although its own SH2 domain is required for dimerization [138]. Considering these searches did not predict in any way the interactions which we had already found to be taking place, we kept these negative results in mind and interrogated AR/STAT3 interactions experimentally.

We demonstrated that pY223AR interacts with pSTAT3 in IL-6 treated LNCaP cells, but not R1881. In PCa cells, STAT3 activation by Y-phosphorylation is important since it allows STAT3 to translocate to the nucleus. Thus, when activated AR binds STAT3, the latter is activated. Our results showed that the STAT3 SH2 domain alone interacts with activated AR; the pY site of STAT3 is not involved in this interaction. This is in line with reports showing AR genomic reorientation in CRPC patients, with AR binding to sites associated with STATs, while AR ChIP-seq on R1881 treated LNCaP cells did not show this same shift in AR binding [39]. This may be explained by the lack of an AR/STAT3 interaction in R1881 treated LNCaP cells, as STAT3 is not phosphorylated and remains cytoplasmic.

The IL-6 induced interaction of STAT3 with AR-V7 in 22RV1 cells is also an important finding, showing that the crosstalks between the IL-6 and androgen pathways can extend to AR-Vs, which have been shown to control a subset of genes transcriptionally regulated by full-length AR [34] and distinct from androgen-independent AR-FL signaling [150]. The lack of an interaction between AR-V7 and STAT3 in untreated 22RV1 cells also shows the importance of STAT3 phosphorylation, which allows nuclear translocation of STAT3 for the interaction to take place. Complementary studies on IL-6 effects on 22RV1 cell growth will follow, showing the effect of STAT3 activation when AR and Fer are already active.

AR-Vs confer resistance to antiandrogens such as enzalutamide, a drug which targets the AR LBD absent in most AR-Vs [34, 36, 139]. AR transcriptional activation in the IL-6 pathway has also been shown to cause resistance to abiraterone and enzalutamide [56, 140]. The

AR/STAT3 interaction is via pY223, in the AF-1 region of the AR NTD necessary for transactivation. This region has already become a potential drug target, because it would bypass resistance mechanisms and potentially target all forms of AR. Advances have been made, although structure-based drug design is problematic because the NTD is disordered [139].

Along these lines, Sintokamide A is part of a family of chlorinated peptides which inhibit AR transcriptional activity by binding to the AF-1 region. Its inhibition is not limited to AR-FL; it blocks activity of AR-V7 and AR-V12 as well. It has been shown to cause regression of AR-positive CRPC xenograft tumors [141]. The EPI family of compounds also bind the AF-1 region of AR and show similar results for specificity and in xenograft tumors [139]. Nevertheless, these two compounds do not bind at the same position in the AR AF-1 domain, as shown by their additive effect in inhibition of AR transcriptional activity. EPI compounds have been shown by nuclear magnetic resonance spectroscopy (NMR) to bind to specific stretches of the Tau-5 (aa 361−537) region in AF-1 [136], while Sintokamide binding has not been further characterized. Interestingly, EPI can inhibit IL-6 mediated AR transcriptional activity and the IL-6 induced interaction between AR and STAT3, while Sintokamide cannot [141]. This means that targeting different parts of the AR NTD (alone or in combination) leads to a broader inhibition of AR activity, as it can target variants, bypass certain point mutations, and stop the activation of AR downstream of various upregulated growth factor and cytokine signaling pathways by binding to different residues of AR.

3. Implication of Other TFs

In line with the study on AR ChIP data from tumors of CRPC cases [39], we searched for AR interactions with c-Myc and E2F1. We found interactions of c-Myc with AR at a basal level, which increased upon IL-6, but not R1881, exposure of LNCaP cells; for E2F1, there was an interaction upon IL-6 or R1881 treatment of cells. These interactions could explain the reorientation of AR DNA binding from known AREs towards DNA sites associated with Myc and E2F [39]. Since E2F1 is known to inhibit androgen-dependent AR activity in LNCaP cells, it would be important to determine whether their interactions result in transcriptional repression or activation in the context of IL-6 vs R1881 [87, 96].

Another meaningful finding is that the AR pY223 motif is necessary for interactions to take place with c-Myc and important for interactions with E2F1 as well. It is not clear which motifs or domains in these TFs would be involved in these interactions, as neither c-Myc nor E2F1 have domains known to bind to pY-motifs. These sites may be viewed as druggavle to block aberrant TF interactions in advanced PCa.

The pY223 motif of AR might not be directly bound to these TFs; other parts of AR might be involved, although the pY223 site would still be necessary (possibly allowing AR translocation to the nucleus in the absence of androgens). Other proteins may also be involved in the complexes between AR and these TFs. *In vitro* binding assays of c-Myc and E2F1 with AR and ARY223F (or specific parts of these proteins) would help to find the domains involved, and whether other proteins are necessary. AR activation might also be causing conformational changes in the AR NTD, allowing for stable interactions with other TFs. NMR studies of AR vs pY223AR NTD, as done for EPI binding to the AR NTD, would show whether there is an important conformational shift in the partially structured stretches upon phosphorylation [136].

Because R1881 triggers an interaction between E2F1 and pY223AR in LNCaP cells, it will be important to determine whether the pY223 of AR is involved in this context, as it is in IL-6. This could be achieved using the methodology developed in this project: co-transfection of PC3 cells with WT vs mutant *AR* cDNA and tagged *E2F1* cDNA, followed by R1881 treatment and IP/western blotting experiments to seek an interaction.

These experiments with mutant AR would also reveal whether non-phosphorylated AR is nuclear and able to form homodimers, as it would occur in normal differentiated luminal cells of the prostate which do not express Fer. As the context may matter, similar experiments may be carried out in less aggressive cells than PC3 (or in normal cells), alongside LNCaP cells knocked down for Fer and treated with R1881.

4. Y-phosphorylation of c-Myc and E2F1

In our search for novel pY-TFs in PCa, we found that c-Myc is Y-phosphorylated in LNCaP and PC3 cells in various conditions, and that this can be done directly by Fer *in vitro*.

These findings are in line with the c-Myc Y-phosphorylation on multiple sites by Abl kinase, as reported in the HEK293 normal kidney cell line [125]. The authors have also shown that pY74 c-Myc is expressed in the cytoplasm of multiple cell lines, and in breast and ovarian cancers [125]. We find that Y-phosphorylation of c-Myc is highest upon FBS or pV exposure of cells, which might be due to the combined effects of Fer, Abl, and possibly other kinases, on the same or different Y residues. Testing other pathways in which these kinases are involved would be important for determining the relevance of c-Myc Y-phosphorylation in PCa, and whether it affects its transcriptional activity or binding partners. Future studies would include known partners of c-Myc: MAX and MAD.

E2F1 Y-phosphorylation upon pV exposure was also observed for the first time. Since we only find it modified when PTPs are inhibited (and TKs maximally activated), we assume that we have not found the pathway in which its phosphorylation would be most important. Testing an array of kinases *in vitro* would be necessary for determining which is responsible for E2F1 Y-phosphorylation; this would also allow us to find the pathway in which activated E2F1 is involved, and study the implications thereof.

Proteomic approaches would identify partners of the Y-phosphorylated c-Myc and E2F1, whereas synthetic phosphor-peptides would be helpful in validating the identified Y residues. Additional studies and IP/ID experiments would help to clarify the role of other Y-phosphorylated proteins with which they interact.

Knowing the Y residue being phosphorylated would also help in determining the role of these modifications. We performed a search for the Y residues in these proteins most likely to be phosphorylated using the NetPhos 3.1 algorithm, which calculates the likelihood of phosphorylation by specific (or unspecified) kinases (Table 3) [142]. These predicted residues should be taken as a starting point, but may not necessarily be observed considering that the same algorithm predicted the phosphorylation of AR on Y223 (score of 0.901) but not that of STAT3 on Y705 (score of 0.431) which activation in the canonical Il-6 pathway is required for pSTAT3 homodimerization and binding to DNA for transcriptional activation [142].

For c-Myc, the predicted residues most likely Y-phosphorylated are found in the NTD, which is important for c-Myc transactivation of target genes [75]. They also correspond to the Y-

residues identified in c-Myc. For E2F1, the residues were in various domains. Y100 is in the cyclin A binding domain (inhibition of DNA binding and transactivation), Y128 is in the DBD, and Y411 in the transactivation domain and pRB binding domain (negative regulator of E2F1) [143].

c-Myc			
Residue	**Context**	**Score**	**Kinase**
16 Y	YDLDYDSVQ	0.967	Unspecified
16 Y	YDLDYDSVQ	0.543	INSR
16 Y	YDLDYDSVQ	0.528	EGFR
32 Y	EENFYQQQQ	0.843	Unspecified
32 Y	EENFYQQQQ	0.647	EGFR
32 Y	EENFYQQQQ	0.526	SRC
74 Y	CSPSYVAVT	0.977	Unspecified
74 Y	CSPSYVAVT	0.510	EGFR
74 Y	CSPSYVAVT	0.501	SRC
E2F1			
Residue	**Context**	**Score**	**Kinase**
100 Y	TDHQYLAES	0.504	INSR
128 Y	EKSRYETSL	0.952	unspecified
128 Y	EKSRYETSL	0.516	INSR
411 Y	EALDYHFGL	0.486	unspecified

Table 3: Prediction of c-Myc and E2F1 pY residues

NetPhos 3.1 results for c-Myc (*top*) and E2F1 (*bottom*) Y-phosphorylation for the three highest scoring residues by specific or unspecified kinases.

We chose to study c-Myc and E2F1 primarily because of their known over-expression in PCa, as showed in this thesis for c-Myc. A few other members of these TF families deserve consideration and would be integrated in future studies as potential candidates for AR partners in PCa. These types of studies would also culminate in ChIP sequencing experiments. The Y-phosphorylation of TFs is also an important research avenue deserving deeper study.

5. Clinical Relevance of STAT3 and c-Myc Expression in PCa

The TK Fer and its substrates AR and STAT3 are part of interrelated complexes where activation by Y-phosphorylation is key for signaling. We designed and generated Abs to investigate how they act in term of mechanisms, but also to determine their clinical significance as biomarkers predicting patient outcome. Of the series Fer/pY714Fer, AR/pY223AR and STAT3/pY705STAT3, STAT3 nuclear expression in tumor cells remained to be studied and was thus integrated into this project. c-Myc was also studied here because of its proposed relationship with AR.

For STAT3, most studies so far have looked at its activation (pY705STAT3) instead of its expression in PCa samples. One study looking at STAT3 expression found that it is higher in PCa than in BPH [49]; another found high (3+) expression of STAT3 in 94.5% of tumors, and therefore looked at pSTAT3 levels instead [50]. We found that STAT3 nuclear expression, as assessed in the CHUM TMA, showed that it is predictive of BCR. The enhanced prognostic value of STAT3 expression when used in combination with pY223AR or pY714Fer for BCR (unpublished observations) is further proof of the importance of targeting this pathway.

The literature on c-Myc indicates that its nuclear expression is strongly positive in PIN and PCa compared to the matched normal epithelium, and that it correlates with tumor stage, presence of metastases, and two year overall survival [70] [71]. Genomic gain and elevated c-Myc mRNA have been shown to be predictive of BCR as well [67, 69]. Here, we find that c-Myc nuclear expression is predictive of BCR, as assessed in the CHUM RP cohort, and its combination to pY223AR expression performs better in predicting BCR than when used alone.

The combination of pY223AR, pY714Fer, Fer, STAT3, and c-Myc as biomarkers showed better prognostic value for BCR (unpublished data). This is an important finding, since the goal is to come up with an array of biomarkers to apply on biopsies to better stratify patients and offer optimal management or therapeutic options. These results also add clinical significance to our biochemical findings and further promote Fer and newly identified TF complexes as novel therapeutic targets for advanced PCa.

CONCLUSION

In CRPC patients, androgenic stimulation is sparse due to ADT. Eventually, most tumor cells that express AR adapt under selective pressure, generally by reactivating AR transcriptional activity by a variety of mechanisms. Tumors are exposed to many growth factors and cytokines, some of which allow androgen-independent Fer-mediated AR activation. This results in AR transcriptional activity different from what is expected in the canonical androgen/AR axis. Here, we showed IL-6 induced AR activation, leading to novel AR interactions with STAT3, c-Myc, and E2F1, which is in line with a reorientation of AR DNA binding from known AREs to motifs associated with members of these TF families in CRPC. The formation of these aberrant complexes might also alter DNA binding sites of STAT3, c-Myc, and E2F1.

Fer is responsible for the phosphorylation of AR, STAT3, and c-Myc. In the case of AR and STAT3, activated AR interacts with STAT3 via its SH2 domain and translocate to the nucleus. We propose that Fer keeps these TFs (and likely others) Y-phosphorylated in the nucleus, thereby allowing them to form aberrant complexes with each other, resulting in novel interactions, as we have shown. Thus, this mechanism may allow the integration of many signals emanating from different upregulated signaling pathways in CRPC, resulting in the reorientation of genomic programs, and thereby contributing to alterations of cell phenotypes that favor PCa progression. Fer may be a novel drug target. Its inhibition would stop IL-6 mediated cell growth through STAT3 signaling (in both AR- and AR+ cells), as well as AR transcriptional activation and interactions with various TFs.

CHAPTER 9: References

1. Aaron, L., O. Franco, and S.W. Hayward, *Review of Prostate Anatomy and Embryology and the Etiology of BPH.* The Urologic clinics of North America, 2016. **43**(3): p. 279-288.
2. Bhavsar, A. and S. Verma, *Anatomic Imaging of the Prostate.* BioMed Research International, 2014. **2014**: p. 728539.
3. Zhou, Y., E.C. Bolton, and J.O. Jones, *Androgens and androgen receptor signaling in prostate tumorigenesis.* Journal of Molecular Endocrinology, 2015. **54**(1): p. R15-R29.
4. Yu, S., et al., *Altered Prostate Epithelial Development in Mice Lacking the Androgen Receptor in Stromal Fibroblasts.* The Prostate, 2012. **72**(4): p. 437-449.
5. Wen, S., et al., *Stromal Androgen Receptor Roles in the Development of Normal Prostate, Benign Prostate Hyperplasia, and Prostate Cancer.* The American Journal of Pathology, 2015. **185**(2): p. 293-301.
6. Statistics, C.C.S.s.A.C.o.C., *Canadian Cancer Statistics 2017*. 2017, Canadian Cancer Society: Toronto, ON.
7. Ayyıldız, S.N. and A. Ayyıldız, *PSA, PSA derivatives, proPSA and prostate health index in the diagnosis of prostate cancer.* Turkish journal of urology, 2014. **40**(2): p. 82-88.
8. Pezaro, C., H.H. Woo, and I.D. Davis, *Prostate cancer: measuring PSA*. Internal Medicine Journal, 2014. **44**(5): p. 433-440.
9. Samaratunga, H., et al., *From Gleason to International Society of Urological Pathology (ISUP) grading of prostate cancer.* Scandinavian Journal of Urology, 2016. **50**(5): p. 325-329.
10. Epstein, J.I., et al., *The 2014 International Society of Urological Pathology (ISUP) Consensus Conference on Gleason Grading of Prostatic Carcinoma: Definition of Grading Patterns and Proposal for a New Grading System.* The American Journal of Surgical Pathology, 2016. **40**(2): p. 244-252.
11. Cheng, L., et al., *Staging of prostate cancer.* Histopathology, 2012. **60**(1): p. 87-117.
12. Litwin, M.S. and H. Tan, *The diagnosis and treatment of prostate cancer: A review.* JAMA, 2017. **317**(24): p. 2532-2542.

13. Ramsay, Alison K. and Hing Y. LEUNG, *Signalling pathways in prostate carcinogenesis: potentials for molecular-targeted therapy.* Clinical Science, 2009. **117**(6): p. 209-228.
14. Karantanos, T., P.G. Corn, and T.C. Thompson, *Prostate cancer progression after androgen deprivation therapy: mechanisms of castrate-resistance and novel therapeutic approaches.* Oncogene, 2013. **32**(49): p. 5501-5511.
15. Quero, L., et al., *The androgen receptor for the radiation oncologist.* Cancer/Radiothérapie, 2015. **19**(3): p. 220-227.
16. van Royen, M.E., et al., *Stepwise androgen receptor dimerization.* Journal of Cell Science, 2012. **125**(8): p. 1970-1979.
17. van der Steen, T., D.J. Tindall, and H. Huang, *Posttranslational Modification of the Androgen Receptor in Prostate Cancer.* International Journal of Molecular Sciences, 2013. **14**(7): p. 14833-14859.
18. Patel, N.K., et al., *Advanced prostate cancer – patient survival and potential impact of enzalutamide and other emerging therapies.* Therapeutics and Clinical Risk Management, 2014. **10**: p. 651-664.
19. Tan, M.H.E., et al., *Androgen receptor: structure, role in prostate cancer and drug discovery.* Acta Pharmacologica Sinica, 2015. **36**(1): p. 3-23.
20. Zhang, G., et al., *Androgen receptor splice variants circumvent AR blockade by microtubule-targeting agents.* Oncotarget, 2015. **6**(27): p. 23358-23371.
21. Thadani-Mulero, M., et al., *Androgen Receptor Splice Variants Determine Taxane Sensitivity in Prostate Cancer.* Cancer research, 2014. **74**(8): p. 2270-2282.
22. Lavery, Derek N. and Iain J. McEwan, *Structure and function of steroid receptor AF1 transactivation domains: induction of active conformations.* Biochemical Journal, 2005. **391**(Pt 3): p. 449-464.
23. Davey, R.A. and M. Grossmann, *Androgen Receptor Structure, Function and Biology: From Bench to Bedside.* The Clinical Biochemist Reviews, 2016. **37**(1): p. 3-15.
24. Chamberlain, N.L., D.C. Whitacre, and R.L. Miesfeld, *Delineation of Two Distinct Type 1 Activation Functions in the Androgen Receptor Amino-terminal Domain.* Journal of Biological Chemistry, 1996. **271**(43): p. 26772-26778.

25. Jenster, G., et al., *Identification of Two Transcription Activation Units in the N-terminal Domain of the Human Androgen Receptor.* Journal of Biological Chemistry, 1995. **270**(13): p. 7341-7346.
26. Simental, J.A., et al., *Transcriptional activation and nuclear targeting signals of the human androgen receptor.* Journal of Biological Chemistry, 1991. **266**(1): p. 510-518.
27. Huggins, C., *Endocrine-Induced Regression of Cancers.* Science, 1967. **156**(3778): p. 1050-1054.
28. Huggins, C., et al., *Studies on prostatic cancer: Ii. the effects of castration on advanced carcinoma of the prostate gland.* Archives of Surgery, 1941. **43**(2): p. 209-223.
29. Chandrasekar, T., et al., *Mechanisms of resistance in castration-resistant prostate cancer (CRPC).* Translational Andrology and Urology, 2015. **4**(3): p. 365-380.
30. Pelekanou, V. and E. Castanas, *Androgen Control in Prostate Cancer.* Journal of Cellular Biochemistry, 2016. **117**(10): p. 2224-2234.
31. Caffo, O., et al., *Splice Variants of Androgen Receptor and Prostate Cancer.* Oncology Reviews, 2016. **10**(1): p. 297.
32. Azoitei, A., et al., *C-terminally truncated constitutively active androgen receptor variants and their biologic and clinical significance in castration-resistant prostate cancer.* The Journal of Steroid Biochemistry and Molecular Biology, 2016.
33. Xu, D., et al., *Androgen receptor splice variants dimerize to transactivate target genes.* Cancer research, 2015. **75**(17): p. 3663-3671.
34. Li, Y., et al., *Androgen receptor splice variants mediate enzalutamide resistance in castration-resistant prostate cancer cell lines.* Cancer research, 2013. **73**(2): p. 483-489.
35. Qu, Y., et al., *Constitutively Active AR-V7 Plays an Essential Role in the Development and Progression of Castration-Resistant Prostate Cancer.* Scientific Reports, 2015. **5**: p. 7654.
36. Antonarakis, E.S., et al., *AR-V7 and Resistance to Enzalutamide and Abiraterone in Prostate Cancer.* New England Journal of Medicine, 2014. **371**(11): p. 1028-1038.
37. Antonarakis, E.S., et al., *Androgen Receptor Splice Variant 7 and Efficacy of Taxane Chemotherapy in Patients With Metastatic Castration-Resistant Prostate Cancer.* JAMA oncology, 2015. **1**(5): p. 582-591.

38. Desai, S.J., et al., *Inappropriate Activation of the Androgen Receptor by Nonsteroids: Involvement of the Src Kinase Pathway and Its Therapeutic Implications.* Cancer Research, 2006. **66**(21): p. 10449-10459.
39. Sharma, Naomi L., et al., *The Androgen Receptor Induces a Distinct Transcriptional Program in Castration-Resistant Prostate Cancer in Man.* Cancer Cell, 2013. **23**(1): p. 35-47.
40. Massie, C.E., et al., *The androgen receptor fuels prostate cancer by regulating central metabolism and biosynthesis.* The EMBO Journal, 2011. **30**(13): p. 2719-2733.
41. Drake, Justin M., et al., *Phosphoproteome Integration Reveals Patient-Specific Networks in Prostate Cancer.* Cell, 2016. **166**(4): p. 1041-1054.
42. Mills, I.G., *Maintaining and reprogramming genomic androgen receptor activity in prostate cancer.* Nat Rev Cancer, 2014.
43. Matsuda, T., et al., *Signal transducer and activator of transcription 3 regulation by novel binding partners.* World Journal of Biological Chemistry, 2015. **6**(4): p. 324-332.
44. Shoelson, S.E., *SH2 and PTB domain interactions in tyrosine kinase signal transduction.* Current Opinion in Chemical Biology, 1997. **1**(2): p. 227-234.
45. Zouein, F.A., et al., *Pivotal Importance of STAT3 in Protecting the Heart from Acute and Chronic Stress: New Advancement and Unresolved Issues.* Frontiers in Cardiovascular Medicine, 2015. **2**: p. 36.
46. Culig, Z., et al., *Interleukin-6 regulation of prostate cancer cell growth.* Journal of Cellular Biochemistry, 2005. **95**(3): p. 497-505.
47. Heinrich, P.C., et al., *Interleukin-6-type cytokine signalling through the gp130/Jak/STAT pathway.* Biochemical Journal, 1998. **334**(Pt 2): p. 297-314.
48. Rocha, J., *The FER Tyrosine Kinase: An Integrator Of Growth-Promoting Factors And Androgens Signaling To Transcription Factors In Prostate Cancer*, in *Faculty of Medicine, Division of Surgical Research*. 2013, McGill University: Montreal. p. 251.
49. Singh, N., et al., *Overexpression of signal transducer and activator of transcription (STAT-3 and STAT-5) transcription factors and alteration of suppressor of cytokine signaling (SOCS-1) protein in prostate cancer.* Journal of Receptors and Signal Transduction, 2012. **32**(6): p. 321-327.

50. Horinaga, M., et al., *Clinical and pathologic significance of activation of signal transducer and activator of transcription 3 in prostate cancer.* Urology, 2005. **66**(3): p. 671-675.
51. Giri, D., M. Ozen, and M. Ittmann, *Interleukin-6 Is an Autocrine Growth Factor in Human Prostate Cancer.* The American Journal of Pathology, 2001. **159**(6): p. 2159-2165.
52. Tam, L., et al., *Expression levels of the JAK/STAT pathway in the transition from hormone-sensitive to hormone-refractory prostate cancer.* British Journal of Cancer, 2007. **97**(3): p. 378-383.
53. Okamoto, M., C. Lee, and R. Oyasu, *Interleukin-6 as a Paracrine and Autocrine Growth Factor in Human Prostatic Carcinoma Cells in Vitro.* Cancer Research, 1997. **57**(1): p. 141-146.
54. Mora, L.B., et al., *Constitutive Activation of Stat3 in Human Prostate Tumors and Cell Lines: Direct Inhibition of Stat3 Signaling Induces Apoptosis of Prostate Cancer Cells.* Cancer Research, 2002. **62**(22): p. 6659-6666.
55. Culig, Z. and M. Puhr, *Interleukin-6: A multifunctional targetable cytokine in human prostate cancer.* Molecular and Cellular Endocrinology, 2012. **360**(1-2): p. 52-58.
56. Liu, C., et al., *Inhibition of constitutively active Stat3 reverses enzalutamide resistance in LNCaP derivative prostate cancer cells.* The Prostate, 2014. **74**(2): p. 201-209.
57. Wu, C.-T., et al., *The role of IL-6 in the radiation response of prostate cancer.* Radiation Oncology (London, England), 2013. **8**: p. 159-159.
58. Gabay, M., Y. Li, and D.W. Felsher, *MYC Activation Is a Hallmark of Cancer Initiation and Maintenance.* Cold Spring Harbor Perspectives in Medicine, 2014. **4**(6).
59. Cascón, A. and M. Robledo, *MAX and MYC: A Heritable Breakup.* Cancer Research, 2012. **72**(13): p. 3119-3124.
60. Dang, C.V., *MYC on the Path to Cancer.* Cell, 2012. **149**(1): p. 22-35.
61. Antony, L., et al., *Androgen Receptor (AR) Suppresses Normal Human Prostate Epithelial Cell Proliferation via AR/β-catenin/TCF-4 Complex Inhibition of c-MYC Transcription.* The Prostate, 2014. **74**(11): p. 1118-1131.
62. Massagué, J., S.W. Blain, and R.S. Lo, *TGFβ Signaling in Growth Control, Cancer, and Heritable Disorders.* Cell, 2000. **103**(2): p. 295-309.

63. Wang, J., et al., *B-Raf activation cooperates with PTEN loss to drive c-Myc expression in advanced prostate cancer.* Cancer research, 2012. **72**(18): p. 4765-4776.
64. Karanika, S., et al., *DNA damage response and prostate cancer: defects, regulation and therapeutic implications.* Oncogene, 2015. **34**(22): p. 2815-2822.
65. Zeman, M.K. and K.A. Cimprich, *Causes and consequences of replication stress.* Nat Cell Biol, 2014. **16**(1): p. 2-9.
66. Dong, J.-T., *Prevalent mutations in prostate cancer.* Journal of Cellular Biochemistry, 2006. **97**(3): p. 433-447.
67. Zafarana, G., et al., *Copy number alterations of c-MYC and PTEN are prognostic factors for relapse after prostate cancer radiotherapy.* Cancer, 2012. **118**(16): p. 4053-4062.
68. Seed, G., et al., *Gene Copy Number Estimation From Targeted Next Generation Sequencing Of Prostate Cancer Biopsies: Analytic Validation and Clinical Qualification.* Clinical Cancer Research, 2017.
69. Hawksworth, D., et al., *Overexpression of C-MYC oncogene in prostate cancer predicts biochemical recurrence.* Prostate Cancer Prostatic Dis, 2010. **13**(4): p. 311-315.
70. Gurel, B., et al., *Nuclear MYC Protein Overexpression is an Early Alteration in Human Prostate Carcinogenesis.* Modern pathology : an official journal of the United States and Canadian Academy of Pathology, Inc, 2008. **21**(9): p. 1156-1167.
71. Zeng, W., et al., *Nuclear C-MYC expression level is associated with disease progression and potentially predictive of two year overall survival in prostate cancer.* International Journal of Clinical and Experimental Pathology, 2015. **8**(2): p. 1878-1888.
72. Udager, A.M., et al., *Concurrent nuclear ERG and MYC protein overexpression defines a subset of locally advanced prostate cancer: Potential opportunities for synergistic targeted therapeutics.* The Prostate, 2016. **76**(9): p. 845-853.
73. Gao, L., et al., *Androgen Receptor Promotes Ligand-Independent Prostate Cancer Progression through c-Myc Upregulation.* PLoS ONE, 2013. **8**(5): p. e63563.
74. Barfeld, S.J., et al., *c-Myc Antagonises the Transcriptional Activity of the Androgen Receptor in Prostate Cancer Affecting Key Gene Networks.* EBioMedicine, 2017. **18**: p. 83-93.

75. Albihn, A., J.I. Johnsen, and M. Arsenian Henriksson, *Chapter 6 - MYC in Oncogenesis and as a Target for Cancer Therapies*, in *Advances in Cancer Research*, F.V.W. George and K. George, Editors. 2010, Academic Press. p. 163-224.
76. Rebello, R.J., et al., *Therapeutic Approaches Targeting MYC-Driven Prostate Cancer.* Genes, 2017. **8**(2): p. 71.
77. Whitfield, J.R., M.-E. Beaulieu, and L. Soucek, *Strategies to Inhibit Myc and Their Clinical Applicability.* Frontiers in Cell and Developmental Biology, 2017. **5**: p. 10.
78. Beltran, H., et al., *Molecular Characterization of Neuroendocrine Prostate Cancer and Identification of New Drug Targets.* Cancer discovery, 2011. **1**(6): p. 487-495.
79. Lee, John K., et al., *N-Myc Drives Neuroendocrine Prostate Cancer Initiated from Human Prostate Epithelial Cells.* Cancer Cell, 2016. **29**(4): p. 536-547.
80. Dardenne, E., et al., *N-Myc Induces an EZH2-Mediated Transcriptional Program Driving Neuroendocrine Prostate Cancer.* Cancer Cell, 2016. **30**(4): p. 563-577.
81. Beltran, H., *The N-myc Oncogene: Maximizing its Targets, Regulation, and Therapeutic Potential.* Molecular Cancer Research, 2014. **12**(6): p. 815-822.
82. Sidaway, P., *Prostate cancer: N-Myc expression drives neuroendocrine disease.* Nat Rev Urol, 2016. **13**(12): p. 695-695.
83. Meng, P. and R. Ghosh, *Transcription addiction: can we garner the Yin and Yang functions of E2F1 for cancer therapy?* Cell Death & Disease, 2014. **5**(8): p. e1360.
84. Udayakumar, T., et al., *The E2F1/Rb and p53/MDM2 Pathways in DNA Repair and Apoptosis: Understanding the Crosstalk to Develop Novel Strategies for Prostate Cancer Radiotherapy.* Seminars in Radiation Oncology, 2010. **20**(4): p. 258-266.
85. Pützer, B.M., *E2F1 death pathways as targets for cancer therapy.* Journal of Cellular and Molecular Medicine, 2007. **11**(2): p. 239-251.
86. Pützer, B.M. and D. Engelmann, *E2F1 apoptosis counterattacked: evil strikes back.* Trends in Molecular Medicine, 2013. **19**(2): p. 89-98.
87. Davis, J.N., et al., *Elevated E2F1 Inhibits Transcription of the Androgen Receptor in Metastatic Hormone-Resistant Prostate Cancer.* Cancer Research, 2006. **66**(24): p. 11897-11906.
88. Malhotra, S., et al., *A Tri-Marker Proliferation Index Predicts Biochemical Recurrence after Surgery for Prostate Cancer.* PLoS ONE, 2011. **6**(5): p. e20293.

89. Liang, Y., Lu, J., Mo, R., He, H., Xie, J., Jiang, F., Lin, Z., Chen, Y., Wu, Y., Luo, H., Luo, Z., Zhong, W., *E2F1 promotes tumor cell invasion and migration through regulating CD147 in prostate cancer.* International Journal of Oncology, 2016. **48**(4): p. 1650-1658.

90. Poppy Roworth, A., F. Ghari, and N.B. La Thangue, *To live or let die – complexity within the E2F1 pathway.* Molecular & Cellular Oncology, 2015. **2**(1): p. e970480.

91. Ren, Z., et al., *E2F1 renders prostate cancer cell resistant to ICAM-1 mediated antitumor immunity by NF-κB modulation.* Molecular Cancer, 2014. **13**: p. 84-84.

92. Libertini, S.J., et al., *E2F1 expression in LNCaP prostate cancer cells deregulates androgen dependent growth, suppresses differentiation, and enhances apoptosis.* The Prostate, 2006. **66**(1): p. 70-81.

93. Udayakumar, T.S., et al., *Antisense MDM2 Enhances E2F1-Induced Apoptosis and The Combination Sensitizes Androgen Dependent and Independent Prostate Cancer Cells To Radiation.* Molecular cancer research : MCR, 2008. **6**(11): p. 1742-1754.

94. Udayakumar, T.S., et al., *ADENOVIRAL E2F1 OVEREXPRESSION SENSITIZES LNCAP AND PC3 PROSTATE TUMOR CELLS TO RADIATION IN VIVO.* International journal of radiation oncology, biology, physics, 2011. **79**(2): p. 549-558.

95. Kumar, A., et al., *Substantial interindividual and limited intraindividual genomic diversity among tumors from men with metastatic prostate cancer.* Nat Med, 2016. **22**(4): p. 369-378.

96. Valdez, C.D., et al., *Repression of Androgen Receptor Transcription through the E2F1/DNMT1 Axis.* PLoS ONE, 2011. **6**(9): p. e25187.

97. Altintas, D.M., et al., *Direct Cooperation Between Androgen Receptor and E2F1 Reveals a Common Regulation Mechanism for Androgen-Responsive Genes in Prostate Cells.* Molecular Endocrinology, 2012. **26**(9): p. 1531-1541.

98. Akamatsu, S., et al., *The Placental Gene PEG10 Promotes Progression of Neuroendocrine Prostate Cancer.* Cell Reports, 2015. **12**(6): p. 922-936.

99. Olsson, A.Y., et al., *Role of E2F3 expression in modulating cellular proliferation rate in human bladder and prostate cancer cells.* Oncogene, 2006. **26**(7): p. 1028-1037.

100. Tao, T., et al., *Autoregulatory feedback loop of EZH2/miR-200c/E2F3 as a driving force for prostate cancer development.* Biochimica et Biophysica Acta (BBA) - Gene Regulatory Mechanisms, 2014. **1839**(9): p. 858-865.
101. Pipinikas, C.P., et al., *Measurement of blood E2F3 mRNA in prostate cancer by quantitative RT-PCR: a preliminary study.* Biomarkers, 2007. **12**(5): p. 541-557.
102. Foster, C.S., et al., *Transcription factor E2F3 overexpressed in prostate cancer independently predicts clinical outcome.* Oncogene, 2004. **23**(35): p. 5871-5879.
103. Drake, J.M., et al., *Oncogene-specific activation of tyrosine kinase networks during prostate cancer progression.* Proceedings of the National Academy of Sciences, 2012. **109**(5): p. 1643-1648.
104. Durocher, Y., A. Chapdelaine, and S. Chevalier, *Tyrosine Protein Kinase Activity of Human Hyperplastic Prostate and Carcinoma Cell Lines PC3 and DU145.* Cancer Research, 1989. **49**(17): p. 4818-4823.
105. Landry, F., et al., *Phosphotyrosine Antibodies Preferentially React with Basal Epithelial Cells in the Dog Prostate.* The Journal of Urology, 1996. **155**(1): p. 386-390.
106. Bourassa, C., et al., *Prostatic epithelial cells in culture: Phosphorylation of protein tyrosyl residues and tyrosine protein kinase activity.* Journal of Cellular Biochemistry, 1991. **46**(4): p. 291-301.
107. Allard, P., et al., *Links between Fer tyrosine kinase expression levels and prostate cell proliferation.* Molecular and Cellular Endocrinology, 2000. **159**(1–2): p. 63-77.
108. Liu, S., et al., *F-BAR family proteins, emerging regulators for cell membrane dynamic changes—from structure to human diseases.* Journal of Hematology & Oncology, 2015. **8**: p. 47.
109. Greer, P., *Closing in on the biological functions of fps/fes and fer.* Nat Rev Mol Cell Biol, 2002. **3**(4): p. 278-289.
110. Oh, M.-A., et al., *Specific tyrosine phosphorylation of focal adhesion kinase mediated by Fer tyrosine kinase in suspended hepatocytes.* Biochimica et Biophysica Acta (BBA) - Molecular Cell Research, 2009. **1793**(5): p. 781-791.
111. Guo, C. and G.R. Stark, *FER tyrosine kinase (FER) overexpression mediates resistance to quinacrine through EGF-dependent activation of NF-κB.* Proceedings of the National Academy of Sciences of the United States of America, 2011. **108**(19): p. 7968-7973.

112. Lennartsson, J., et al., *The Fer Tyrosine Kinase Is Important for Platelet-derived Growth Factor-BB-induced Signal Transducer and Activator of Transcription 3 (STAT3) Protein Phosphorylation, Colony Formation in Soft Agar, and Tumor Growth in Vivo.* The Journal of Biological Chemistry, 2013. **288**(22): p. 15736-15744.

113. Priel-Halachmi, S., et al., *FER Kinase Activation of Stat3 Is Determined by the N-terminal Sequence.* Journal of Biological Chemistry, 2000. **275**(37): p. 28902-28910.

114. Zoubeidi, A., et al., *The Fer Tyrosine Kinase Cooperates with Interleukin-6 to Activate Signal Transducer and Activator of Transcription 3 and Promote Human Prostate Cancer Cell Growth.* Molecular Cancer Research, 2009. **7**(1): p. 142-155.

115. Chen, T., L.H. Wang, and W.L. Farrar, *Interleukin 6 Activates Androgen Receptor-mediated Gene Expression through a Signal Transducer and Activator of Transcription 3-dependent Pathway in LNCaP Prostate Cancer Cells.* Cancer Research, 2000. **60**(8): p. 2132-2135.

116. Rocha, J., et al., *The Fer tyrosine kinase acts as a downstream interleukin-6 effector of androgen receptor activation in prostate cancer.* Molecular and Cellular Endocrinology, 2013. **381**(1–2): p. 140-149.

117. Mostaghel, E.A., et al., *Intraprostatic Androgens and Androgen-Regulated Gene Expression Persist after Testosterone Suppression: Therapeutic Implications for Castration-Resistant Prostate Cancer.* Cancer Research, 2007. **67**(10): p. 5033-5041.

118. Sellers, W.R., et al., *Stable binding to E2F is not required for the retinoblastoma protein to activate transcription, promote differentiation, and suppress tumor cell growth.* Genes & Development, 1998. **12**(1): p. 95-106.

119. Vo, B.T., et al., *The interaction of Myc with Miz1 defines medulloblastoma subgroup identity.* Cancer cell, 2016. **29**(1): p. 5-16.

120. Choudhury, K.R., et al., *A Robust Automated Measure of Average Antibody Staining in Immunohistochemistry Images.* Journal of Histochemistry and Cytochemistry, 2010. **58**(2): p. 95-107.

121. Budczies, J., et al., *Cutoff Finder: A Comprehensive and Straightforward Web Application Enabling Rapid Biomarker Cutoff Optimization.* PLOS ONE, 2012. **7**(12): p. e51862.

122. Hao, Q.L., N. Heisterkamp, and J. Groffen, *Isolation and sequence analysis of a novel human tyrosine kinase gene.* Molecular and Cellular Biology, 1989. **9**(4): p. 1587-1593.
123. Iwanishi, M., M.P. Czech, and A.D. Cherniack, *The Protein-tyrosine Kinase Fer Associates with Signaling Complexes Containing Insulin Receptor Substrate-1 and Phosphatidylinositol 3-Kinase.* Journal of Biological Chemistry, 2000. **275**(50): p. 38995-39000.
124. Ueda, T., N. Bruchovsky, and M.D. Sadar, *Activation of the Androgen Receptor N-terminal Domain by Interleukin-6 via MAPK and STAT3 Signal Transduction Pathways.* Journal of Biological Chemistry, 2002. **277**(9): p. 7076-7085.
125. Lobo, V.J.S.-A., et al., *Dual regulation of Myc by Abl.* Oncogene, 2013. **32**(45): p. 5261-5271.
126. Huyer, G., et al., *Mechanism of Inhibition of Protein-tyrosine Phosphatases by Vanadate and Pervanadate.* Journal of Biological Chemistry, 1997. **272**(2): p. 843-851.
127. Goel, M.K., P. Khanna, and J. Kishore, *Understanding survival analysis: Kaplan-Meier estimate.* International Journal of Ayurveda Research, 2010. **1**(4): p. 274-278.
128. Bradburn, M.J., et al., *Survival Analysis Part II: Multivariate data analysis – an introduction to concepts and methods.* British Journal of Cancer, 2003. **89**(3): p. 431-436.
129. Godoy-Tundidor, S., et al., *Interleukin-6 and oncostatin M stimulation of proliferation of prostate cancer 22Rv1 cells through the signaling pathways of p38 mitogen-activated protein kinase and phosphatidylinositol 3-kinase.* The Prostate, 2005. **64**(2): p. 209-216.
130. Ng, S.S.W., et al., *Antitumor Effects of Thalidomide Analogs in Human Prostate Cancer Xenografts Implanted in Immunodeficient Mice.* Clinical Cancer Research, 2004. **10**(12): p. 4192-4197.
131. Pasder, O., et al., *Downregulation of Fer induces PP1 activation and cell-cycle arrest in malignant cells.* Oncogene, 2006. **25**(30): p. 4194-4206.
132. Lee, S.-H., et al., *Synapses are regulated by the cytoplasmic tyrosine kinase Fer in a pathway mediated by p120catenin, Fer, SHP-2, and β-catenin.* The Journal of Cell Biology, 2008. **183**(5): p. 893-908.
133. Kogata, N., et al., *Identification of Fer Tyrosine Kinase Localized on Microtubules as a Platelet Endothelial Cell Adhesion Molecule-1 Phosphorylating Kinase in Vascular Endothelial Cells.* Molecular Biology of the Cell, 2003. **14**(9): p. 3553-3564.

134. Paardekooper Overman, J., et al., *Phosphoproteomics-Mediated Identification of Fer Kinase as a Target of Mutant Shp2 in Noonan and LEOPARD Syndrome.* PLoS ONE, 2014. **9**(9): p. e106682.

135. Babon, Jeffrey J., et al., *The molecular regulation of Janus kinase (JAK) activation.* Biochemical Journal, 2014. **462**(1): p. 1-13.

136. De Mol, E., et al., *EPI-001, A Compound Active against Castration-Resistant Prostate Cancer, Targets Transactivation Unit 5 of the Androgen Receptor.* ACS Chemical Biology, 2016.

137. Altschul, S.F., et al., *Gapped BLAST and PSI-BLAST: a new generation of protein database search programs.* Nucleic Acids Research, 1997. **25**(17): p. 3389-3402.

138. Obenauer, J.C., L.C. Cantley, and M.B. Yaffe, *Scansite 2.0: proteome-wide prediction of cell signaling interactions using short sequence motifs.* Nucleic Acids Research, 2003. **31**(13): p. 3635-3641.

139. Antonarakis, E.S., et al., *Targeting the N-Terminal Domain of the Androgen Receptor: A New Approach for the Treatment of Advanced Prostate Cancer.* The Oncologist, 2016.

140. Liu, C., et al., *Niclosamide suppresses cell migration and invasion in enzalutamide resistant prostate cancer cells via Stat3-AR axis inhibition.* The Prostate, 2015. **75**(13): p. 1341-1353.

141. Banuelos, C.A., et al., *Sintokamide A is a Novel Antagonist of Androgen Receptor that Uniquely Binds Activation Function-1 in its Amino-Terminal Domain.* Journal of Biological Chemistry, 2016.

142. Blom, N., et al., *Prediction of post-translational glycosylation and phosphorylation of proteins from the amino acid sequence.* PROTEOMICS, 2004. **4**(6): p. 1633-1649.

143. Zachariadis, M.G., VG, *E2F1 (E2F transcription factor 1).* Atlas Genet Cytogenet Oncol Haematol., 2009. **13**(11): p. 812-816.

144. Ojemuyiwa, M.A., R.A. Madan, and W.L. Dahut, *Tyrosine kinase inhibitors in the treatment of prostate cancer: taking the next step in clinical development*. Expert Opinion on Emerging Drugs, 2014. **19**(4): p. 459-470.

145. Drake, J.M., et al., *Metastatic castration-resistant prostate cancer reveals intrapatient similarity and interpatient heterogeneity of therapeutic kinase targets.* Proceedings of the National Academy of Sciences, 2013. **110**(49): p. E4762-E4769.

146. Wang, Y., et al., *Reciprocal regulation of 5α-dihydrotestosterone, Interleukin-6 and interleukin-8 during proliferation of epithelial ovarian carcinoma*. Cancer Biology & Therapy, 2007. **6**(6): p. 864-871.

147. Lin, D.-L., et al., *Interleukin-6 Induces Androgen Responsiveness in Prostate Cancer Cells through Up-Regulation of Androgen Receptor Expression*. Clinical Cancer Research, 2001. **7**(6): p. 1773-1781.

148. Ueda, T., et al., *Ligand-independent Activation of the Androgen Receptor by Interleukin-6 and the Role of Steroid Receptor Coactivator-1 in Prostate Cancer Cells*. Journal of Biological Chemistry, 2002. **277**(41): p. 38087-38094.

149. Zelivianski, S., et al., *Multipathways for transdifferentiation of human prostate cancer cells into neuroendocrine-like phenotype.* Biochimica et Biophysica Acta (BBA) - Molecular Cell Research, 2001. **1539**(1): p. 28-43.

150. Hu, R., et al., *Distinct transcriptional programs mediated by the ligand-dependent full-length androgen receptor and its splice variants in castration-resistant prostate cancer*. Cancer Res., 2012. 72(14): p. 3457-3462.